THE OPTIMISATION OF PEBBLE GRINDING

by

T PILLAY

A thesis submitted in fulfilment of the academic
requirements for the degree Master of Science in
Engineering, at the School of Chemical Engineering,
University of KwaZulu-Natal

Durban

2012

ABSTRACT

Secondary pebble milling is an attractive alternative to using ball-mills. It is of particular interest in older mines where tonnage has been reduced, spare mills are available and savings in operating cost are essential to ensure the financial success of the mine. Ball-mills in a conventional two-stage milling circuit can be converted to pebble mills and pebbles can be obtained by allowing a fraction of the feed to bypass the tertiary crusher. The aim of this work was to investigate the effect of pebbles size and mill speed on secondary grinding efficiency at a gold mine. Pebble mills are used at the mine for secondary grinding, using a pebble feed size of 65mm/35mm.

Semi-batch tests were performed on a bulk sample of the ore, using a 1.2 m diameter mill. Various mill speeds and two pebble feed size ranges were tested (i.e. 65mm/35mm and 44mm/28mm).Various size fractions of pebbles were marked using spray paint and weighed before and after each experiment to determine a mass loss function. The steady state size distribution for a given feed size was predicted using an empirical model which incorporates this function.

It is well known that smaller grinding media are more efficient for fine grinding, as a result of a larger surface area to volume ratio. The experiments confirmed this. It was expected that the use of smaller pebbles would result in an increase in pebble consumption, but the pebble consumption actually decreased, when the smaller pebbles were used. This phenomenon is thought to be due to the removal of the larger rocks, resulting in a decrease in impact forces on the pebbles, and hence a lower surface wear rate. A substantial improvement in secondary grinding efficiency (defined as the kWh spent to produce a ton of material finer than 75 μm or Work Index) was observed by reducing the pebble feed size. Grinding efficiency was improved further by reducing the mill speed from 83.5% of critical speed to a typical ball-milling speed of 69%. The results of these batch grinding tests show that simple changes to equipment may lead to a more efficient use of power, a finer grind and better extraction of gold.

Tests in a laboratory-scale mill were used to compare pebble milling to ball milling, using the same size range for the pebbles and balls. The pebbles were more efficient, resulting in a reduction of 26% in the power required per ton of product, for the same product size distribution. However, the reduced power draw requires a 42% increase in mill volume. However if spare mills are available then this poses no problem.

PREFACE

I, Terrence Pillay declare that unless indicated, this thesis is my own unaided work and that it has not (in part or whole) been submitted to any other universities or academic institutes.

_____

T. Pillay

As the candidate's supervisor, I, Prof. B.K. Loveday approved this thesis for submission.

_____

Prof. B.K. Loveday

ACKNOWLEDGEMENTS

TABLE OF CONTENTS

LIST OF FIGURES

LIST OF TABLES

xiv

NOMENCLATURE

Symbol	Description	Unit
CS	Critical Speed	rpm
CoC	Centre of circulation	-
d^{av}	Average diameter of rock	m
d^{bottom}	Lower limit of the size interval	m
d^{s}	Arithmetic average of the limits of size interval	m
d^{top}	Upper limit of the size interval	m
F	Force	N
f_r	Number of rotations of mill	-
f_{SF}	Shape factor function	-
g	Acceleration due to gravity	m/s^2
J	Percentage mill filling	-
k_s	Specific wear rate correction factor	-
M	Mass of fines	kg
m^{av}	Average mass of a rock	kg
M^{feed}	Mass fraction of rocks in feed	-
M^{p}	Predicted mass of rocks	kg
m^{p}	Predicted mass fraction of rocks	-
m^{s}	Mass of a sphere	kg
m^{sphere}	Mass of a reference sphere	kg
m^{T}	total mass of rocks in model	kg
M^{tp}	Total predicted mass of rocks	kg
m^{TS}	Total mass of sampled rocks	kg
m_w	Mass of weigh used for static calibration	kg

NLP	No load power	*mV*
n^m	Total number of rocks in model	-
n^s	Number of rocks in sample	-
P	Power	*W*
r	Mill radius	*m*
RPM	Revolutions per minute	*rpm*
R_s	Specific wear rate as determined from rock tagging procedure	*1/min*
s	Distance	*m*
SF	Shape factor	-
t	Time	*min*
V	Voltage	*mV*
W	Work	*J*
WI	Grinding efficiency or work index	*kwh/t*
Δt	Change in time	*min*
κ	Angle of repose	*Radians*
ρ_{rock}	Density of rock	*kg/m³*
τ	Rotational torque	*Nm*
φ	Mill speed	*% CS*

Important subscripts

i	Denotes a rock originally from size *i*	
0	Denotes that given property of rock evaluated at time *t=0*	
t	Denotes that given property of rock evaluated at time *t*	
t+1	Denotes that given property of rock evaluated at time *t+1*	

1. INTRODUCTION

Size reduction is usually the first step in any mineral processing circuit. It is achieved by various methods of crushing and grinding ore to liberate the valuable minerals from the gangue. Size reduction is by far the most expensive operation in most concentrators and Jones and Holmberg (1996) estimate that up to 70 % of the total cost may come from size reduction. According to Jones and Holmberg (1996) the ―selection of the optimum size reduction method is essential to the financial success of a mine".

Crushing is used to reduce the ore to a size that is suitable for grinding. Grinding is conventionally done in two stages using a metallic grinding media to grind the ore to the final required product size. The problem with this method of grinding is that the grinding media (usually made out of steel) also wear away. The cost of ball consumption is significant, particularly when alloy steel balls are used. The latter is required when the downstream process is flotation of sulphide minerals. Older mines where tonnage has decreased may be looking to save on cost in order to ensure the financial success of the mine. The use of selected pieces of ore as pebbles may be an attractive option to replace balls for secondary grinding.

A recent analysis of the design of the Nkomati nickel ore concentrator has demonstrated that operating costs are reduced significantly when pebble mills are used for secondary grinding, in place of ball mills. There was no significant increase in capital cost and the case for pebble milling should be re-visited. It is envisaged that some of the existing single-stage SAG mills on South African gold mines could be converted to two-stage autogenous grinding (AG) mills, with closed circuit crushing applied to the primary stage.

The grinding plant at the reference gold mine was designed to use secondary pebble milling. At this mine the primary rod mill is operated in open circuit while the secondary pebble mill is operated in close circuit with cyclones (two-stage). The current practice at the gold mine is to feed relatively large pebbles between 65 mm to 35 mm to the secondary pebble mill. In view of recent work at UKZN on the use of small pebbles, it appears that significant improvements to grinding efficiency may be obtained in the pebble mills at the mine, by using a wider range of pebble sizes.

The aim of this work was to investigate the effect of pebble feed size and mill speed on secondary grinding efficiency at the gold mine. This may lead to the more efficient use of power, a finer grind and better extraction of gold. It is a well understood principle that smaller balls (or

in this case pebbles) are needed for fine grinding as they have a larger surface area to volume ratio than larger balls. However this means the rate of consumption of the smaller pebbles increases, as does the amount of critical size particles, as the rocks undergo an initial rounding stage which produces pebbles but also chips. However by altering the natural size distribution of the pebbles and setting a new optimised size distribution, it was envisaged that the fore mentioned problems could possibly be overcome.

2. LITERATURE REVIEW

2.1 Introduction

The term comminution is used to define any process which involves a reduction in size of solid material. Comminution or size reduction is usually the initial stage of any mineral processing circuit. Kelly and Spottiswood (1982) explain that size reduction is necessary to:-

- ➢ Liberate valuable minerals from the gangue so that they can be separated, to produce a concentrate of valuable minerals.
- ➢ To provide a product that meets a certain specification with respect to shape and size.
- ➢ Increase the area available for chemical reactions.

There are various methods by which size reduction may be achieved. The methods are grouped according to the initial particle size. The first stage of size reduction is usually mining where large ore bodies are broken with the use of explosives. All subsequent size reductions down to about 25 mm are referred to as crushing while further reductions in size are considered to be grinding. Both crushing and grinding are more economical when done in stages. This is referred to as primary, secondary or tertiary crushing/grinding depending on the number of stages (Kelly and Spottiswood, 1982).

Grinding is further divided in terms of the type of mill used, the type of grinding media and whether grinding is done using wet or dry conditions. This work involves an investigation of size reduction by means of grinding hence subsequent comments on comminution or size reduction will refer to grinding.

The wet tumbling mill still remains the most common method for grinding. The tumbling mill uses a grinding medium to essentially shatter the ore into smaller fragments. The grinding media could include steel rods or balls, ceramic balls or even the ore itself. Jones and Holmberg (1996) stated that a tumbling mill which uses the ore itself as a grinding medium is referred to as an autogenous grinding (AG) mill while a tumbling mill which uses a combination of steel/ceramic media and the ore itself is referred to as semi-autogenous grinding (SAG). Size reduction in an autogenous grinding mill occurs mainly due to shattering of particles. However not all ores have suitable fracture characteristics for fully autogenous grinding (FAG). An alternative is to use secondary pebble milling, where the ore enters as a finely crushed material and is ground further by selected pieces of the ore itself (called pebbles) which act as a grinding media. (Kelly and Spottiswood, 1982)

2.2 Analysis of comminution methods

A study of the most common comminution circuits was done in order to have a better understanding of the role of pebble milling. It also gave insight into the possible change from a conventional type milling to pebble milling. Koivistoinen (1995) describes the advantages and disadvantages of 9 common comminution methods which are discussed below. In addition two more common methods (more common in gold mining) namely rod mill - pebble mill grinding and run-of-mine grinding are also discussed.

2.2.1 Single-Stage Ball mill grinding

Single stage ball milling has its advantages as it has a relatively simple flowsheet and is capable of producing a stable throughput. The disadvantages are that it requires fine crushing which is expensive in terms of both capital and operating costs and operating costs are further increased by the high cost of grinding balls. The grain size distribution is not optimal for flotation and the fineness of the grind is difficult to adjust. A typical single stage ball milling circuit is shown in Figure 2-1. (Koivistoinen, 1995)

2.2.2 Rod mill - Ball mill grinding

A rod mill/ball mill combination is efficient in terms of energy consumption, with a simple flow sheet capable of producing a stable throughput. The production of slimes is low due to the good grain size distribution. The fine crushing needed here is only a little cheaper than in single stage ball milling which is offset by the increased cost of rods and balls. Worn rods need to be removed regularly, resulting in downtime and labour costs. The fineness of the grind is difficult to adjust, especially downwards. A typical rod mill/ ball mill circuit is shown in Figure 2-2. (Koivistoinen, 1995)

2.2.3 SAG- Ball mill grinding

The trend in mining has been towards processing progressively lower grades of ore, recovered from large open-pit mines. The economies of scale have resulted in the use of large semi-autogenous grinding (SAG) primary mills and followed by large ball mills. Large balls (100 to 150mm diameter) are used in the SAG mills to provide fine crushing of the ore lumps. Capital and operating costs are reduced as no fine crushing is required. However, the large balls damage the liners, and ball and energy consumption are high. Although the flowsheet is rather simple, the circuit is hard to adjust and control thus causing an unstable throughput with high slimes production. A typical SAG-ball milling circuit is shown in Figure 2-3. (Koivistoinen, 1995)

2.2.4 SABC Grinding

The term SABC refers to a SAG/ball-mill circuit, in which the SAG mill has pebble ports, for discharge of pebbles, which are crushed using a closed-circuit crusher. The double elimination of critical size material results in a high throughput and a more stable flow, but difficulties arise when steel balls enter the crushing circuit. A typical SABC grinding circuit is shown in Figure 2-4. (Koivistoinen, 1995)

2.2.5 ABC Grinding

In addition to SAG ball milling the ABC grinding circuit produces a more stable throughput and eliminates the need for steel balls in the primary stage. A typical ABC grinding circuit is shown in Figure 2-5. (Koivistoinen, 1995)

2.2.6 Traditional two stage autogenous grinding

The two-stage autogenous grinding circuit eliminates the need for metallic grinding media completely. Apart from the savings in operating expenditure, the elimination of metallic grinding media also has advantages in flotation. Although the circuit is relatively easy to control it produces an unstable throughput. Fine crushing is needed which is expensive and variation in ore characteristics may require ore blending. Traditional two-stage autogenous grinding produces a high volume of slimes in the primary stage and high overall energy consumption. A traditional two stage autogenous grinding circuit is shown in Figure 2-6. (Koivistoinen, 1995)

2.2.7 Boliden grinding circuit

The flowsheet is highly simplified and requires moderate capital investments. The elimination of metallic grinding media and the need for fine crushing has advantages as previously discussed. There is no way of eliminating the critical size matter which can lead to low and unstable throughput. This method of grinding consumes high amounts of energy, produces excessive slimes and it is difficult to adjust and control. A typical Boliden grinding circuit is shown in Figure 2-7. (Koivistoinen, 1995)

2.2.8 High pressure roll grinding

In this method of size reduction a large portion of comminution is achieved by crushing. It has a very simple flowsheet however the need for fine crushing is essential. The rolls require constant turning and the fineness of the product may vary. A typical high pressure roll grinding circuit is shown in Figure 2-8. (Koivistoinen, 1995)

2.2.9 Outogenous grinding method

In this method of grinding the operating and capital costs are very low due to the elimination of fine crushing and rod or ball cost. The absence of iron ions from production improves flotation. Production of slimes is low and energy usage is quite moderate. The circuit is easy to adjust and control producing a relatively constant throughput. The planning and operating of this circuit could be complicated. A typical Outogenous grinding circuit is shown in Figure 2-9. (Koivistoinen, 1995)

2.2.10 Rod mill - Pebble mill grinding

With relatively low energy consumption and a simple flow sheet a Rod mill - Pebble mill circuit is capable of producing a stable throughput. The production of slimes is low due to the good grain size distribution. Less expensive than a rod mill – ball mill grinding circuit due to the savings in balls in the secondary mill. Size of grinding media easily adjusted to adjust fineness of grind. No way of dealing with the build-up of critical particles in the secondary mill. A typical rod mill – pebble mill circuit is shown in Figure 2-10.
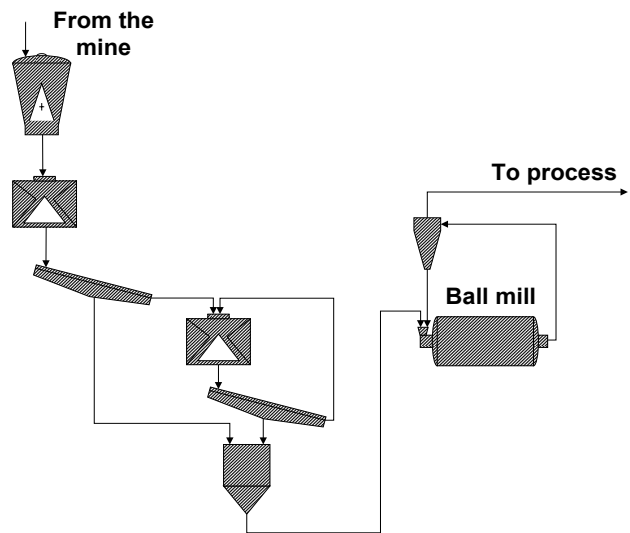
Figure 2-1: Single stage ball mill grinding
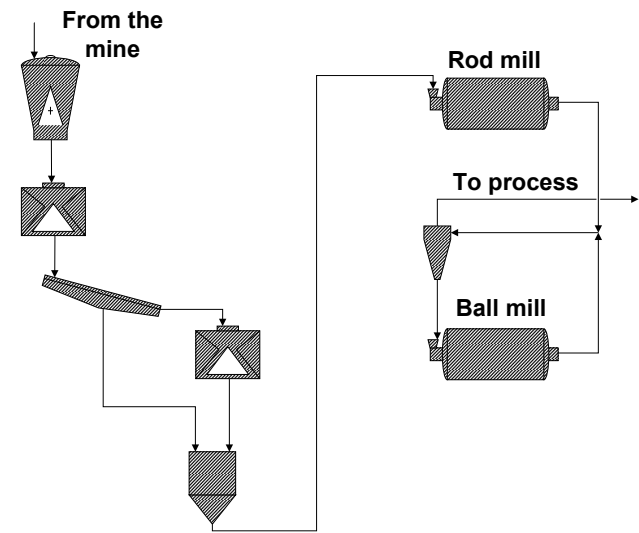
Figure 2-2: Rod mill – Ball mill grinding
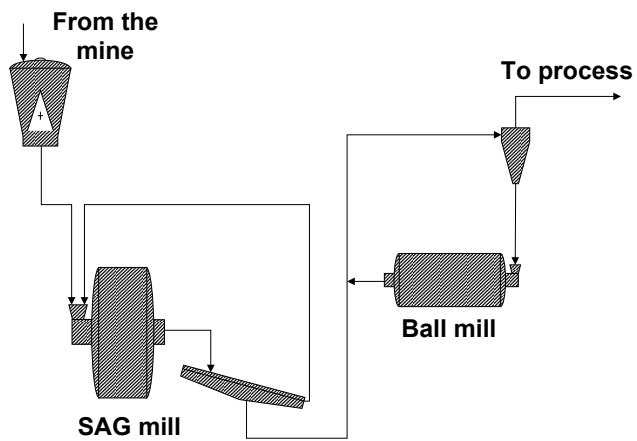
Figure 2-3: SAG – Ball mill grindin
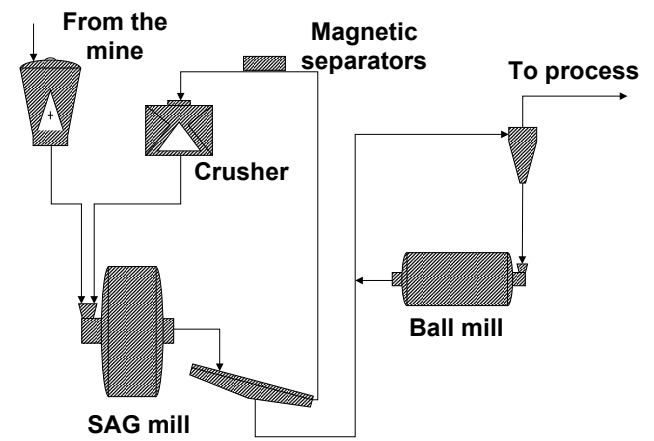
Figure 2-4: SABC Grinding
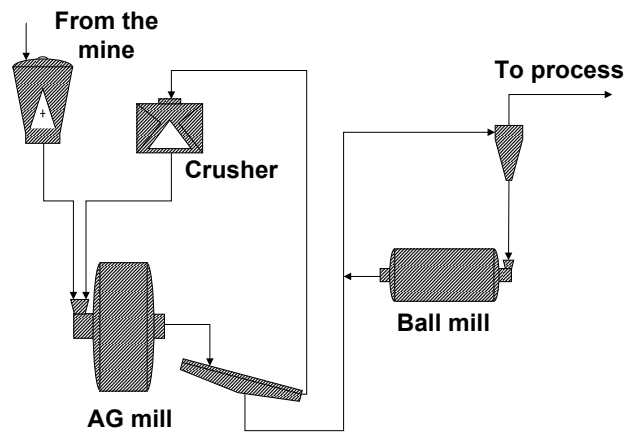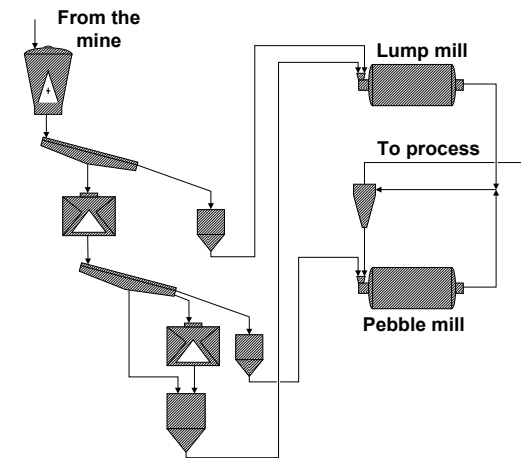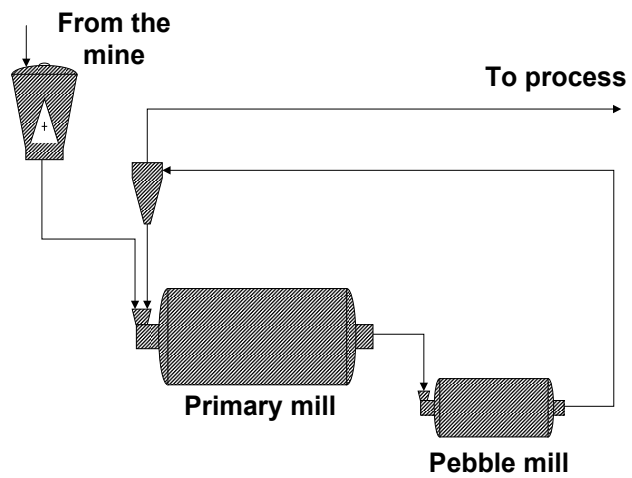
7

From the mine

To process

Crusher

Ball mill

AG mill

From the mine

Lump mill

To process

Pebble mill

From the mine

To process

Primary mill

Pebble mill

From the mine

Ball mill

To process

High pressure rolls

From the mine

Lump mill

To process
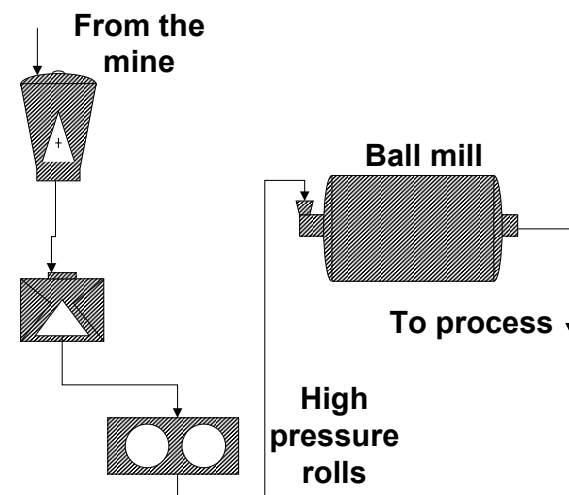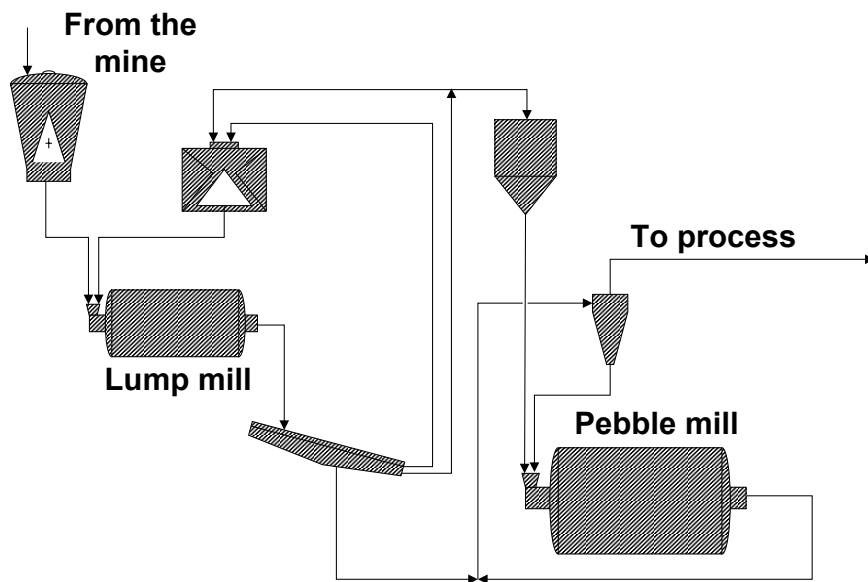
Pebble mill

Figure 2-9: Outogenous grinding

From the mine

Rod mill

To process
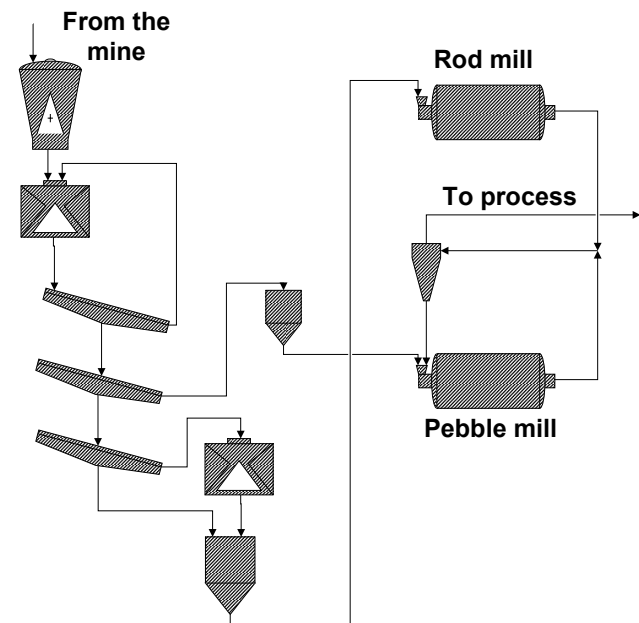
Pebble mill

Figure 2-10: Rod mill – Pebble mill grinding

9

2.2.11 South African single-stage ROM Mills

Most modern autogenous grinding (AG)/semi-autogenous grinding (SAG) mills available today are either one of type of two general types. The South African type mills are characterised by diameter to length ratios of less than one and are given the term low aspect (LA) ratio mills. On the other hand Australian/North American mills are characterised by diameter to length ratios of greater than two and are given the term high aspect (HA) ratio mills. While the initial capital cost is lower for a LA ratio mills, for a specific grind, a LA ratio mill consumes more power per ton of product than a HA ratio mill. (Jones and Holmberg, 1996)

The South African style AG/SAG mills have been termed by locals as a run-of-mine (ROM) mills. Powell et al. (2001) stated that South African style AG/SAG mills operate in a completely different window' to Australian/North American AG/SAG mills. The key differences are highlighted in Table 2-1.

Table 2-1: Differences between South African ROM and conventional AG/SAG mills (Powell et al., 2001)

	AG/SAG	*South African RoM*
Speed, % critical	70-80%	75-90%
Charge Filling, % total mill volume	20-30%	35-45%
Ball filling, % total mill volume	4-15%	15-35%
Internal length	3-5 m	5-12 m
Aspect ratio, diameter/length	0.7-2	0.5-0.8
Recycle stream	Trommel oversize & pebble crusher	Cyclone underflow/fine screen
Application	Primary grind	Single stage to final product

The reason for the differences stem from historic reasons instead of operational reasons as described by Powell et al. (2001). By feeding the run-of-mine ore directly to the mill, existing pebble mills were easily converted to ROM mills and primary ball milling was no longer required. (Powell et al., 2001). Figure 2-1 shows the circuit for a ROM mill.
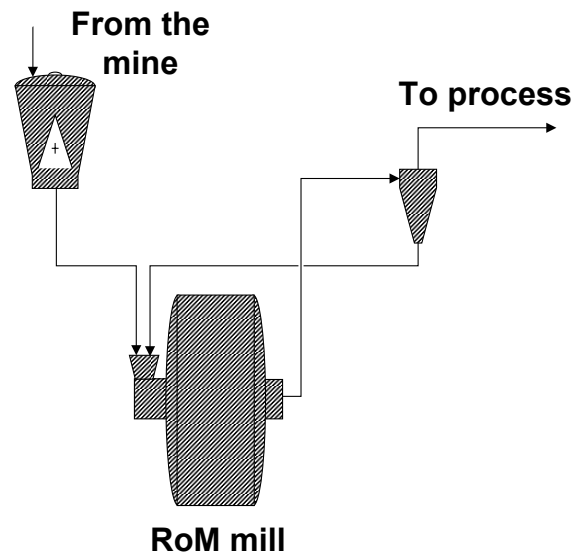
Figure 2-11: Run of mine mill

In order to maximise the amount of energy transferred to the charge, South African ROM mills are operated at maximum power draw. This is achieved by progressively increasing the ore feed rate to the mill until a drop in power is noticed. The feed rate is then maintained to ensure that mill is operated at maximum power draw. The feed rate is increased if a drop in power is observed. This ensures a maximum power draw and maximum feed rate. To ensure the mill operates within the maximum power range, a 40% or more volumetric filling is maintained and the mill is operated at relatively high speeds (70-90% critical) which thus determines the characteristics of the South African ROM mill.(Powell et al., 2001)

2.3 Autogenous grinding

The word autogenous is derived from Latin and means something that is born of its self. The term can describe a single mill or an entire grinding circuit. A mill is referred to as autogenous if the grinding media is already in the feed. A circuit is referred to autogenous if the grinding media is naturally obtained from that mine. Although the media may not mot be mixed in the feed it may be obtained by screening the crusher product or pebble ports and feeding it separately to the mill.(Koivistoinen et al., 1989). The latter, referred to as pebble milling is dealt with in this work with the former certainly implicated in the results.

2.3.1 History of autogenous and semi-autogenous grinding

Although some may consider grinding a primitive practice, autogenous grinding was only introduced in about 1880. The popularity of pebble grinding was on the increase and the pebbles used were naturally occurring and found on beaches. In 1908 the first paper regarding autogenous grinding was delivered to the American Institute of Mining and Metallurgical Engineers. In 1930 Alvah Hadsel installed the Hadsel crushing and pulverising machine in the Beebe Gold mine in California. The device used a high drop principle against a stationary plate. However, mechanical failures occurred when processing harder ores and decreases in capacity where observed.

The Hardinge Company noticed the potential of Hadsel's mill and in 1940 collaborated to produce the redesigned Hardinge-Hadsel Mill. This lead to the production and installation of the Hardinge Cascade mill which was similar to the mills produced in Canada by the Aerofall Company. It was soon discovered that some ores developed a tendency to produce a critical size particles which caused a decrease in capacity. This was controlled by adding pieces of railroad track or large steel balls. (Wipf, 1996)

By 1959 autogenous grinding became popular and various commercial applications began as did significant worldwide installations. (Jones and Holmberg, 1996). A census of all known autogenous and semi-autogenous mills installed before 1996 is available from Jones and Holmberg (1996). The authors estimate that through 1995 hundreds of AG/SAG mills were sold with a total installed power of 2,100,000 kW. A more recent census is available from Stuart and Jones (2001). Here the authors estimate that in the year 2000 alone 1075 AG/SAG mills were sold increasing the total installed power to 2,700,000 kW. This shows the growth of AG/SAG mills with an increase of 17% in five years.(Jones and Holmberg, 1996, Stuart and Jones, 2001).

On the gold mines of the Witwatersrand pebble milling (sometimes referred to as tube milling) has been used since the late 1920's. Initially the method involved hand picking larger pieces of

rock up to 150 mm in diameter to be used as grinding media or pebbles. As crushing and screen applications were introduced it was soon realised that the larger screened fraction could serve as pebbles. This is now common practice when dealing with gold bearing reefs. The properties of the rock as well as mining procedure allow the use of pebble milling thereby reducing the cost associated with grinding. However sometimes the supply of pebbles is not enough to fulfil the requirements for grinding, in which case supplementary grinding media is added. The supplementary media is usually in the form of steel balls. Another form of pebble milling called run-of-mime (ROM) milling is becoming a more popular route on newer mines as well as extensions on existing mines. The addition of metallic media is frequently necessary for the efficient operation of a ROM mill. (Howat and Vermeulen, 1988)

2.3.2 The change to Pebble Milling

Comminution still remains one of the most vital processes required in the mineral industry. According to (Musa and Morrison, 2009) grinding may consume about 75% of the total electrical energy used by a concentrator. Secondary pebble milling is thus an economical option for older mines where tonnage is being reduced and the cost associated with grinding contributes a substantial amount to the total operation cost. (Loveday and Dong, 2000). Loveday (2001) showed that small pebbles could be used to replace steel balls. According to Loveday and Naidoo (1997) for South African gold mines many cases have shown that pebbles are the most efficient grinding media. An ample supply of potential pebbles are available from the crusher, however in order to maintain the same throughput, the low density of the pebbles requires the mill volume to be increased. (Loveday (2010). Figure 2-12 shows the increase in mill volume if steel balls in a conventional ball mill are completely replaced by pebbles. However in this test the pebbles used were relatively small and angular and very inefficient. The author suggested that larger pebbles (once rounded) grind with a similar efficiency as ceramic balls. This gives a more realistic and reasonable increase in mill volume as shown in Figure 2-12. However this poses no problems for older mines were the tonnage has been reduced, spare mills are available and savings operating cost are essential for economic reasons.(Loveday, 2010).
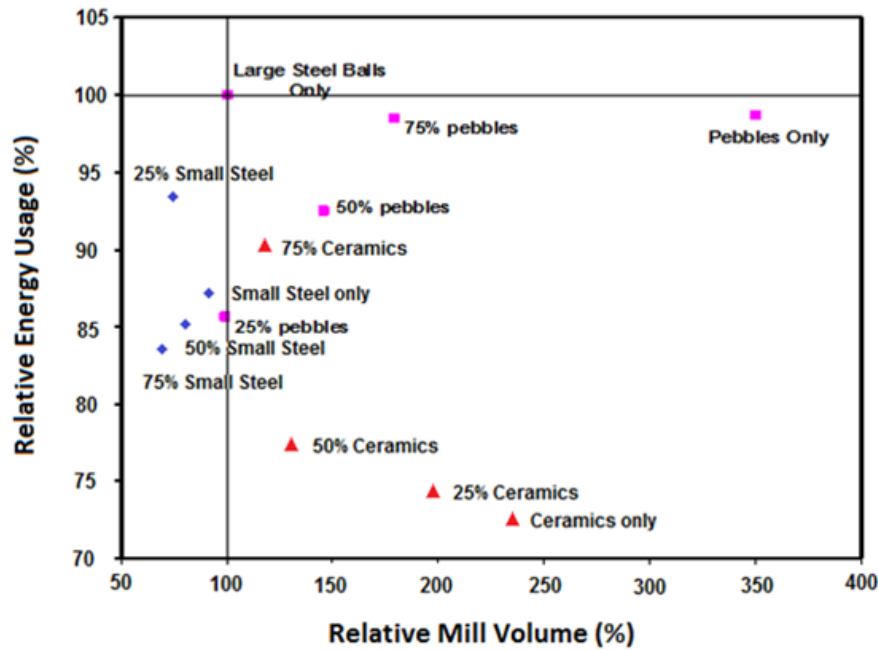
Figure 2-12:Relative energy use for fines production versus relative mill volume. (Loveday, 2010)

2.3.3 Ore variation

The seemingly simplistic approach of pebble milling is not without its share of added complications. Loveday and Dong (2000) stated that changes in ore characteristics and variations in the feed size distribution may produce an inconsistent grind. The problem according to Powell et al. (2009), is that variations in the ore type and size distribution affect the operation of a SAG or ROM mill. The author used a simple logic flow

Variable ore → variable operation → variable grind → variable recovery → possibility of lower recovery

Charge density, volume and size distribution determine the mill load characteristics which in turn determine grinding rates. Any change in feed characteristics causes a change in the mill load characteristics which thus affects the grinding rates which further affects the mill load characteristics. The mill will respond to this disturbance in a non-linear iterative manner until a new point of equilibrium is reached. This process is demonstrated in Figure 2-13. (Powell et al., 2009)

14
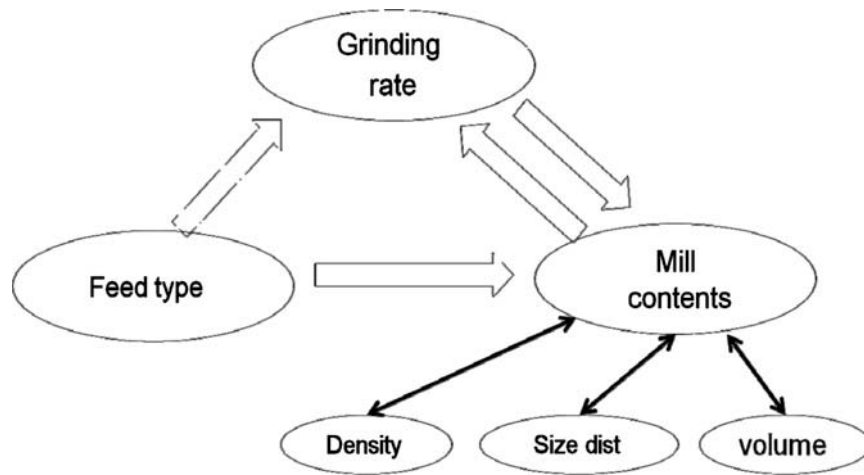
Figure 2-13: Interaction of various milling parameters. (Powell et al., 2009)

A change in feed size distributions may also occur due to segregation as the ore is moved through shafts and stored in bins. (Hahne et al., 2003). In cylindrical bins the coarsest ore fractions tend to move towards the walls. (Rantanen S. et al., 1996). Mellberg and Soderman (1996) state that the problem of variation of feed size distribution can be solved by separating ore into fractions or by size blending.

Any change to the properties of the feed ore will affect the mill load and thus the breakage rates and mechanism in the mill. The optimum feed to the mill with respect to size distribution should contain sufficient larger rocks to efficiently break the smaller particles. Hahne et al. (2003) stated that the mill charge is not only affected by the feed size distribution but also by ore hardness. These disturbances in mill feed properties affect the mill performance and will also affect the fineness of the grind.(Hahne et al., 2003)

2.3.4   Critical particle size

According to Wipf (1996) ―the critical size of material is the dominant factor when mined ore is hard, competent and amenable to impact breakage to an acceptable size". Rantanen S. et al. (1996) define the critical size fraction as the size of pebbles that is not able to break up smaller pebbles and not able to be broken up by larger particles. A semi-autogenous mill (SAG) uses steel balls together with natural grinding media to prevent the accumulation of critical sized pebbles. It also increases the mills ability to deal with ores of varying hardness which in turn leads to an increase in capacity and efficiency.(Loveday and Dong, 2000, Jones and Holmberg, 1996)

2.3.5 Size of grinding media

According to Kelly and Spottiswood (1982) the size of the media is a compromise between two conflicting factors. A decrease in media size causes an increase in area for grinding thus the capacity increases. An increase in particle size creates larger forces between grinding surfaces meaning that larger particles can be broken. As mill speed and diameters increases the energy input to the media increases thus allowing smaller media to be used. Larger media are needed when dealing with harder ores.(Kelly and Spottiswood, 1982)

Figure 2-14 demonstrates a well-known principle in ball milling, that the size of the grinding media should be selected depending on the size of the particles. According to Holmberg and Lidström (1993) particle breakage occurs as a result of forces propagating though planes of weakness present in the particle itself. The plane of weakness could include micro cracks or inhomogeneity. As the particle gets smaller, the probability of a flaw existing decreases while the strength increases thus making it more resistant to forces applied by the media. Hence when using a fixed media size, as the particle size decreases the rate of breakage drops.

Loveday (2010) stated that the pebbles may not have the same momentum as steel balls and an equivalent charge of pebbles may not exert sufficient pressure. Hence from Figure 2-14, larger rocks are needed to grind coarser material and smaller pebbles to ensure effective grinding of the smaller particles. However the term small pebbles is of concern. The pebbles must be large enough as not to fall victim to the forces exerted by the larger rocks but small enough to optimise the grind. (Loveday, 2010).
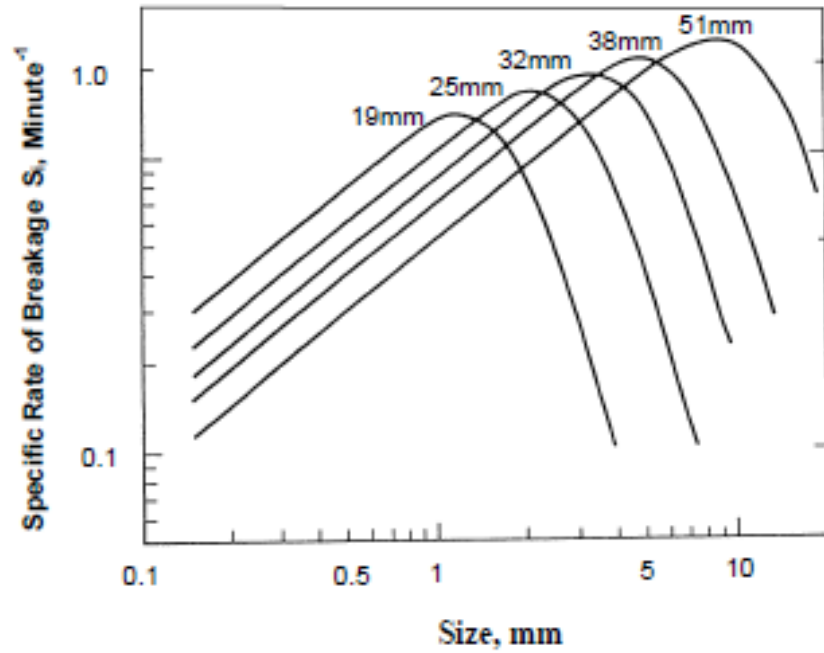
Figure 2-14:Change in breakage rates of particles for various balls sizes(Austin et al., 1984)

The Empire mine, a subsidiary of Cleaveland-Cliff Inc, employs fully autogenous grinding. McIvor and Greenwood (1996) state that the Empire mine reduced the pebble size used as grinding media in the secondary mill to improve the grinding efficiency. The original size of -63.5 mm +31.8 mm was changed to -63.5 mm +22.2 mm however improvements were not well documented. Further plant testing revealed that even small pebbles could be used with -63.5 mm +12.7 mm pebbles showing a 4% reduction in pebble mill energy requirement. All top deck screens have been changed to 12.7mm. (McIvor and Greenwood, 1996)

2.3.6   Theory of pebble wear

The wear of the media (balls or pebbles) causes the mill charge to reach a steady state size distribution, sometimes referred to as a seasoned charge. The amount of makeup material is normally determined by the drop in power draw. The make-up material is usually fed in fixed sizes, which determine the charge size distribution. (Kelly and Spottiswood, 1982).

According to Loveday and Whiten (2002) the wear rate of rocks (or pebbles) in an AG/SAG mill determine the capacity and efficiency of the mill. Loveday and Naidoo (1997) provided a new definition for the specific wear rate of rocks. The new definition considers the mass loss of rocks per unit time but takes into account the mass of the specific rock. It is defined mathematically by Loveday and Naidoo (1997) as:

$$R_S(D) = -\left(\frac{dM}{dt}\right)\left(\frac{1}{M}\right)$$

(2.1)

17

The specific wear rate (R_s) provides a relationship which demonstrates how efficiently a rock is converted to fines. As rocks enter the mill it is usually rounds rapidly as sharps edges and weak planes are quickly eliminated. After this initial ‚fast chipping' phase the rocks (pebbles) wear away at a rate determined by the size. The size distribution of fines produced from each rock is usually similar regardless of the parent rock size. (Loveday and Whiten, 2002). The specific rate is also converted to a corresponding rate of diameter change (k) (mm/h) by the following expression as described by Loveday and Whiten (2002):

$$R_S(D) = \frac{3k(D)}{D} \qquad (2.2)$$

The authors were able to determine the size distribution of the mill charge by examining images of the static charge. Using image analysis techniques both the abrasion rate (mm/h) and the specific wear rate (1/h) was determined. The results are shown in Figure 2-15 and Figure 2-16. The graphs show that between 20 mm and 80 mm the abrasion rate stays relatively constant while the specific rate falls, showing a decrease in area per unit mass. Due to an increase in mass, larger impact forces are created which causes ‒localized surface crumbling and pitting" according to Loveday and Whiten (2002). This is the cause of the increase in abrasion rate for the larger rocks.
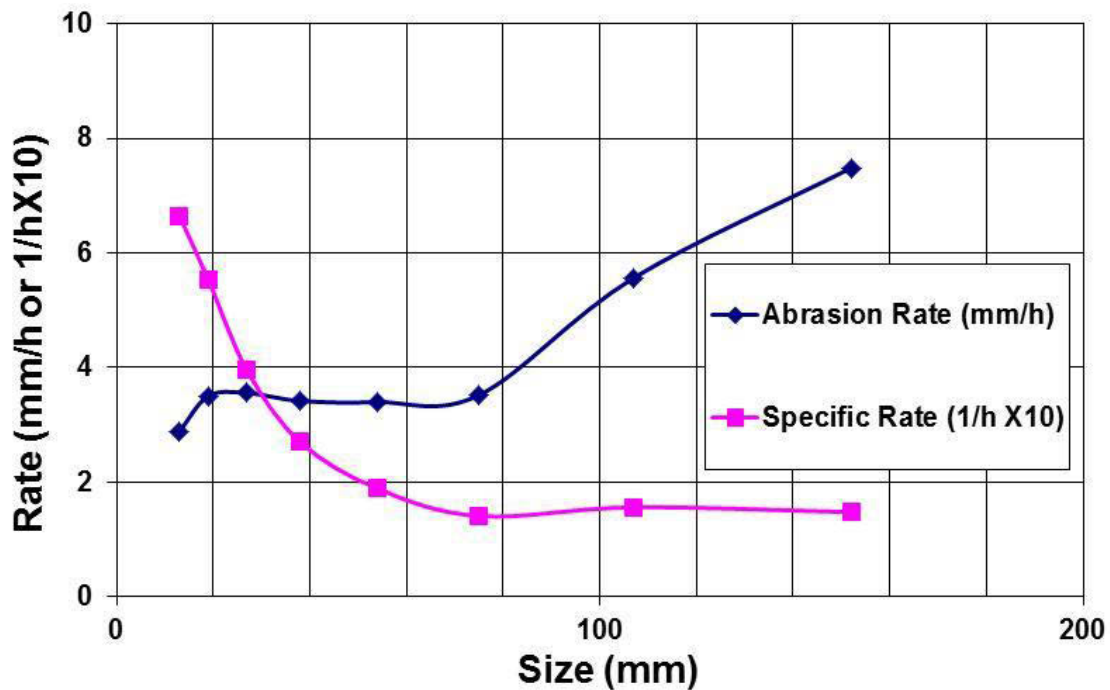
Figure 2-15: Abrasion rate and specific rate at high charge level

18
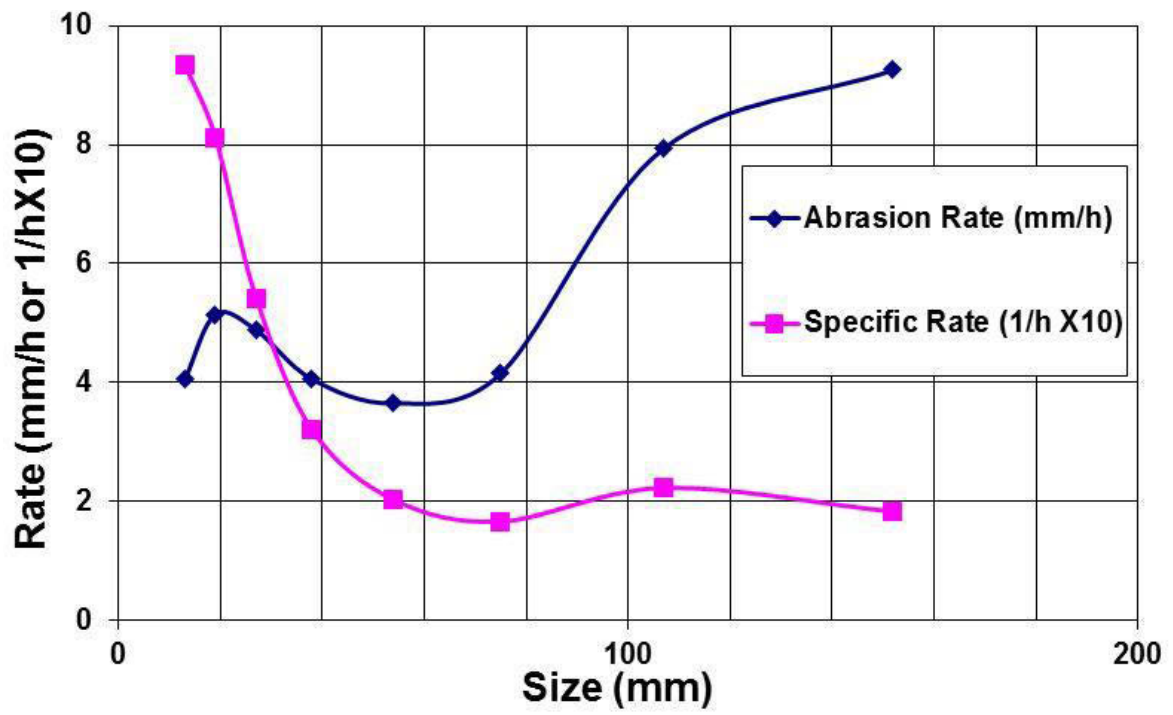
Figure 2-16: Abrasion rate and specific rate at low charge level

2.4 Charge Motion

There are many publications regarding the motion of charge within a tumbling mill in which authors make assumptions and simplifications which are somewhat unrealistic, according to Powell and Nurick (1996a). One of the main problems in the literature is that the particle on particle interactions between grinding media are neglected and only the charge visible at the end window of a mill is examined.

In an effort to better characterise the charge structure within a mill, Powell and Nurick (1996a) conducted studies on charge motion and gave proper definitions of the observed regions. Their study included ball motion deep within the charge using three-dimensional filming techniques. Powell (2004) also stated that an improvement in milling efficiency may be achieved through a better understanding of the charge motion.

According to Powell (2004) the charge motion within a tumbling mill may be characterised by the various regions as shown in Figure 2-17.
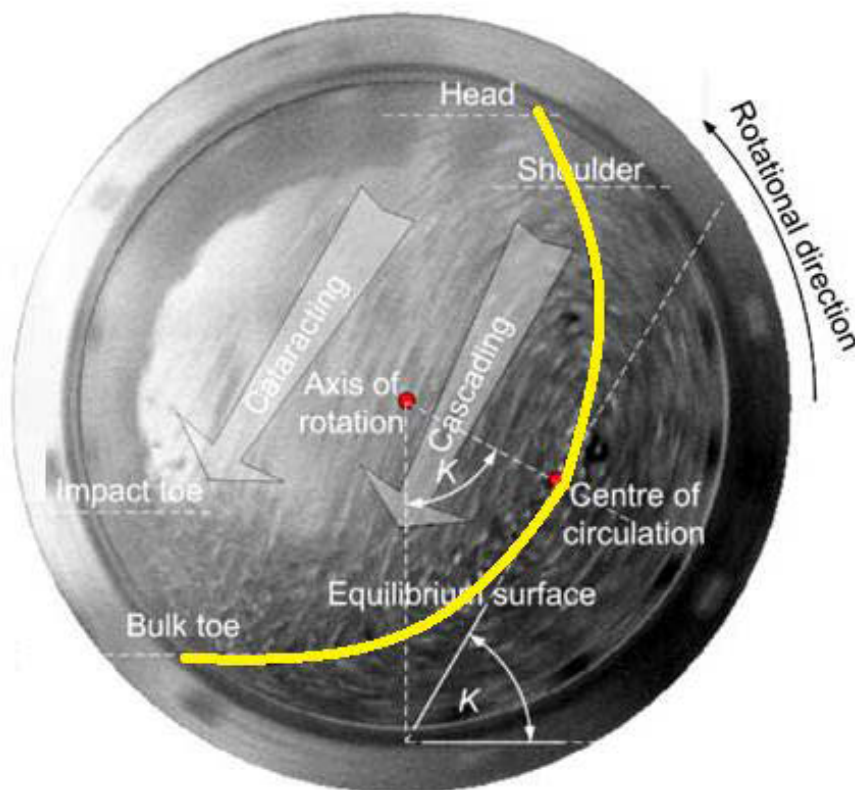
Figure 2-17: Trajectory of the charge motion in tumbling mill (Powell, 2004)

Table 2-2: Definitions of regions in mill.(Powell and McBride, 2004)

Name	Description
Head	Highest point of charge trajectory
Shoulder	Uppermost point at which material leaves the mill shell
Bulk toe	Point of intersection of tumbling charge motion with mill shell
Impact toe	The region where cataracting charge impacts on the mill shell
En masse	Bulk region of the charge moving in an upward direction
Centre of circulation (CoC)	Axis about which all charge in the mill circulates
Equilibrium surface	Surface separating the rising en masse charge from the descending charge
Angle of repose	Cascade angle of the charge

In the past many authors have represented the angle of repose using the line which joins the shoulder and toe. According to Powell and Nurick (1996a) at high speeds this representation becomes an impractical definition of both the angle of repose and of the equilibrium surface. The equilibrium surface is the line which separates the ascending ‗en masse‗ charge from the descending charge. Powell and Nurick (1996a) states that in principle, the equilibrium surface should start from the toe and end at the shoulder and pass through two turning points. The two turning points are at the top and bottom of the charges‗ concentric path. The surface must also pass through the centre of circulation (*CoC*) of the charge as seen by the yellow line in Figure 2-17.

A tangent to the equilibrium surface at the centre of circulation (*Co*C) is always perpendicular to the radius which passes from the centre through the *CoC*. This same tangent subtends an angle with the horizontal that is equal to angle of repose (κ) which defines the angular location of the *CoC*. The distance between the *CoC* and the centre of the mill is known as the radial position of the *CoC*. The radial position of the *CoC* changes with varying mill speeds. At a very low speed when the top layer of balls starts to cascade, the radial position of the *CoC* is a minimum one layer below the surface of the charge. Thus there exists an initial radial position of the *CoC* which corresponds to a minimum angle of repose both of which are dependent on the type of ore and the mill volumetric filling. Powell and Nurick (1996a).

The angle of repose increases as the speed of the mill is increased and the radial position of the *CoC* moves outward, towards the mill shell. This is because most of the charge is cateracting and cascading inside the *CoC*. However when the speed continues to increase the radial position of the *CoC* starts to move back towards the centre of the mill, into a central hollow region. Cascading is eliminated and the entire charge begins cateracting downward. As the speed of the mill approaches critical, circular path of the charge becomes larger. At the critical speed when the entire charge starts to centrifuge the centre of the mill becomes the *CoC*. The angle of repose starts out at a minimum value and moves towards 90°C which is the maximum value that can be reached.

The upward movement of the mill shell causes the balls in the en masse region to be driven in an upward direction. The angular velocity of the charge and the mill shell may not be the same. The degree of slip is defined by (Powell and Nurick, 1996b) to be the ratio of the balls angular velocity and the mills angular velocity. As the ball descends from the cascading or cateracting region it slams the toe of the charge and may even land directly on the mill liner or lifter. This impact causes larger pieces of ore to be fractured or crushed. The majority of the energy transfer takes place in this region. (Powell and Nurick, 1996b)

According to Powell and Nurick (1996b) as the speed of the mill increases the charge begins to spread out. The ratio of the cascading charge to the en masse charge increases as does the rate of circulation of the charge. Thus the particle on particle interaction increases and it can be concluded that an increase in mill speed increases the grinding rate. However at speeds above 90% critical, the balls land directly on the mill liner or lifter. Moodley (1997) stated that in a ball mill all energy transferred to the balls should be ideally transferred to the ore and a loss in efficiency can occur when the balls impact the mill. However in autogenous grinding, the fact that the ore impacts the mill liners or lifter is not considered a total power loss as these impacts can result in rock breakage. Moodley (1997) concluded that varying speeds give different charge motions which could result in different grinds. Thus a study of charge motion is essential if one requires a product with a specific size distribution.

According to Radziszewski (2002) a charge profile is separated in to three zones characterised by the type of grinding taking place in that zone as shown in Figure 2-18. In the grinding zone media slide over one another and break material that is trapped between them. In the tumbling zone media roll over one another breaking material in low energy impacts. In the crushing zone media re-enters the charge breaking material in high energy impacts.
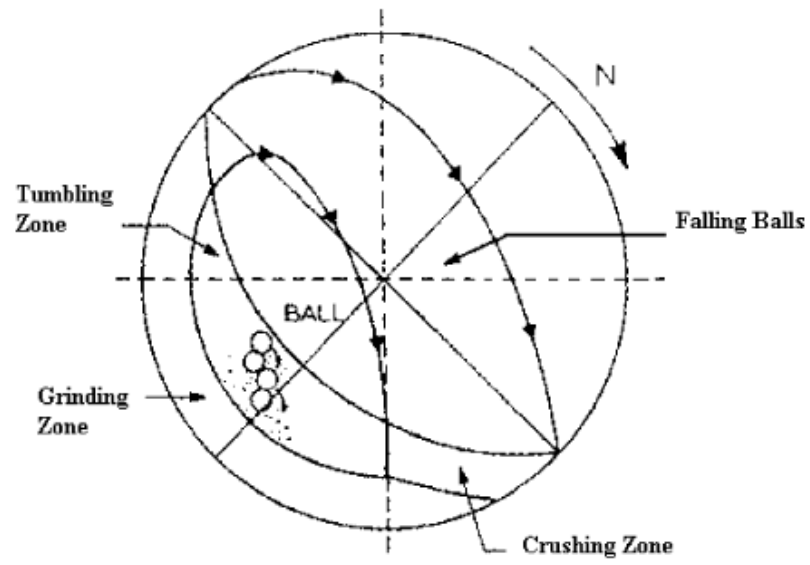
Figure 2-18: Charge profile showing various regions (Radziszewski, 2002)

2.5 Mechanisms

Stanley (1974) conducted a study which aimed to represent the mechanisms in an autogenous mill mathematically. Autogenous milling is here defined as ―a process in which the size of the constituent pieces of a supply of rock is reduced in a tumbling mill purely by the inaction of the pieces, or by the interaction of the pieces with the mill shell, no other grinding medium being employed." The definition covers both run-of-mine milling which has a non-continuous feed size distribution and pebble milling which has a continuous feed size distribution.

Stanley (1974) stated that size reduction in an autogenous mill differs from a size reduction in a ball mill in two ways. Firstly he explains that size reduction in autogenous milling occurs by two main modes which are abrasion and crushing. Abrasion, as defined by (Stanley, 1974) is the ―the superficial detachment of relatively fine material from the surface of larger pieces; it results in the slow ‗whittling away' of a central core with the concomitant production of an increasing quantity of fine detritus". According to Naidoo (2000) the abrasion mechanism occurs when two larger particles move ‗parallel to their plane of contact'. A special case of abrasion referred to as attrition takes place when a smaller particle becomes trapped between two larger particles as this parallel movement takes place. Crushing or better termed impact grinding is defined to be ―the disintegration of smaller particles due to the propagation of crack networks through them". This mechanism is caused by the perpendicular impact of a larger particle at the plane of contact. The point of contact could be another rock or the mill shell or liner. The mechanisms are shown graphically in Figure 2-19.
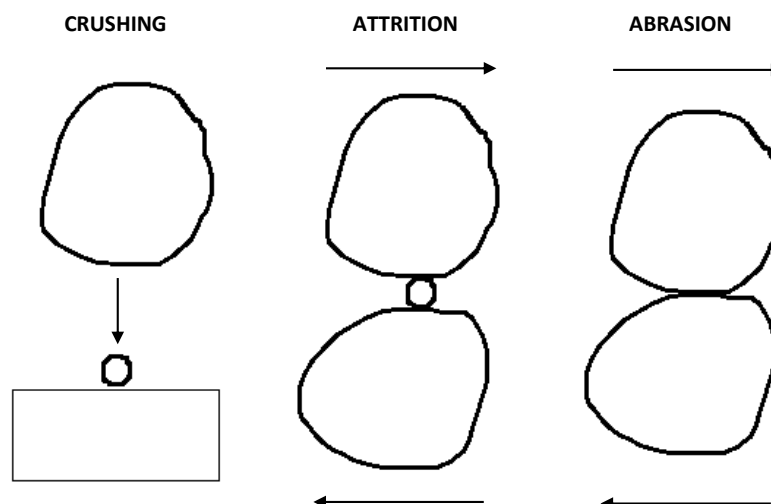
Figure 2-19: Mechanism of fracture

Secondly he states that the grinding parameters of the load are highly dependent on the mill feed since the mill load is generated from the mill feed.

Stanley (1974) conducted experiments in a 1.6 m diameter by 0.3 m mill operating at 70 per cent of critical speed in closed circuit with a 75 mm cyclone. The closed-circuit experiments lasted about 8 hours which is adequate time to establish equilibrium.

By visually examining the size fractions in the equilibrium charge the limits of abrasion and crushing were determined as well as the transition zone between abrasion and crushing. The upper limit of the transition zone is the size above which no breakage occurs and the lower limit the size below which no abrasion occurs. In doing so it is possible to determine the size interval in which rounded pebbles do not exist. (i.e. the pebbles disappear due to breakage). From the results of this experiment Stanley (1974) was able to generate Figure 2-20 which demonstrates the typical breakage-rates (R).

The breakage rate of the coarsest fraction increases, and peaks at the crushing limit. The breakage rate then drops drastically and stays at this low value for several size fractions. These fractions are the critical fractions of the ore as defined earlier. The rate then starts to rise and peak around the abrasion limit. This is followed by a number of pseudo peaks and when the last of the pseudo peaks has been passed the breakage rate starts to decrease before giving a ―final upward kick in the final interval‖.
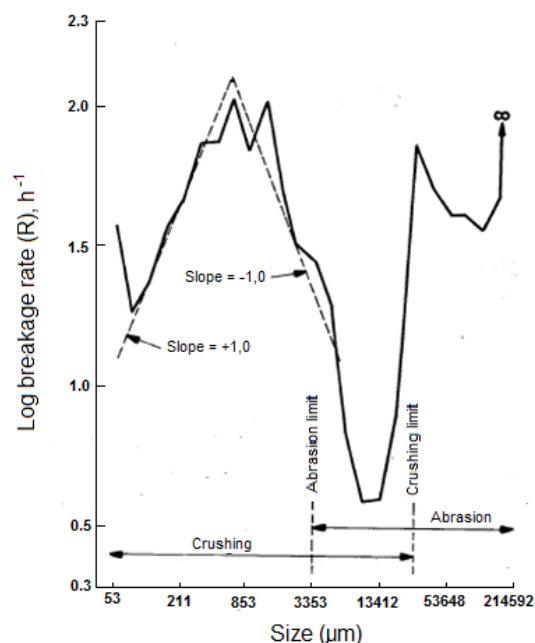
Figure 2-20: Typical breakage rate functions(Stanley, 1974)

Austin et al. (1987) conducted studies in an effort to demonstrate the physical processes that occur during autogenous grinding. The authors concluded that that net breakage process may be calculated by summing up the breakage rates of three distinct breakage regions each of which has its own associated specific rate of breakage. Figure 2-21 shows the typical selection function pattern which demonstrates three distinct breakage regions.

The first region shows a rise in breakage rates as the particles are broken down by the grinding media. Normal breakage occurs as smaller particles are ―nipped" between the pebbles or steel balls. This is shown in region 1 and the principle is well understood. Abnormal breakage occurs when the particles are too large to be broken by the media. It is demonstrated by the decrease in breakage rates as the media is not able to effectively break larger particles. The rate of breakage in this region becomes abnormal as it is made up of normal fracture, and chipping caused by a ―less violent impact". (Stanley, 1974). The third region demonstrates the principal of self-breakage and shows the increase in breakage rate with size. Self-breakage occurs by the tumbling action of the larger rocks. When the particles reach a certain size the grinding media is not able to effectively break the larger rocks. However, the rocks will reach a size at which they will be able to break due to the impact of their own fall. Thus in region 3 of Figure 2-21 the breakage rate increases as the particle size increases.
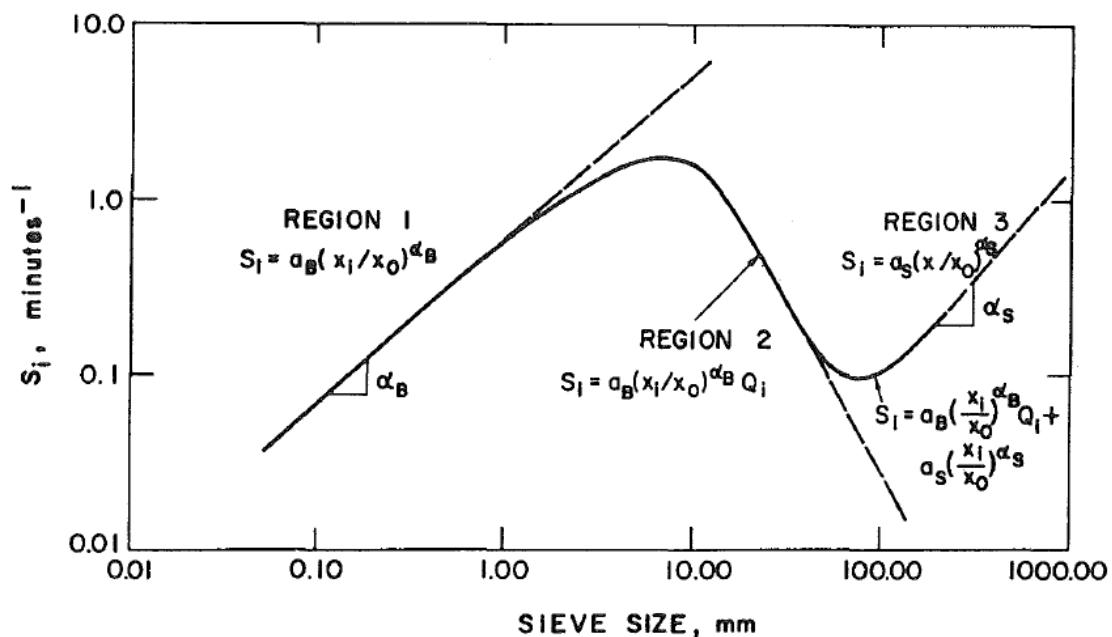
Figure 2-21: Typical trend of specific rate of breakage (Austin et al., 1987)

The tests conducted by Austin et al. (1987) were done in an effort to demonstrate the grinding mechanisms of fracture breakage, chipping and abrasion. These batch tests were conducted in a 600 mm diameter mill that was 300 mm in length. The feed ore was numbered with a dye in an effort to track the weight of individual lumps as a function of time. These weights were expressed as the radius of a sphere having the equivalent weight. The results of the test are shown in Figure 2-22, which shows the linear decrease of weight caused by abrasion. A mean abrasion rate is calculated which is expressed as K in mm/min. The value of K does not stay constant over a wide size interval. This value may however be assumed to be constant over given size intervals.

Austin et al. (1987) explains that for a given size interval the sudden weight changes are due to chipping while complete disappearance is caused by disintegrative fracture. According to the authors ―the results indicated that pure abrasion gave relatively low rates of weight loss, so abrasion and chipping were combined to give an overall chipping-abrasion rate." Figure 2-23 gives a graphical summary of the process.
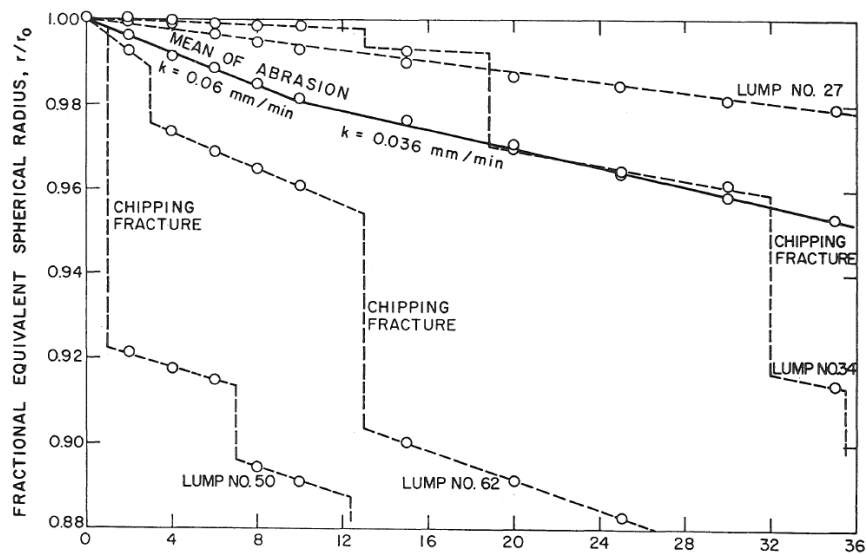
Figure 2-22:Change in equivalent spherical radius of rocks with time.(Austin et al., 1987)

CHIPPING — ABRASION   FRACTURE
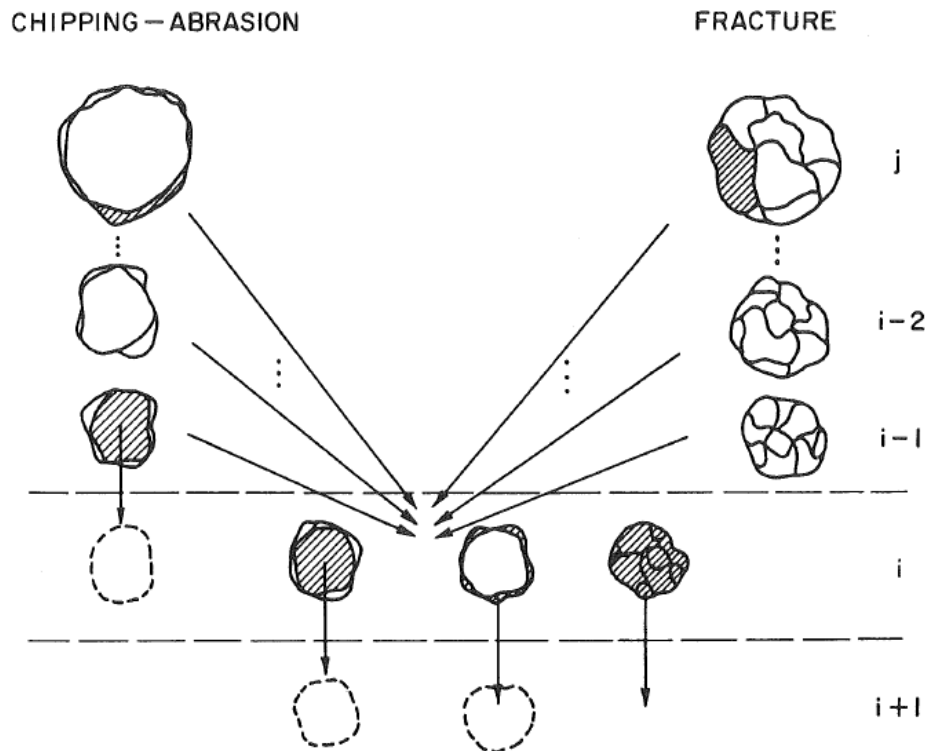
Figure 2-23: Graphical description of the mass balances of chipping-abrasion and fracture.(Austin et al., 1987)

Figure 2-24shows the proportion of mass loss due to fracture, due to fragments from chipping-abrasion and mass loss from cores abrading and moving into a smaller size faction. Austin et al. (1987) concluded that the proportion of these mechanisms remain relatively constant.

Figure 2-25 shows that despite keeping the mill conditions the same for each run, the specific breakage rate of the traced ore decreases with time. Austin et al. (1987) explains that the feed ore is relatively irregular with a high surface area to weight ratio and thus chip-abrade away rapidly. This causes rounding of the rocks into pebbles which chip-abrade slower. It can be concluded from the directly proportional relationship of Figure 2-24 that the fracture component has the same relationship. Austin et al. (1987) say that the entire system essentially behaves like a ―mixture of weaker material which disappears more rapidly, leaving stronger rounded pebbles, which disappear more slowly." Figure 2-26 shows breakage can be approximated using a simple binary mixture. The authors concluded that the ore used in this test was suitable for autogenous grinding due to the fact that the ore produced rounded pebbles that act as balls. The rate of breakage for autogenous grinding is low requiring a large mill volume when compared to ball milling. However the chipping-abrasion process generates a large amount of fines which could compensate for the low rate of breakage and give circuits with grinding energies that are similar to that of conventional grinding.
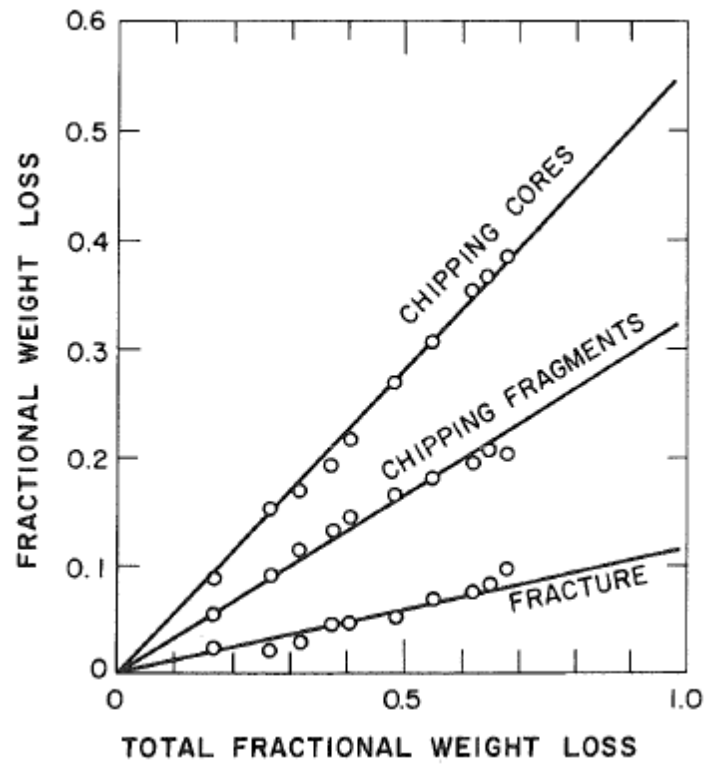
Figure 2-24: Contributions of the individual breakage mechanisms.(Austin et al., 1987)
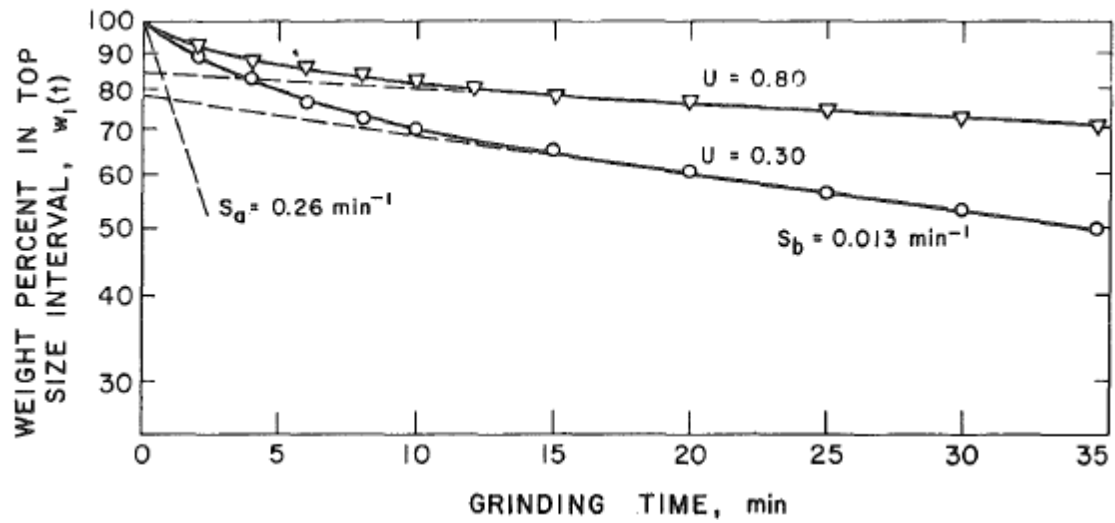
Figure 2-25: Rates of self-breakage.(Austin et al., 1987)
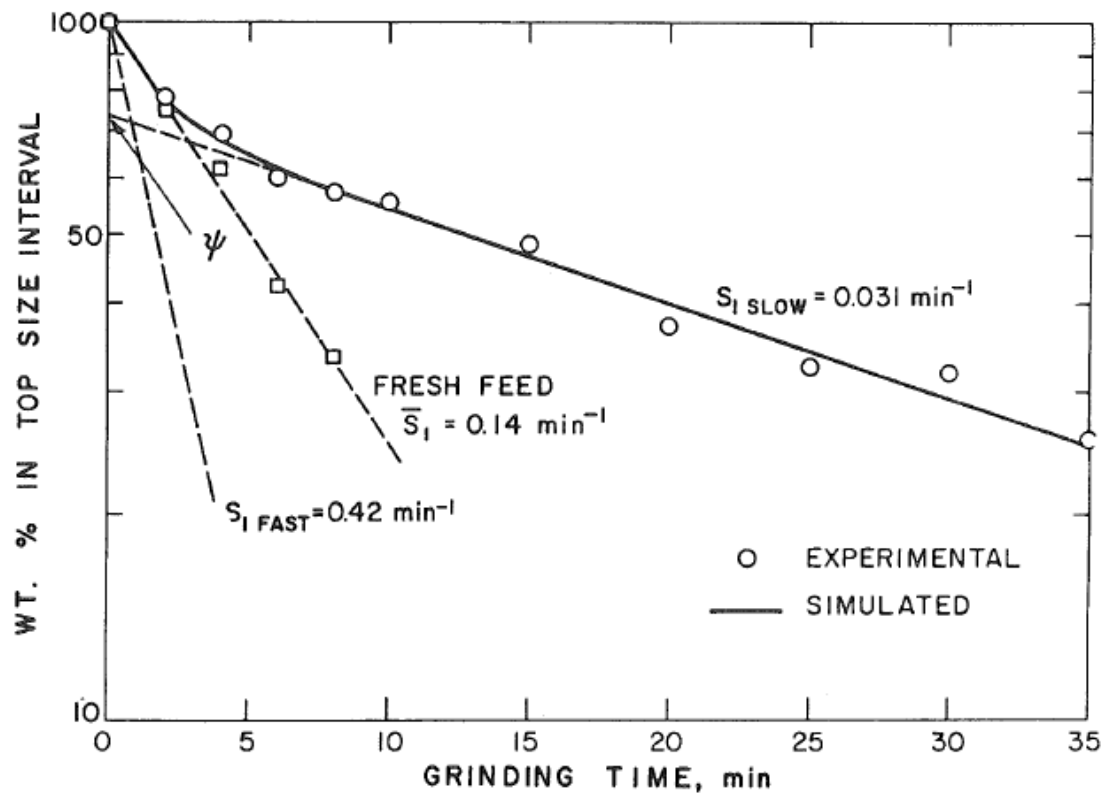
Figure 2-26: Combined rate of breakage-chipping.(Austin et al., 1987)

2.6 The Gold Mine

The gold mine involved in this study has recently embarked on project which aims at processing old surface rock dumps (SRD's) containing gold. These SRD's are mainly low grade waste rock (like the ones shown in Figure 2-27) that was obtained from shaft sinking and development operations. These mining operations began more than 40 years ago and over that time massive SRD's have accumulated. These SRD's contain a fair amount of gold bearing material (like the ones shown in Figure 2-28) which were lost during the tramming and hauling operations. The overall grade of the dump normally ranges between 0.2 to 0.9 g/t and some mines process the entire rock dump. Some mines try screening the dump and blending the material finer than 16 mm, which normally have a higher gold content of between 0.8 to 1.0 g/t with normal run of mine feed. Apart from screening no other ore preparations methods are used. The processing of SRD produces gold, backfill and industrial aggregate resulting in positive cash flow. It also allows for the concurrent rehabilitation of SRD sites well ahead of the mines scheduled closure thereby reducing closure liability. (Ketelhodt, 2009)
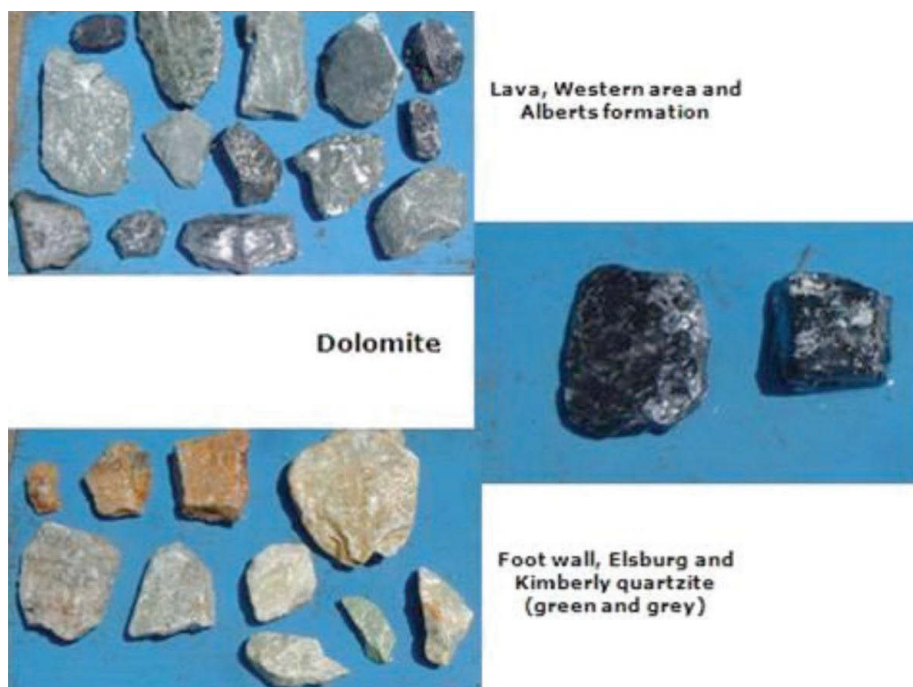
Figure 2-27: Low grade waste rock (Ketelhodt, 2009)
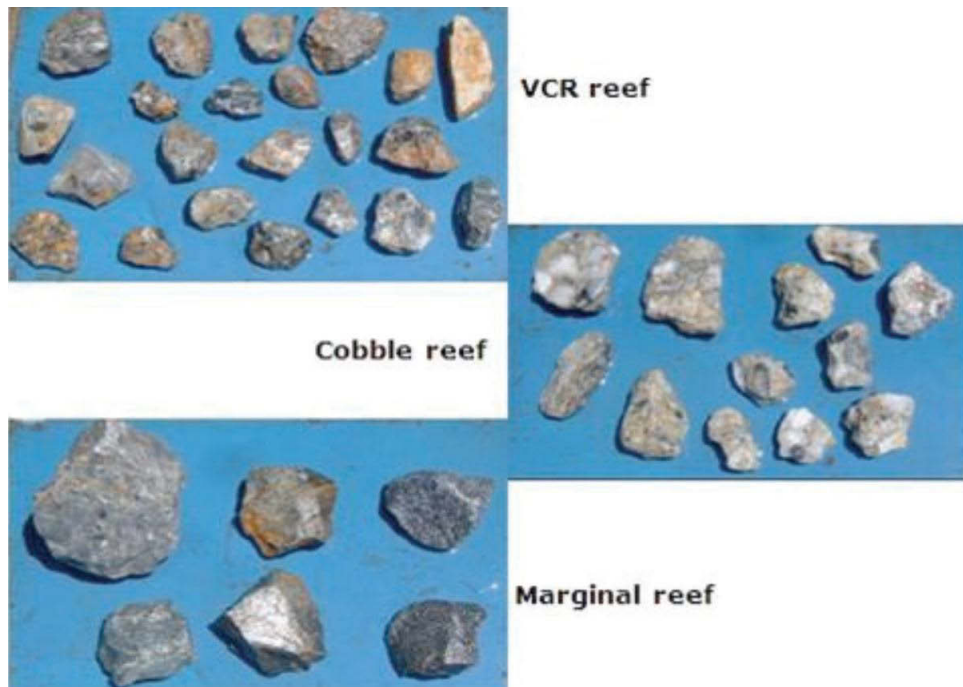
Figure 2-28: Gold bearing rock (reef) (Ketelhodt, 2009)

Table 2-3: Head grades of various rock types (Ketelhodt, 2009)

Rock Types	Au (g/t)
VCR	14.50
Cobble	3.70
Marginal	0.55
Dolomite	<0.08
Lava	<0.08
Green Quartz	<0.08
Grey Quartz	<0.08

3. METHODOLGY

The aim of this work was to investigate the effects of mill speed and pebble feed size on secondary grinding efficiency at a South African gold mine. Grinding, at the mine is achieved by a rod-pebble milling circuit. The crushed ore first enters an open circuit rod mill and is ground further by two pebble mills operated in closed circuit with cyclones. The pebble mills, which have diameters of 4.27 m and a length of 6.71 m, are operated at 83.5% critical speed using a pebble feed size of 65 mm to 35 mm. Plant data revealed that the above operating conditions of the mill produced a product with a grind of 75% passing 75 μm.

The test mill, used for this research needed to simulate secondary grinding at the mine. It also needed to be large enough to subject the rocks to forces that are capable of breaking them but small enough to be operated by a single person and use a relatively small amount of ore sample that can be easily loaded and unloaded. Loveday et al. (2006) explained that a mill with a diameter of 1.2 m is a very convenient size for research and under similar conditions a 1.2 m mill produced similar rates of rock attrition and breakage as experienced in 1.8 m diameter pilot mill.

Samples of ore were obtained from the mine and crushed at Mintek to produce rocks (pebbles) ranging in size from 65 mm to 17 mm. The -17 mm fraction was crushed further to produce a simulated rod mill product (pebble mill feed) with a top size of 3.3 mm. Locked-cycle batch tests were performed on samples of the ore, with the conditions adjusted to achieve the target of 75% passing 75 μm. A locked cycle test is series of repetitive batch tests which aims to simulate a continuous circuit. A simple batch test was performed in the first cycle, after which the rounded pebbles were re-used in subsequent cycles. A full locked cycle test may last up to 10 cycles where the final cycles mimic a steady state, (i.e. Fresh (unrounded) rocks within the designated size range, were added after each cycle, to make up for the loss in pebble mass during the previous cycle). The ‗product', which is equivalent to the cyclone overflow in the operating circuit, was separated from the pebbles using a 3.3mm screen. The locked-cycle test was done in order to firstly determine the milling time required to produce the correct per cent passing so that a base case could be established. Secondly it was done to determine the steady state size distribution of the charge.

The steady-state size distribution of the charge is a function of pebble feed size. In order to determine the steady size distribution for different feed sizes, each feed size requires locked-cycle tests. This would have been time consuming as a locked cycle tests require many cycles

and consumes a large amount of ore before steady-state is achieved. Instead, an empirical model was developed to predict the steady-state size distribution for any pebble feed size range. The mill was simulated operating at steady state with a new pebble feed size, at different speeds. The power drawn by the mill and the per cent passing 75 μm was measured for each operating condition. This was used to calculate the secondary grinding efficiency (*WI*) which is defined as the power consumed to produce ton of material finer than 75 μm.

3.1 Experimental Equipment

3.1.1 The 1.2 m diameter mill

Grinding tests were conducted in a rubber lined mill that had an inside diameter of 1190 mm and a length of 310 mm. The mill, which was installed at the University of KwaZulu-Natal in 2003, was initially used for SAG testing by Loveday (2010) who showed that the mill could be used to determine the optimum conditions for pebbles. In an effort to minimise noise and more importantly fracture caused by impact between rocks and the steel shell, the inner shell of the mill was rubberised. The mill was fitted with 40 mm high lifters as shown in Figure 3-1. The end of the mill is closed off by bolting a steel plate over the end. This steel plate had an aperture cut into it allowing for loading and unloading of ore into the mill. During operation the cavity was closed off by bolting a door over it, as shown in Figure 3-2. The extra weight added by the door would have caused the mill to be imbalanced during rotation. This was overcome by attaching counter weight for balance. The mill was rotated using a motor and gearbox with a variable speed drive.

Figure 3-1: Test mill with endplate removed to show lifter configuration

Figure 3-2: Mill with endplate bolted showing door for loading ore

3.1.2 Power measurement

The power drawn was determined using the torque measurement method, which according to Naidoo (2000) is the simplest method of determining the true net power drawn by the mill charge. The method uses the torque of the mills rotation coupled with the mills rate of rotation (*RPM*) to determine the total power draw. A full derivation of the power equation is given in Appendix A. The no load power (*NLP*) which is defined as the power used to rotate the mill shell

35

is a function of mill speed. For a given mill speed the *NLP* is determined by measuring the power used to spin an empty mill. The true net power drawn is then given by the total power drawn minus the *NLP*.

The power equation is a relationship between power and torque. In order to determine the power one needed to determine the torque with which the mill rotates. This was made possible by the setup of the motor and gear box assembly as shown in Figure 3-3. It can be seen that the motor and gearbox assembly is hung from two bearings attached to the main drive shaft. The drive shaft becomes a pivot point so that the entire assembly is free to swing. In order to rotate a load with a given mass at a constant speed the motor applies a rotational force (torque) to the mill shell. As the motor tries to apply this force stress is induced on the motor which causes it to move or swing. The force required to restrain this movement is directly proportional to the torque applied and is measured using a strain gauge installed between the motor and the frame. The signal from the strain gauge is converted to a voltage signal which is logged on a computer. A record is necessary as the torque varies significantly during the operation of the mill, and averaging is required.

3.1.3   Torque Calibration

The voltage generated by the load cell was meaningless and a calibration of the torque measuring system was done in order to determine a relation between torque and voltage. This was done by hanging different masses from the shell of the mill as shown in Figure 3-4. The motor was locked into position and the weight opposed the normal direction of rotation.

Each mass caused a torque on the mill shell which was relayed back to the motor. Since the motor was locked into place this torque was detected by the strain gauge and the signal sent to a computer where it was converted into a voltage. The torque caused by the hanging mass was determined as the force exerted by the mass ($m_w g$) multiplied by the radius of the shell (*r*) since the string used to suspend the weight is a tangent to the mill shell. This procedure was repeated for different masses so that a plot of torque vs voltage could be obtained. The results of the static calibration of the power measuring equipment are available in Appendix B.

Figure 3-3: Motor and gearbox setup used to rotate mill
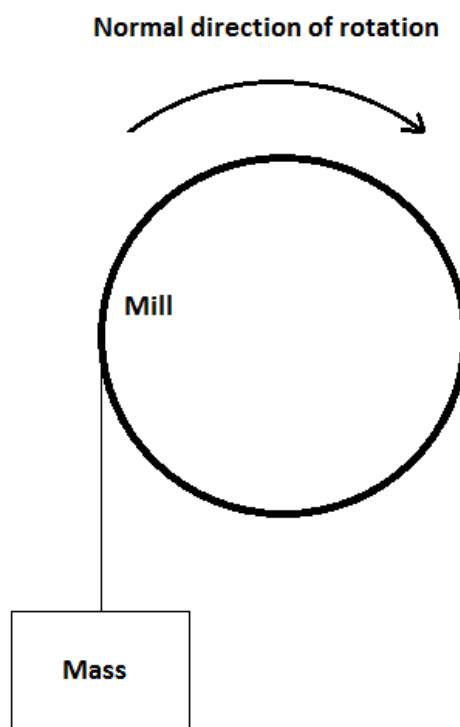
Figure 3-4: Procedure for calibration

3.2 Experimental procedure

Due to the delays in acquiring the gold ore sample and the limited amount available preliminary test work was done using a local ore from a nearby quarry. A large quantity of pebbles was available which allowed for the commissioning of the experimental equipment. It also allowed experimental techniques and procedures to be perfected in preparation for the actual gold ore.

3.2.1 Preliminary Tests

The local ore was first separated into size fractions using grids that were made by welding steel bars together to create square apertures of predetermined sizes. The grids were attached to buckets lids so that the passing material could be collected in buckets as shown Figure 3-5. The ore was separated into three size fractions, 75/65mm, 65/53mm, and 53/37.5mm. From each size fraction 60 rocks were selected and tagged. Initially the rocks were tagged by spray painting each size fraction a different colour and checking for paint remaining in the grooves. However this was rather cumbersome due to the number of times this process was going to be repeated so the tagging process was changed. The new tagging process involved cutting various groove patterns onto the rock surface using an angle grinder. An "×", "#" and "+" pattern were used to distinguish between 75/65 mm, 65/53 mm, and 53/37.5 mm size fraction respectively as shown in Figure 3-6.The mass of rock in each size was determined allowing for initial average mass per rock to be calculated. This also made it possible to determine an initial shape factor (*SF*). The shape factor for a group of rocks in a given size fraction is defined as the ratio of the rocks average mass to that of a sphere which has a diameter equivalent to the arithmetic average of the top and bottom size fractions.

The mill was then loaded with the marked rocks and "spectator rocks" were added in order to ensure a volumetric filling of 30%. According to Loveday (2010) the low level of charge in the mill simulates the impacts experienced in a larger mill. The average density of the local ore was 2898 kg/m^3 and the total mass in the mill amounted to 143.52 kg. In order to simulate true grinding conditions this test included a feed consisting of river sand and water. The mass of sand used was approximately 30 kg and the slurry contained equal amounts of solids and water on a volume basis. The slurry filled all the voids in the charge and the mill speed was set at 69% of critical. The critical speed (*CS*) of a mill is defined as the speed at which the smallest particles in the charge start to centrifuge. The first two runs had a duration of 15 minutes whereas in all subsequent runs the duration was increased to 30 minutes. This was done in order to demonstrate the initial rounding phase of fresh rock as described by Loveday and Naidoo (1997). After each run, the rocks were removed by hand washed individually and in an effort to recover the marked

rocks. The smaller material was screened at 3.3 mm, to separate the fines which were discarded. After the marked rocks in each size fraction were found they were counted and weighed which allowed for the new average mass to be calculated. The shape factor (*SF*) was recalculated after each run. Broken rocks, like the one shown in Figure 3-7 were discarded. The total mass of rocks (marked and spectator) were determined. Fresh make up rock was added to maintain a 30% volumetric filling, and a fresh sample of river sand used. This locked cycle test was repeated until the mass loss of the pebbles (pebble consumption) or the top up of fresh make up rock reached a steady state.
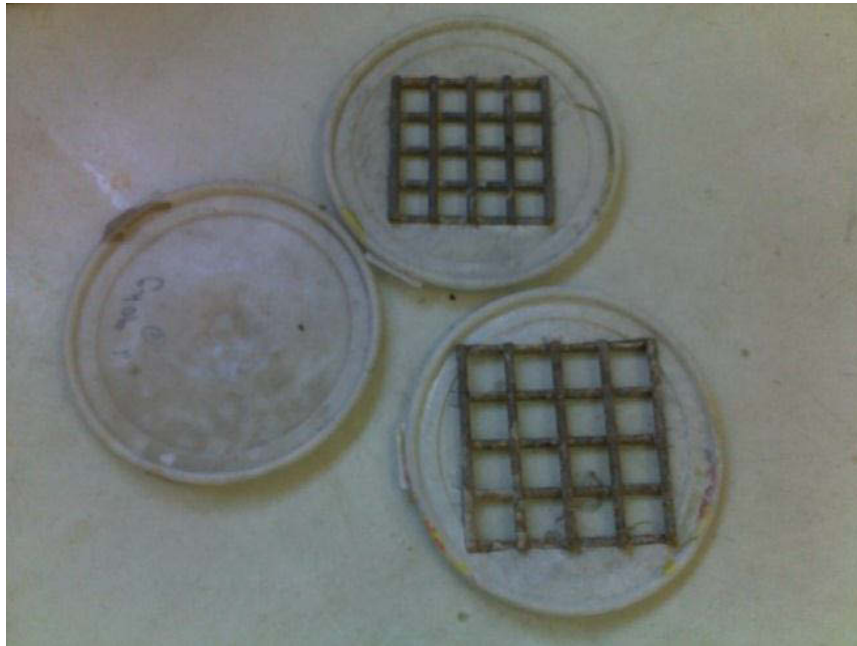
Figure 3-5: Screens attached to bucket lids

Figure 3-6: Tagged rock showing various patterns

Figure 3-7: Fractured rock

3.2.2 Gold ore preliminary tests

On arrival, the gold ore was first screened in order to determine the natural distribution of the rocks as produced by the crusher. The sample itself was too large for complete screen analysis and hence, sub samples were taken in order to determine the natural size distribution of the rocks. Care needed to be taken when obtaining sub samples as segregation according to size may have taken place during delivery process. To avoid false size distributions the ore was first mixed and samples were taken from different locations on the stockpile. The sub samples with masses ranging from 50 kg to 100 kg were screened and an average size distribution determined.

Preliminary test experience demonstrated that screening was quit cumbersome. The area available for screening from self-made screens was too small and due to the thickness of the bars the rocks would jam between bars. It was decided that the screening process would become much less labour intensive if better equipment was used. Custom made wire mesh screens with apertures of 53 mm, 44 mm and 35 mm were ordered from Ludowici Meshcape. The mesh was 480 mm square and sheet metal was welded along the edges as seen in Figure 3-8. This allowed for the screen to fit over a rubbish bin as shown in Figure 3-9.

Figure 3-8: Custom made wire mesh screens

Figure 3-9: Screen on rubbish bin during sreening

The sample of gold ore was made up of 700 kg of waste rock, 100 kg of reef rock, and 57×20 kg of rod mill product. The rod mill product which is actually the feed to the pebble mill was simulated by further crushing of the ore. This gave a product with a top size of 3.3 mm. The fines were conveniently packed in 20 kg bags. Once again complete analysis of each bag was not possible so sub samples of a bag were taken using the cone and quartering method and the sample was screened to determine the per cent passing 75 µm. Various random samples of bags were also tested to check if the size distribution varied from bag to bag. The screen sizes used for the charge and the fines size distribution are shown in Table 3-1.

Table 3-1: Screen sizes used for sizing

Fines screen sizes (µm)	Charge screen sizes (mm)
3300	65
1180	53
425	44
300	35
212	28
150	16
106	11.2
75	3.3

The mill was then loaded with a distribution of waste rocks between 65 mm and 35 mm in size. The density of the gold ore was 2644 kg/m^3 and 132.27 kg of the ore ensured that mill was volumetrically filled to 30%. The feed to the mill consisted of 20 kg of rod mill product and 25 l of water. The mill was then run for 30 minutes at 83.5 % of the critical speed in order to pass the initial rounding phase of the rocks. After the first run the contents of the mill were screened using a 3.3 mm screen, in an effort to separate the fines. A screen size of 3.3 mm was chosen as an arbitrary split between fines and pebbles. A size distribution was performed on the +3.3 mm particles which were eventually returned to the mill. The -3.3 mm particles were discarded. The total mill charge was weighed and fresh make up added with a distribution of pebbles between 65 mm and 35 mm. A fresh sample of rod mill product was used for the next run which had duration of 30 minutes. This process was repeated until the mass of top up and the size distribution of the charge reached a steady state.

Now that the charge had reached a steady state, the next step was to determine the time of grind by producing a milling curve. As before fresh make up rock was added to rounded pebbles and a fresh sample of rod mill product used. A milling curve is basically a plot of milling time against per cent passing 75 μm. The mill was then run for 15 minutes at 83.5 % of the critical speed after which the pulp was passed through a 3.3 mm screen as before. However, now a particle size distribution (*PSD*) was done on the -3.3 mm particles in an effort to determine the per cent passing 75 μm. (For ease of understanding, the experimental procedure for the screening of fines will be discussed later). Now that the per cent passing 75 μm of fresh rod mill product (i.e. milling time of zero) and the per cent passing 75 μm after 15 minutes of milling was determined, an estimation of the required per cent passing 75 μm (i.e. 75%) was obtained by assuming a linear fit. The time required was estimated to be approximately 35 minutes which was the duration of the next run. The process was repeated and the per cent passing 75 μm was found to be 76.2%. The mill was now operating at the mines operating conditions producing approximately the correct per cent passing 75 μm.

The next step was to determine the specific wear rate of the rocks which was an important factor used in the model to predict steady state size distribution. The groove cutting method used in preliminary testing was not practical because the rocks were now a lot smaller. Instead, marking was achieved by spray painting rocks with different colours where each colour represented a different size fraction. The first step was to determine the specific wear rate of rounded waste rocks. Rounded waste rock was separated into various size fraction and random samples of rocks were taken from each size fraction. The rocks from each size fraction were then counted and

weighed in order to determine the average mass of a rock within that respective size fraction. The shape factor was also determined for the waste rocks. The rocks were then painted using an aerosol paint and left in the sun to dry for an hour as shown in Figure 3-10. The marks rocks were then milled for 35 minutes using the exact same procedure as mentioned before. After milling, the fines were discarded and each rock was washed and examined for remnant traces of paint in order to identify the size of the rock as shown in Figure 3-12. After all painted rocks were recovered, the rocks were recounted and reweighed and the average mass determined. Knowing the time of grind and the average mass loss of the rock within a given size fraction, a specific wear rate graph could be plotted for rounded waste rocks. This procedure was repeated for fresh waste rock in order to determine the specific wear rate during the initial rounding phase. The painted fresh waste rock is shown in Figure 3-11. In order to investigate whether the reef rocks and waste rocks wear at the same rate the entire process was repeated for rounded reef rocks.

Figure 3-10: Marked rounded rock ready for milling

Figure 3-11: Marked fresh rock ready for milling

Figure 3-12: Recovered rock showing remanant paint in grooves

3.2.3 Gold ore tests

The mill speed was first set by adjusting the gear ratio and timing the number of revolutions per minute (*RPM*) using a stopwatch. Once the speed is confirmed the *NLP* was determined. Rounded rock from a previous run was separated into size factions using the custom made screens. According to the prediction the mass of rock in each size fraction is set in order to simulate a charge size distribution that has already ‚reached steady state'. A portion of rounded rock from the feed size fraction is replaced by fresh rock. This is done in order to simulate the fresh pebble feed at the mine. A 20 kg sample of fresh rod mill product is added together with 25 litres of water and the mill is bolted shut. The mill and a stopwatch are then switched on simultaneously. The data logging system was then switched on. During operation the *RPM* was checked in order to ensure that the mill was operating at the correct speed. Each run had duration of 35 minutes as determined by the milling curve. For this section of testing the duration of each run was kept constant irrespective of operating conditions.

After 35 minutes both the mill and data logging system was switch off. The mill was then started and stopped quickly to set the door and drainage port in the correct position. The drainage plug was then opened allowing the pulp to pass through a 3.3 mm screen and collect in a plastic drum as shown in Figure 3-13.

Figure 3-13: Pulp exiting mill through drainage port

The rocks in the mill were then dug out by hand and rinsed in a bucket of water before being set aside. To ensure the maximum recovery of fines the inside of the mill was flushed with water to

removed remaining fine material. The water used to wash the rocks was added to the bucket containing the fines. The -3.3 mm particles were allowed to settle in buckets overnight so that excess water could be removed.

The pebbles were then screened and the mass of rock in each size fraction determined allowing for a size distribution to be obtained. The steady state size distribution of the pebbles was verified if the size distribution of the rocks after milling remained constant. Any -3.3 mm particles were returned to the bucket of fines.

Excess water was siphoned into another bucket using a hosepipe as shown in Figure 3-14. The fines were then mixed in order to remove particles stuck to the bottom. Ideally the most accurate option would be to screen the entire bucket of fines. This would be rather inconvenient and take a long time. A good representative sample that was small enough to handle was obtained by using a riffle splitter to split the ore as shown in Figure 3-15. Each time the ore is split the mass of the ore is halved. This splitting process was repeated five times to produce two identical samples weighing 32 (i.e. 2^5) times less than the original sample. Each sample was then wet screened through a 75 micron sieve placed on vibrating platform as shown in Figure 3-16. The -75 μm was pressure filtered to remove excess water as shown in Figure 3-17. The resulting -75 micron filter cake together with the +75 micron fraction from wet screening was placed in an oven together to dry overnight.

Once dry, a size distribution was done on the +75 micron fraction. Any -75 micron particles remaining were mixed with the -75 micron particles from pressure filtering and the total mass determined. This allowed for a per cent passing 75 μm to be obtained. This fine screening process was repeated on the duplicate sample so that an average could be obtained. This was considered as one run which took about three days to complete. Two runs were performed for each operating condition in order to determine the correct top up mass of fresh rock and have a duplicate run so that and average could be obtained.

The main variables tested in this work were mill speed and pebble feed size. Three different mill speeds were tested as well as one smaller feed size of pebbles. For ease of understanding the order in which these variables were tested are shown in Table 3-2.

Figure 3-14: Exccess water being shiphegnd off from pulp

Figure 3-15: Sample being split using a riffle slitter

Figure 3-16: Wet screenig on a vibratin jig

Figure 3-17: Pressure filtering eqiupment

Table 3-2: Testing order of mill speed and pebble feed size

Run I.D.	Pebble feed size (mm)	Mill speed (% critical)	Volumetric Filling (%)
Run 01a	65-35	83.5	30
Run 01b	65-35	83.5	30
Run 02a	44-28	83.5	30
Run 02b	44-28	83.5	30
Run 03a	44-28	75	30
Run 03b	44-28	75	30
Run 04a	65-35	75	30
Run 04b	65-35	75	30
Run 05a	44-28	69	30
Run 05b	44-28	69	30
Run 06a	65-35	69	30
Run 06b	65-35	69	30
Run 01c	65-35	83.5	30

3.2.4 Tests at 40% volumetric filling

The selection of a 30% volumetric filling was based on conservation of ore and limiting the effort involved in loading and unloading the mill. It was decided that a few more tests would be done at 40% volumetric filling to confirm the findings on pebble size. It was assumed that the rate of consumption of pebbles would be proportional to pebble mass and power/pebble mass. This provided an accurate estimate and a duplicate run was only performed if the actual wear rate was not the same as predicted. The time required for milling was determined by keeping the energy input per kg of fine material entering constant for each corresponding mill condition. This was done by running the mill at a given speed for 22 minutes while measuring the power. The time interval used was arbitrary but sufficient enough to ensure relatively constant power consumption. The mill was then stopped and according to the power used the time was recalculated assuming a constant *kwh/t* of fine material entering for that same speed at a lower filling. A sample calculation of the recalculated time is available in Appendix C. After running

for the recalculated time the mill was stopped and the contents emptied. The entire screening process was then repeated on the pebbles and the fines. The order for this testing procedure is shown in Table 3-3.

Table 3-3: Testing order at higher volumeteric filling

Run I.D.	Pebble feed size (mm)	Mill speed (% critical)	Volumetric Filling (%)
40 Run 01	44-28	83.5	40
40 Run 02	44-28	75	40
40 Run 03	44-28	69	40
40 Run 04	65-35	69	40
40 Run 05	65-35	75	40
40 Run 06	65-35	83.5	40

3.3 Volumetric filling and Speed Testing

The effect of volumetric filling and speed on the power draw is well known. However most tests use data from small mills which are not very accurate. This work gave an opportunity to test these variables on a large scale.

3.3.1 Experimental Procedure

The same 1.2 m diameter mill used for previous test work was used to test these variables. The mill speed was first set to 69% critical. The next step involved the loading of 132 kg of rocks with a similar size distribution as used before to ensure a mill volumetric filling of 30%. The power measuring system, the stopwatch and the mill were then switched on simultaneously. In order to generate sufficient data points the mill was run for two minutes for a given set of operating conditions. The power measuring system was then paused to allow for the change of mill speed. During this time the stopwatch was kept running in order to measure the total time spent at a given speed. The speed was considered to be changed when the required *RPM* of the mill was verified. The time was noted while the power measuring system and the stopwatch was restarted. This procedure was repeated for different critical speeds up to 90% critical.

The time measuring procedure was done in order to determine the approximate time spent at each speed. Since wear rate is a function of mill speed and volumetric filling the total wear from the test at 30% filling was estimated by summing the wear at each speed. It is important to note that the wear rate also increases proportionally with volumetric filling. This allowed for the wear rate at higher volumetric filling to be calculated by the ratio of the wear rate at 30% volumetric filling. In order to return the volumetric filling to 30% the rocks that were worn away were first replaced. The filling was increased to 40% by the addition of about 50 kg of rocks. There is a proportional increase in fines and water, however one has to account for the fact the rocks wear into fines. The mill was now 40 % filled at 90% critical speed. The speed changing procedure was repeated for the new filling for different critical speeds down to 69%. The order of the test procedure is shown in Table 3-4.

Table 3-4: Order of testing

Run I.D.	Volumetric Filling (%)	Mill speed change (% critical)				
svRun 1	30	69	75	80	85	90
svRun 2	40	90	85	80	75	69
svRun 3	45	69	75	80	85	90
svRun 4	50	90	85	80	75	69
svRun 5	55	69	75	80	85	90

3.4 Comparison to steel balls

The comparison tests were conducted a smaller mill will an internal diameter of 0.3 m and length of 0.3 m as shown in Figure 3-18. The mill was rotated using a 1 BhP variable speed DC motor. The shell of the mill was made using mild steel with eight lifters fitted. The power measuring systems and its calibration worked on the same principle as before. The results of the static calibration of the power measuring equipment are available in Appendix B.

3.4.1 Experimental procedure

Rounded rocks from previous work were screened into various fractions. A steady state size distribution when feeding 44/28 mm pebbles was simulated. As before some of the rounded rock in the feed size range was replaced with fresh rock to simulate continuous top up. The mill was filled to 40% by volume which amounted to 11.2 kg of rocks. The required mass of fines was 1.69 kg and 2.16 litres of water was added. Since the rod mill samples were in 20 kg bags a riffle was used to split the sample in order to obtained smaller representative sub samples of the required mass.

The pebbles were charge into the mill and the door bolted shut. The fines and water were mixed together and fed through a port in the middle of the mill endplate using a funnel. The need for a grinding curve was eliminated by ensuring that the energy input per mass of fine material entering was kept constant when compared to the 1.2 m diameter mill. This was done by running the mill at a given speed for 5 minutes while measuring the power. The mill was then stopped and according to the power used the time was recalculated assuming a constant *kwh/t* of fine material entering. After running for the recalculated time the mill was stopped and the contents emptied. As before a size distribution was performed on the pebbles in order to determine the wear rate and a particle size distribution was performed on the fines in order to determine the per

cent passing 75 μm. The run was repeated in order to determine the correct fresh rock top up and so that an average can be obtained.

The next step was to compare the efficiency of the pebbles to steel balls. An exact size distribution of steel balls was made up as shown in Figure 3-19. The mass was higher but the mass fraction in each size range was identical. The same procedure for pebbles was then repeated using steel balls. Again two runs were performed so that an average can be obtained.

Figure 3-18: Setup of the 0.3 m diameter mill

Figure 3-19: Various size fractions of pebbles and steel balls

4. RESULTS AND DISCUSION

4.1 Preliminary test work

Preliminary testing on a local quartzite ore gave an opportunity to investigate how rocks of different sizes are worn away. Doing this for the entire load would be very inconvenient due to the large mass present in each size fraction so instead a method of rock tagging was employed. It is important that the tagging process not affect the characteristics of the rocks. After milling, the original size of a rock could be identified by the type of pattern cut into it. Even if a rock were to leave a size interval and drop to a size range down or further the marking on the rock would reveal the size range from which the rock was originally in. In the event of complete breakage (referred to as cleavage) the rock was discarded from the data set. This was because the breakage event was probably due to direct impact on a lifter. The probability of cleavage was found to be relatively low.

The number of samples provided a sufficiently large data set. This coupled with the number of repeated runs allowed the average mass of a rock in a given size, both before and after milling to be determined quite accurately.

The mass fraction remaining is the ratio of the remaining average mass to the original average mass. The results for each size fraction are shown in Figure 4-1, Figure 4-2 and Figure 4-3 respectively. The change in average mass as a function of time for all size fractions is shown in Figure 4-4.

The graphs demonstrate two stages each with different grinding rates. During the first 15 minutes an increase in the grinding rate is observed. This is due to the fact that fresh rocks have a lot of sharp edges and planes of weakness that are broken of relatively quickly. This initial rounding process, often referred to as fast chipping, results in a central core which wears away at a relatively constant rate (note the slope of the dotted lines is about 0.0011 min^{-1}). The cores are relativity strong and are worn away due to abrasion and slow chipping. This causes a slower wear rate which remains constant with time and even with size as shown by Figure 4-1, Figure 4-2 and Figure 4-3. However as the core reaches certain size the rate of wear shoots up as the smaller cores are crushed by larger rocks.
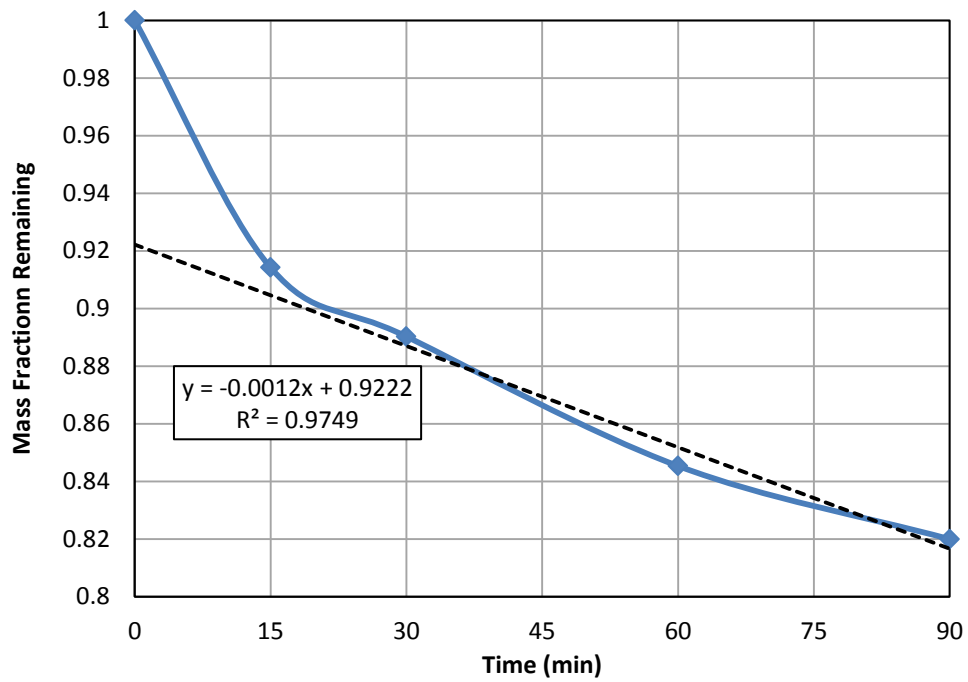
Figure 4-1: Mass fraction remaining for 75/65 mm rocks

$y = -0.0012x + 0.9222$
$R^2 = 0.9749$
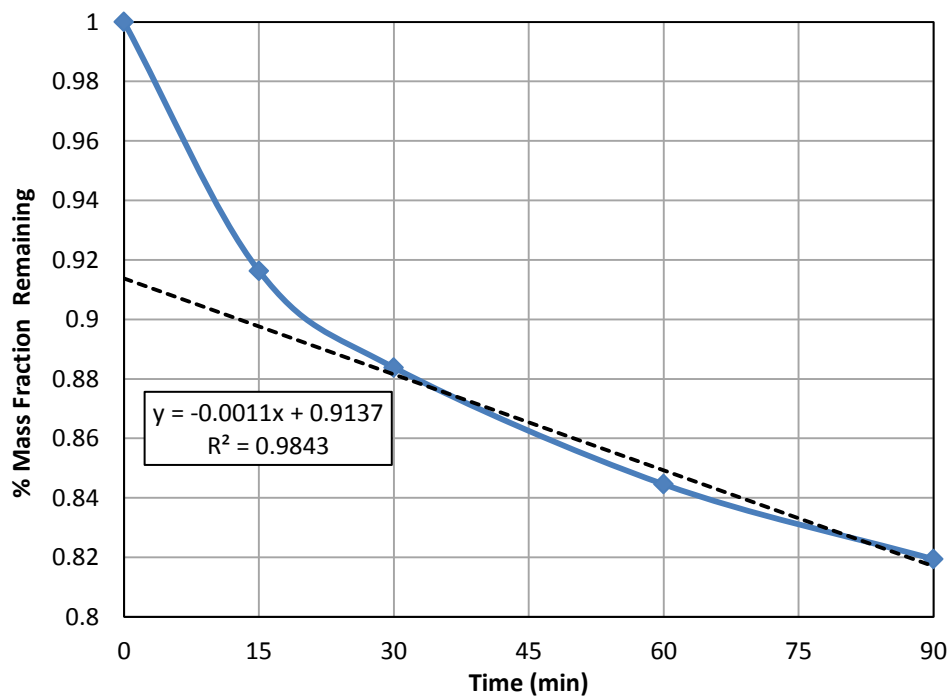
Figure 4-2: Mass fraction remaining for 65/53 mm rocks

$y = -0.0011x + 0.9137$
$R^2 = 0.9843$

57
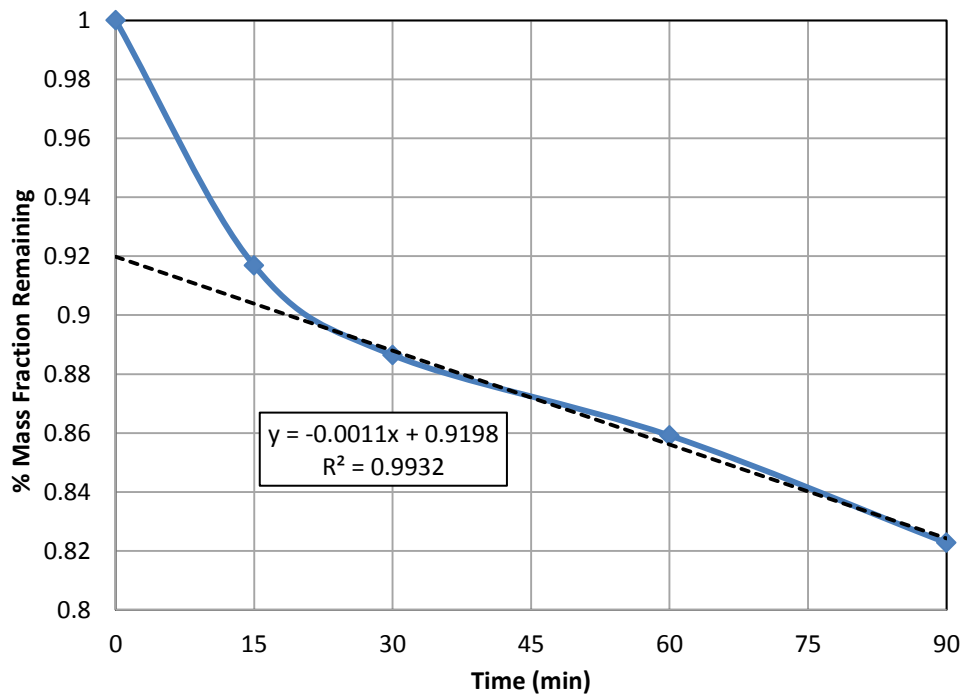
Figure 4-3: Mass fraction remaining for 53/37.5 mm rocks
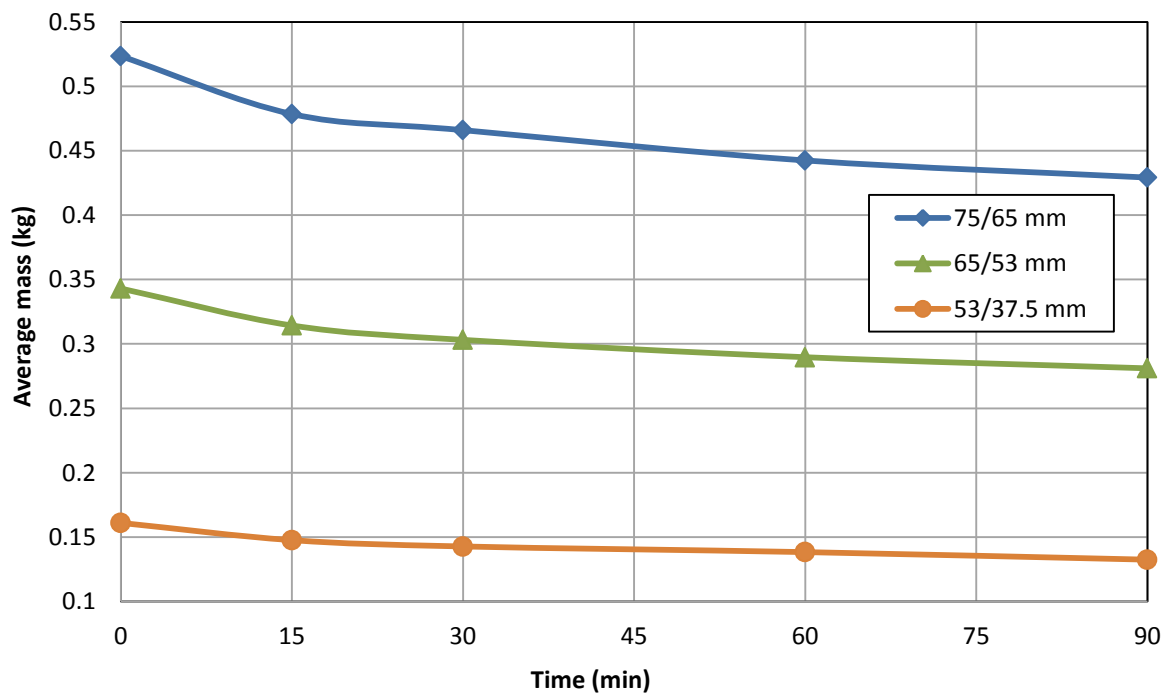
Figure 4-4: Average mass vs Time

At this stage the results indicated that the smallest average particle size tagged was still within this constant wear region. Smaller particles needed to be tracked in order to find this transition zone. The method of tagging rocks by cutting grooves into the surface was useful as it allowed

58

for multiple runs to be performed without retagging after each run. However, for smaller rocks this method was not practical. The size of the rocks made it difficult to tag and it was evident that the tagging procedure would create planes of weakness thus affecting the characteristics of the rocks. Spray-painting was used as an alternative method of measuring the wear of samples of the smaller rocks. A different colour was used to identity each size range. The smaller size ranges were 37.5/26.5 mm, 26.5/22.4 mm, 22.4/16 mm.

Figure 4-5 is a graph showing the specific wear rate as a function of average size in screen fractions for various types of rocks. The specific wear rate is defined as the rate of mass loss per unit mass. It shows how fast a rock is abraded away relative to its own mass. The graph shows that larger rocks have a relatively constant specific wear rate. However for a rock size around about 45 mm a change in the trend is observed. A rapid increase in the specific wear rate is observed in a relationship that is inversely proportional to size. The trends observed are similar to that published by Loveday and Whiten (2002). The authors tested ore on a pilot plant scale obtaining specific wear rates between 0.0025 min^{-1} and 0.0033 min^{-1}. The difference between the two graphs demonstrates the initial fast chipping phase. The fact that the two graphs are equidistant from each other throughout the size range shows that a change in trend at this same size is also observed during the fast chipping phase.
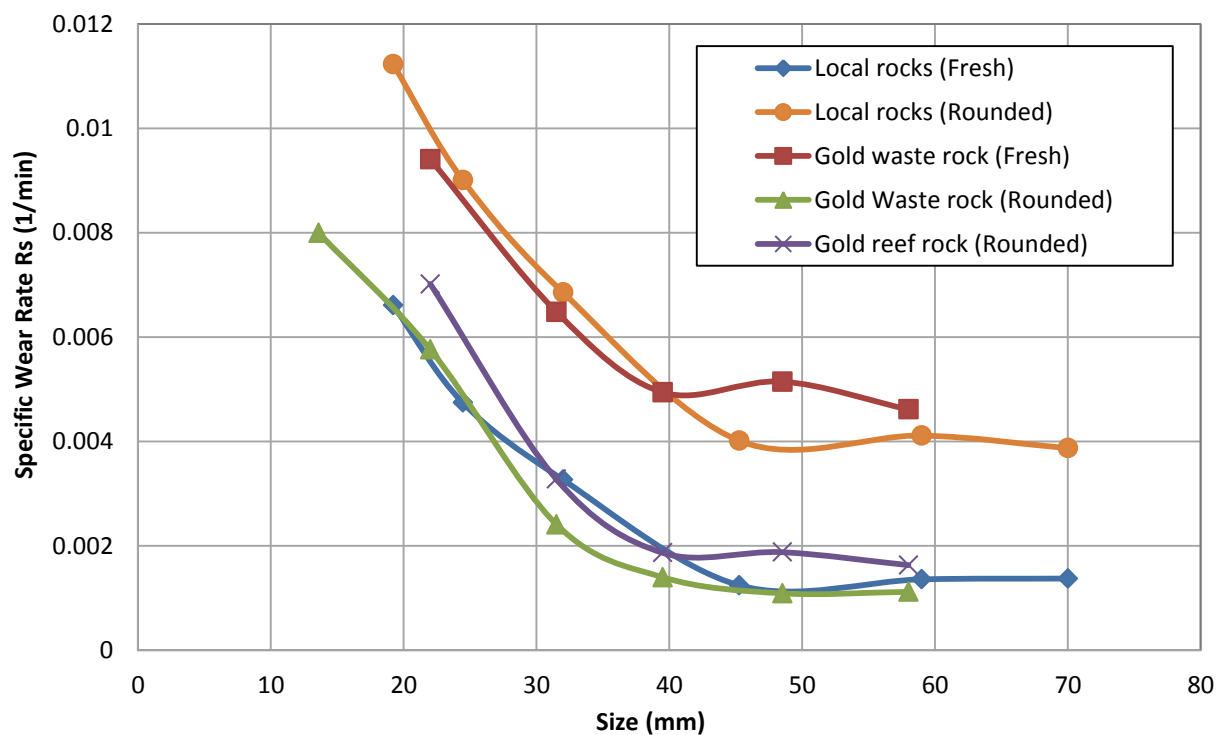
Figure 4-5: Specific wear rate for various types of rocks

59

The method of marking the larger rocks enabled the size distribution of marked rock to be tracked as it is worn away. The combined size distribution of the marked is shown in Figure 4-6. The graph shows that for any given feed size distribution the charge will reach a constant size distribution. The irregular shape of the fresh rock sometimes caused a rock to be held up in an ‗inœrrect' size fraction. This is quickly corrected by the fast chipping phase which as mentioned breaks off sharp edges and planes of weakness. This allows a rock that was previously held up by a sharp edge to enter a smaller ‗œrrect' size fraction. This phenomenon is evident in Figure 4-6. It can be seen that the feed size distribution changes rapidly during the first 15 minutes. After that the rocks enter the second phase of wear and thus the gradual change in size distribution. The main mechanism during this phase is abrasion which is defined the detachment fine material from the surface of larger rocks. Although this process is a relatively slow one it may still cause a large mass to leave a size fraction and thus cause a change in size distribution. This occurs when a rock is close to the lower limit in a size range. Figure 4-6 shows how the gradually change size distribution until a constant size distribution is achieved. It is important to note that this constant size distribution is not a steady-state size distribution because the marked rock was not topped up continually.
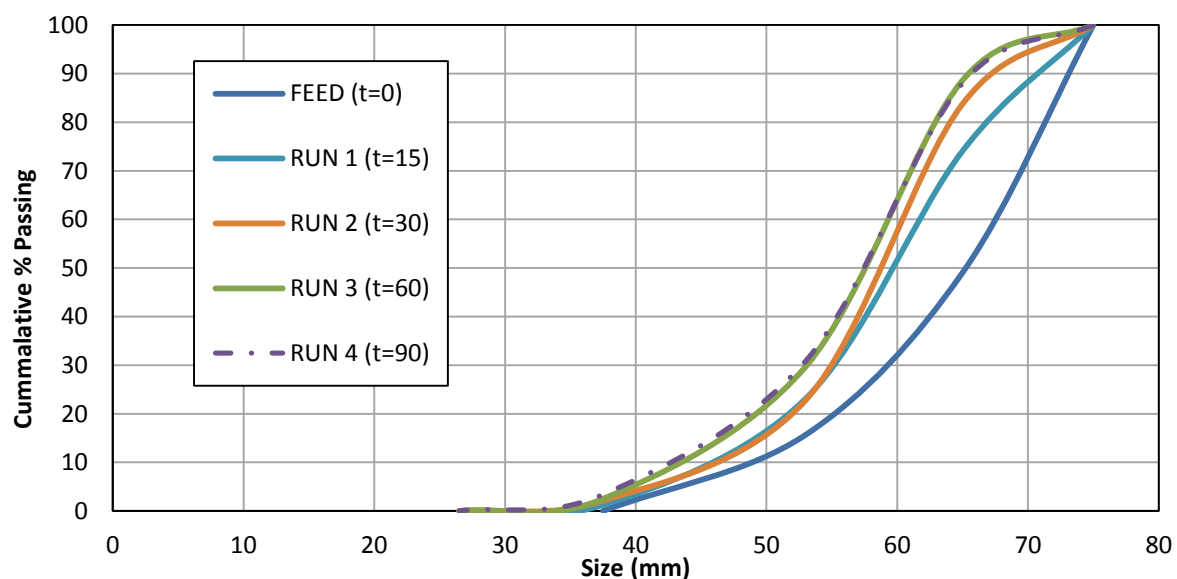
Figure 4-6: Change in size distribution with time

A visual examination of the screened charge, was used to determine the size at which pebbles no longer exists. Table 4-1shows that between 16-11.2 mm, some fracture occurs, while below 11.2 mm, no rounded pebbles were found. Thus 11.2 mm was the taken as the lower limit for pebbles and particles between 11.2-3.3 mm were considered to be chips or scats. A large proportion of

these chips are progenies of the fast chipping phase. In a closed circuit the inability to deal with these chips results in an accumulation of chips which may be detrimental to the grinding process.

The average mass allowed the shape factor of the rocks to be traced as a function of time. The shape factor is a good indicator of the rounding procedure of fresh rock. The general idea is shown in Figure 4-7. Figure 4-8 is a plot of shape factor versus time, combining all tagged rocks in the selected size fraction. This plot shows how rocks of a fixed ‗size' change shape and hence mass. The rapid shift in the shape factor is due to a rapid change in the rocks average mass. This rapid change takes place during the fast chipping phase and is the probable reason for sudden changes in the charge size distribution. The anomaly observed at the 75/65 mm fraction is thought to be due to the fact that it represents the largest feed size fraction where rocks may leave the size fraction but may not enter since new feed is not added.
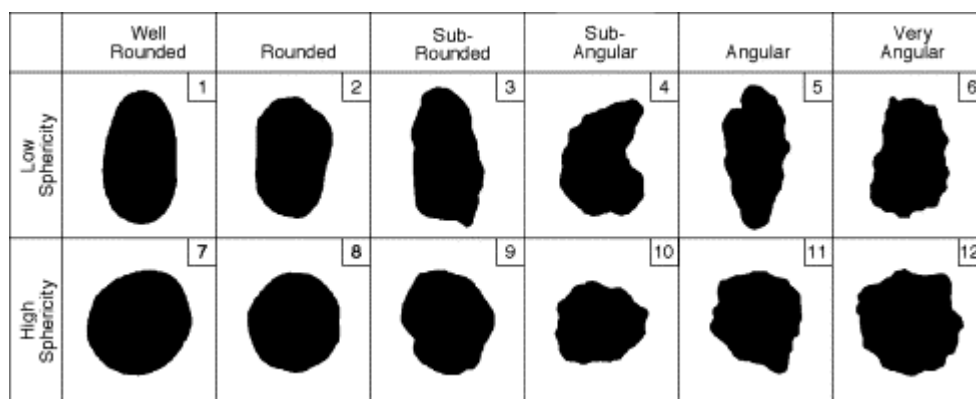
Figure 4-7: Rounding of fresh rock (MacLeod, 2002)
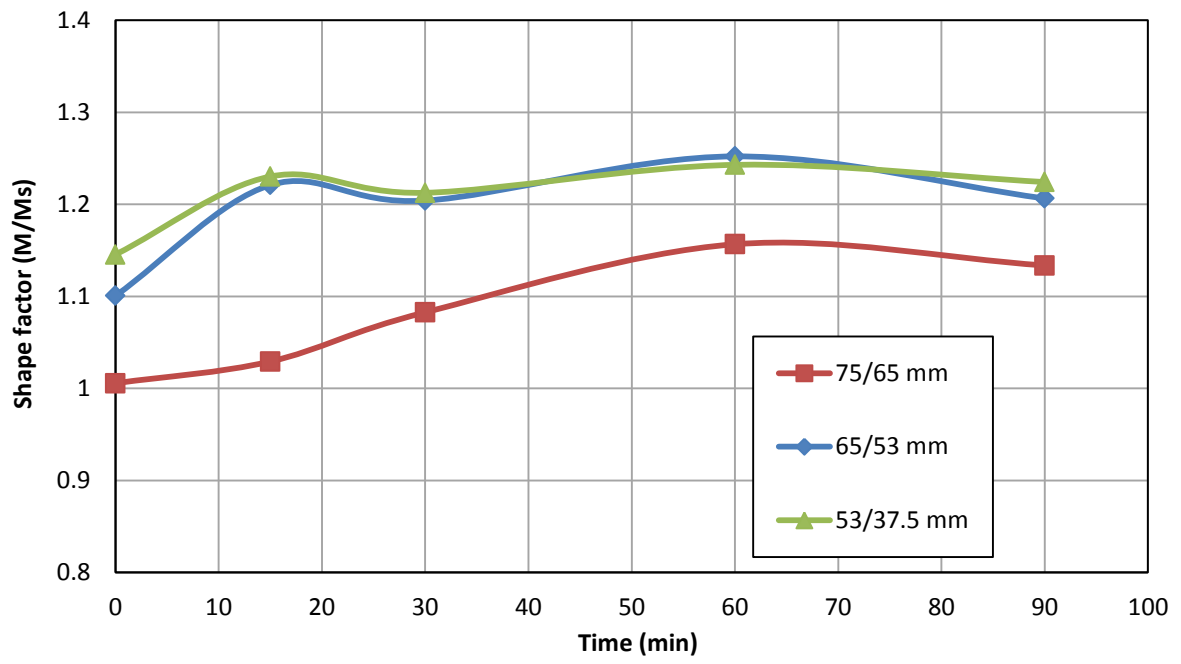
Figure 4-8: Combined change in shape factor for various size fractions

Size Range (mm)	Image	Observation
37.5-26.5		Pebbles present
26.5-22.4		Pebbles present
22.4-19		Pebbles present
19-16		Pebbles present
16-11.2		Pebbles present with some fracture
11.2-3.3		No rounded pebbles present

4.2 Preliminary tests on gold ore

The natural size distribution exiting the crusher at Mintek is shown in Figure 4-9. The closed side setting was kept constant so that the size distribution matched the mines size distribution.

Using the cone and quartering method a good representative sample for size analysis was obtained. Figure 4-10 represents the average size distribution of the product produced by Mintek using fine crushing and screening at 3.3 mm to simulate the rod-mill product.
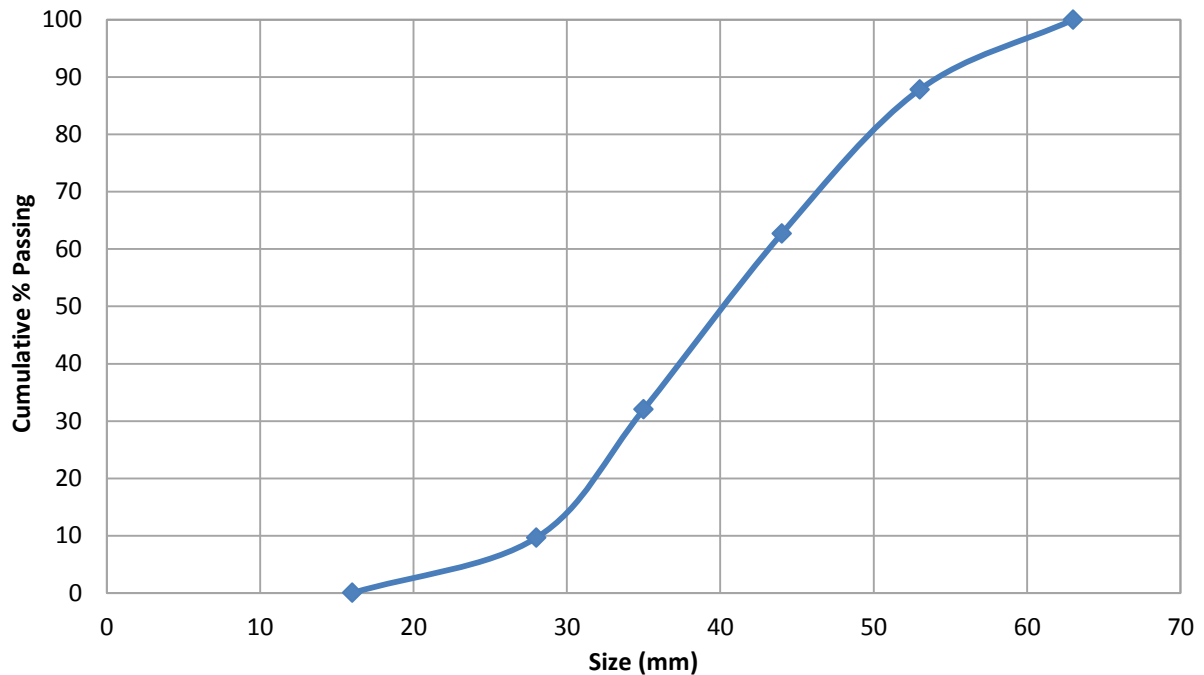
Figure 4-9: Natural size distribution of rocks from crusher
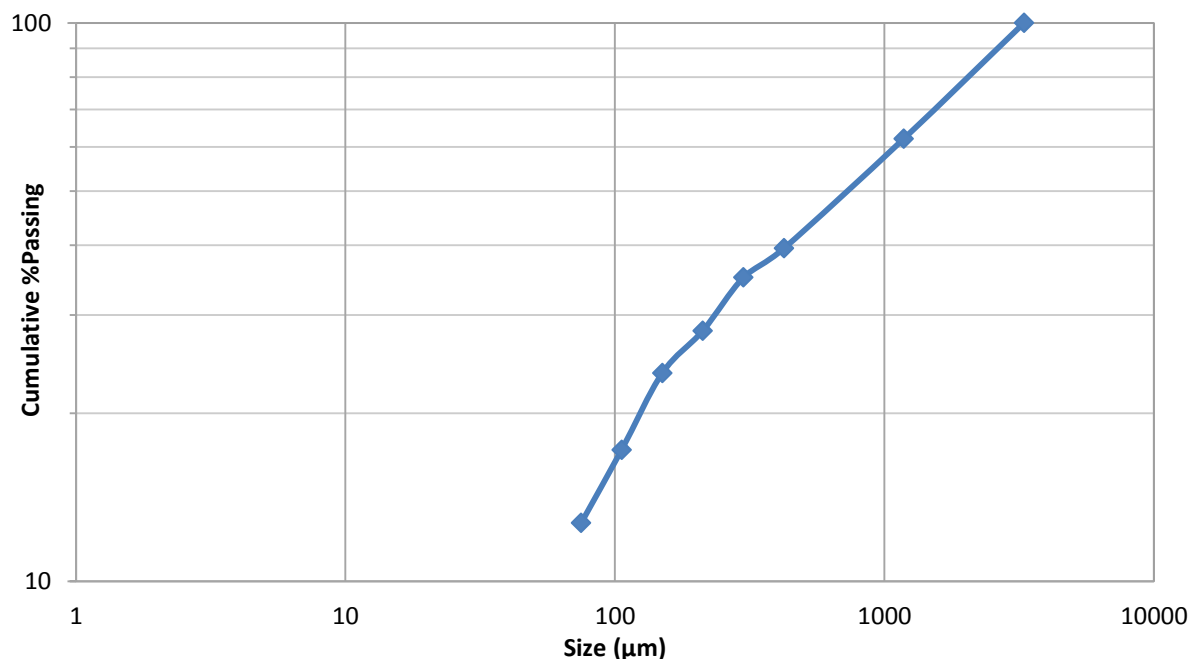
Figure 4-10: Size distribution of simulated rod mill product

The mill was filled to 30% by volume which was a manageable amount of material to load and unload, and it provided more cascading in the milling action. In order to have a base case to which all runs could be compared to, the first task was to replicate the mines operating conditions while trying to reproduce the results. By periodically feeding pebbles between 65/35mm the rate at which the pebbles are fed eventually reaches a steady state. The mass of fresh top up rock as function of time is plotted in Figure 4-12. It can be seen that during the fast chipping phase (which last around 30 minutes) a peak in feed rate is observed after which the rate of top up remains relatively constant. This change in top up of fresh rock, until a steady state is reached is related to the change in size distribution of the charge until a steady state size distribution is reached as shown in Figure 4-11. It can be seen that during the first 30 minutes the size distribution changes rapidly as mentioned earlier. This corresponds to the rate of top up of fresh rock. After this phase the rocks wear away at a constant rate as is evident in both Figure 4-11 and Figure 4-12.
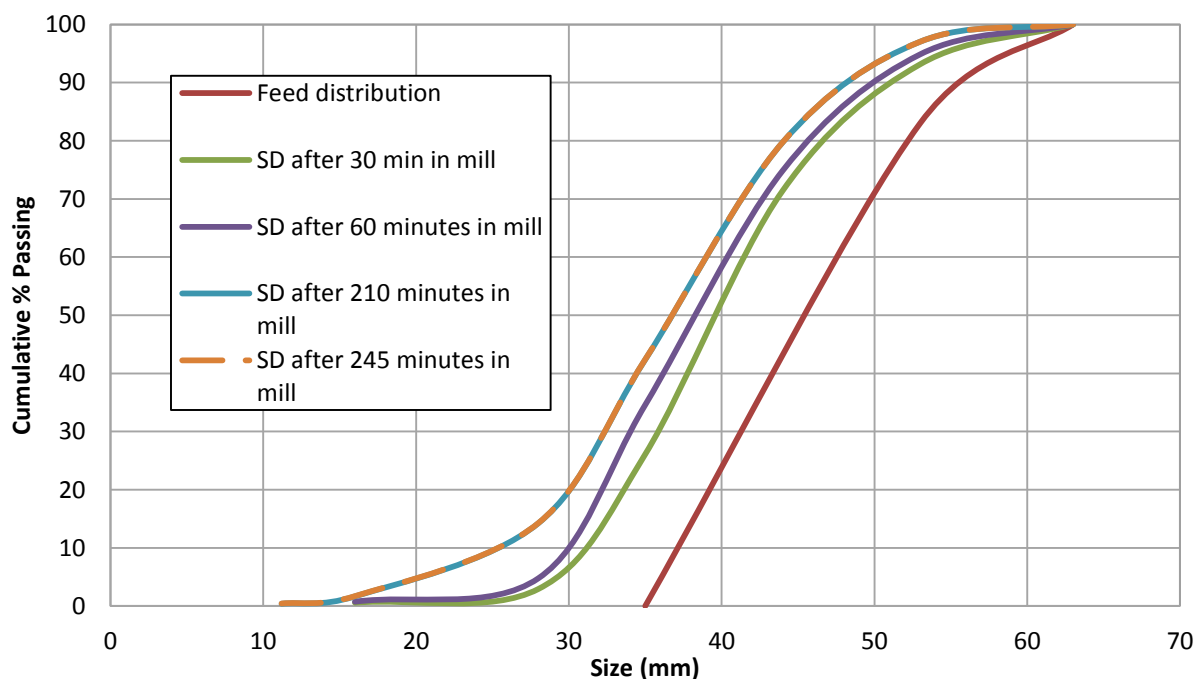
Figure 4-11: Size distribution vs time
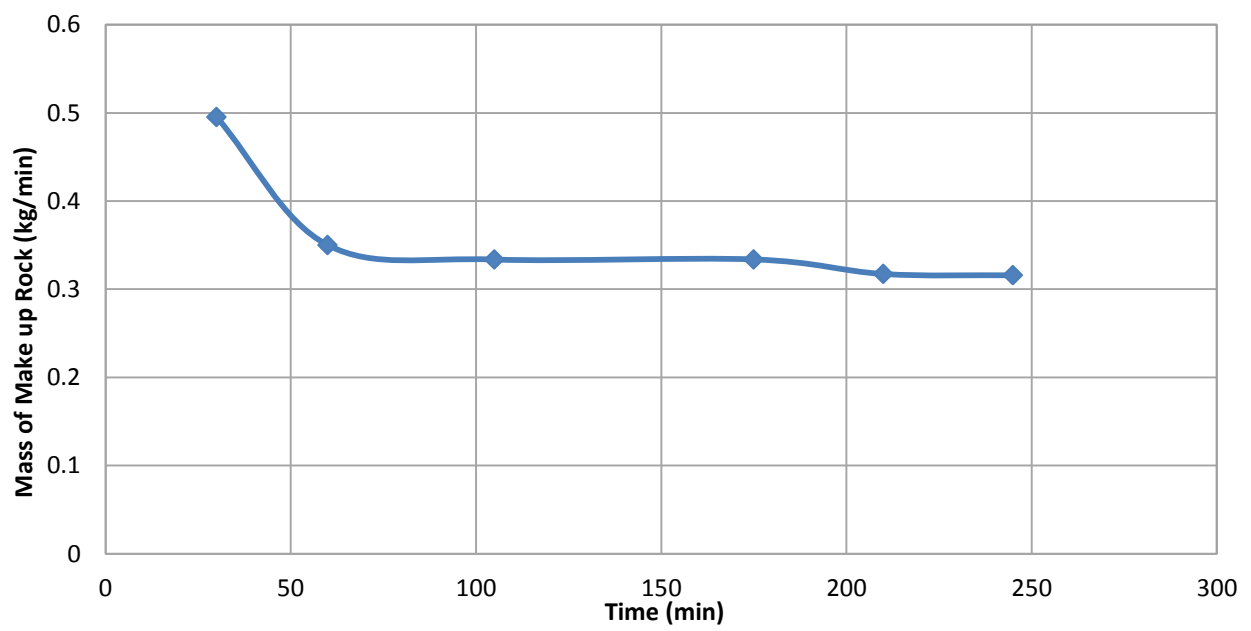
Figure 4-12: Rate of make-up rock as charge reaches steady state

The milling curve obtained for this ore under these milling conditions is shown in Figure 4-13. The target grind of 76.2% passing 75 µm was obtained in 35 minutes. Hence, for this section of testing all runs had a duration of 35 minutes.
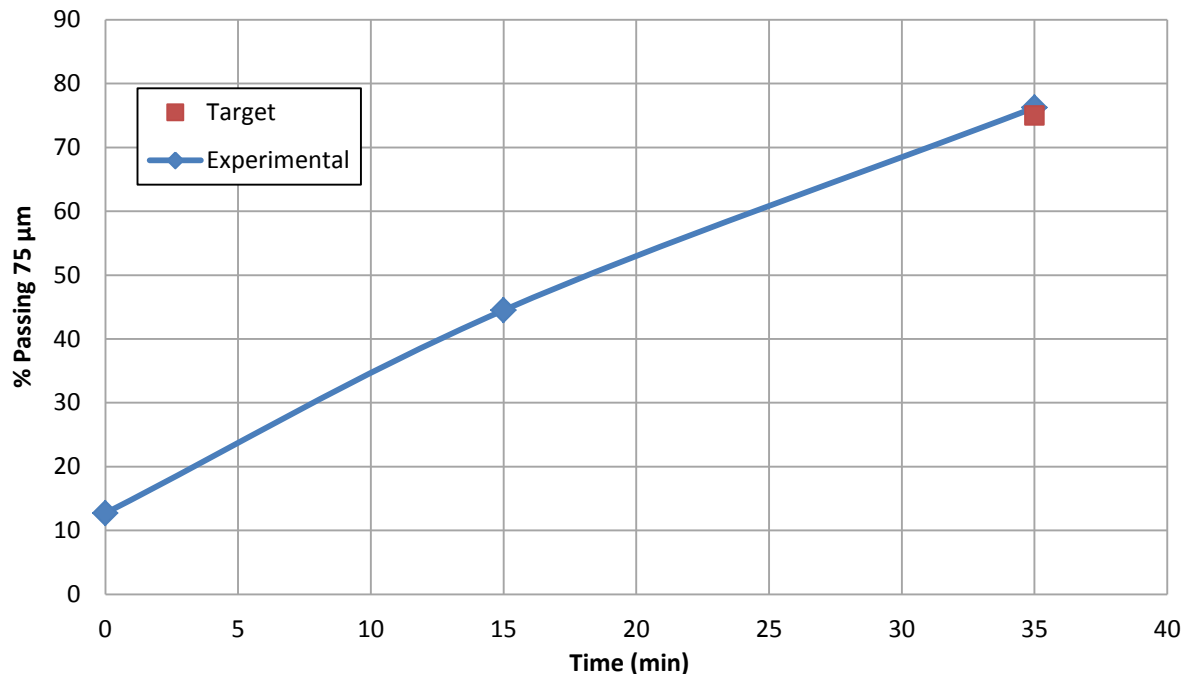
Figure 4-13: Milling curve

The preliminary work on rock wear generated an adequate stock of rounded pebbles. The rounded pebbles were mainly waste rock but also had some reef rocks that were deliberately fed with the fresh top up. This was done because at the mine during the transportation of ore, some gold bearing reef rock gets misplaced with the waste rock. The specific wear rate was determined for rounded waste rock, rounded reef rock and fresh waste rock. The spray painting technique was chosen over the angle grinding technique for tagging as the former is less labour intensive and causes no damage to the rocks. The specific wear rate as a function of size is plotted in Figure 4-5. The specific wear rates of rocks from the local quarry are also shown. The trends observed for both waste and reef rocks are similar to that obtained for the local ore. The data for ore, reef and local quarry rock is approximately the same, with a distinct difference between fresh rock and rounded rock. The point at which the slope changes could be an indication of some intermediate sized rock. Rocks below this size are wearing away faster and are less likely to accumulate in the charge.

The fast chipping phase of the fresh rock for both waste rock and local ore is also displayed in Figure 4-5. The larger fresh waste rock loses more mass during the fast chipping phase than similar sized fresh local ore. This was expected as a visual examination revealed that the waste

rock had much more sharper edges than the local ore. This may be an influence of the different closed side settings of the crusher from which the respective ore came from. It also may be attributed to the characteristics of the different type of ore.

4.3 Model for predicting steady state pebble size distribution

A locked cycle test is very useful when simulating a continuous system and mimicking steady state. The problem is that many cycles are needed before steady state is reached. Apart from this being resource consuming, it may also be time consuming requiring an inconveniently large amount of work to be done by an operator. The main aim of the locked cycle test in this work was to determine the steady state size distribution of the charge for a given pebble feed size. The problem with this is that a steady state size distribution is highly dependent on the pebble feed size. This implies that for every change in pebble feed size a new steady state size distribution would be required. It was thus decided that in the interest of this work and future work to come that a simple empirical model be developed to predict steady state size distribution for a give pebble feed size. This model would be a resource and time saving tool. It would thus allow future work to test various size distributions without requiring large amount of ore.

The model is very empirical and makes many assumptions which imply that it may not be able to predict steady state correctly. However since the testing is actually done, if steady state was predicted incorrectly, the predicted size distribution will only help steady state to be reached sooner. The method of predicting the steady-state size distribution will be explained below.

In order to predict the size distribution for a given ore type three pieces of information was needed. The first parameter required in the model was the specific wear rate (R_s) function. This data was available from earlier test work. (See Figure 4-5)

The second piece of information required, dealt with the size distribution of the feed. Since locked cycle tests were already performed using a pebble feed size of 65/35 mm and steady state charge size distribution data available, the model was first used to predict the steady state size distribution with a 65/35 mm pebble feed size. The feed size distribution of rocks between 65/35 mm was determined by screening carefully selected samples and is shown in Figure 4-14 and Table 4-2.
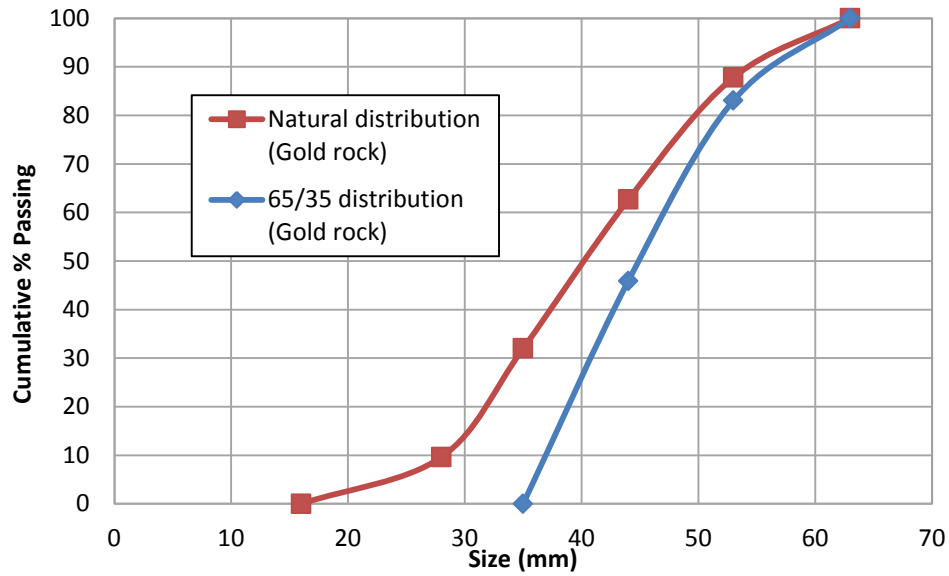
Figure 4-14: Size distribution of rocks between 65/35 mm.

Table 4-2: Natural size distribution of rocks between 65/35 mm

Size (mm)		Mass (kg)	Mass %(mf)	% Passing
65	53	7.75	16.94	100
53	44	17	37.16	83.06
44	35	21	45.90	45.90
35	28	0	0	0
28	16	0	0	0
16		0	0	0
		45.75		

The third parameter used in the model was the shape factor (*SF*). As discussed earlier the shape factor for a group of rocks in a given size fraction is defined as the ratio of the rocks average mass to that of a sphere that has a radius equivalent to the average of the top and bottom size fractions. This required the average mass of the rocks in a size fraction be determined by counting as many rocks as possible and weighing the total mass. This then allowed a shape factor of the rocks in every feed size fraction to be determined as follows:

The initial average mass (i.e. *t=0*) of a rock originally from size interval *i* is given by:

$$m_{0,i}^{av} = \frac{m_i^{TS}}{n_i^{S}} \qquad (4.1)$$

Where

$m_{0,i}^{av}$ = Initial average mass of a rock originally from size interval i. (kg)

m_i^{TS} = Total mass of sampled rocks originally from size interval i. (kg)

n_i^s = Number of rocks in sample

The relationship between the mass of a sphere at time t originally from size interval i and diameter of that same sphere is given by:

$$m_{t,i}^s = \frac{\pi \times \left(d_{t,i}^{av}\right)^3}{6} \times \rho_{rock} \qquad (4.2)$$

Where

$m_{t,i}^s$ = Mass of a sphere from size interval i. (kg)

$d_{t,i}^{av}$ = Diameter of a sphere at time t originally from size interval i. (m)

The mass of a reference sphere that has a radius equivalent to the average of the top and bottom size of interval i was determined as follows:

$$m_i^{shpere} = \frac{\pi \times (d_i^s)^3}{6} \times \rho_{rock} \qquad (4.3)$$

Where

m_i^{shpere} = Mass of a reference sphere from size interval i. (kg)

ρ_{rock} = Density of rock (kg/m^3)

d_i^s = Arithmetic average of the limits of size interval i (m) given by:

$$d_i^s = \frac{d_i^{top} + d_i^{bottom}}{2} \qquad (4.4)$$

Where

d_i^{top} = Upper limit of the size interval i (m)

d_i^{bottom} = Lower limit of the size interval i (m)

Assuming that the rock size initially starts at the average size of interval i then:

$$d_i^s = d_{0,i}^{av} \tag{4.5}$$

Where

$d_{0,i}^{av}$ = Initial average diameter of a rock originally from size interval i. (m)

This assumption implies that:

$$m_{0,i}^s = m_i^{shpere} \tag{4.6}$$

$m_{0,i}^s$ = Initial average mass of a rock originally from size interval i. (kg)

The shape factor is now the ratio of the average mass to the mass of a sphere and was determined as follows:

$$SF_{t,i} = \frac{m_{t,i}^{av}}{m_{t,i}^s} \tag{4.7}$$

Where

$SF_{t,i}$ = Shape factor of rocks at time t originally from size interval i.

So the initial SF is given by:

$$SF_{0,i} = \frac{m_{0,i}^{av}}{m_{0,i}^s} \tag{4.8}$$

Where

$SF_{0,i}$ = Initial shape factor of rocks at time t originally from size interval i.

Now that specific wear rate, the feed size distribution, and the SF of the rocks are known it is first assumed that 100 kg of rocks initially enter the mill. This mass enters in different fractions (m_i^{feed}) as determined from the size distribution tabulated in Table 4-2. This allows the total initial mass ($t=0$) in a given size fraction to be determined as follow:

$$m_{0,i}^T = 100 \times m_i^{feed} \tag{4.9}$$

Where

$m_{0,i}^T$ = initial total mass of rocks in model originally from size interval i. (kg)

m_i^{feed} = mass fraction of rocks from size interval i in feed

The total number of rocks in the model at any given time t originally from size interval i is given by:

$$n_{t,i}^m = \frac{m_{t,i}^T}{m_{t,i}^{av}}$$ (4.10)

Where

$n_{t,i}^m$ = number of rocks in model at time t originally from size interval i.

$m_{t,i}^T$ = Total mass of rocks at time t originally from size interval i. (kg)

So the initial average mass ($t=0$) originally from size interval i as determined from equation 4.1 allows the initial number of pebbles in model originally from size interval i.

$$n_{0,i}^m = \frac{m_{0,i}^T}{m_{0,i}^{av}}$$ (4.11)

Where

$n_{0,i}^m$ = Initial number of rocks in model originally from size interval i.

Using the total mass of rocks at time t originally from size interval i, the specific wear rate (R_s) was used to determine the total mass at next time interval. The specific wear rate (R_s) is a function of time, rock diameter and charge size distribution. The introduction of a specific wear rate correction factor (k_s) is used to account for the variation of specific wear with charge size distribution. A detailed explanation of the specific wear rate correction factor is given in Chapter 4.4.

$$m_{t+1,i}^T = m_{t,i}^T - m_{t,i}^T \times k_s R_S\big(t, d_{t,i}^{av}\big) \times \Delta t$$ (4.12)

Where

$m_{t+1,i}^T$ = Total mass of rocks at time $t+1$ originally from size interval i. (kg)

R_S = Specific wear rate as determined from rock tagging procedure (1/min)

k_s = Specific wear rate correction factor.

Δt = Time increment (min)

Assuming the total number of rocks in model remains constant then:

$$n_{t+1,i}^m = n_{t,i}^m = n_{0,i}^m \qquad (4.13)$$

Where

$n_{t+1,i}^m$ = number of rocks in model at time $t+1$ originally from size interval i

This then allowed the total mass of rocks at time $t+1$ originally from size interval i to be converted to an average mass at time $t+1$ originally from size interval i.

$$m_{t+1,i}^{av} = \frac{m_{t+1,i}^T}{n_{t+1,i}^m} \qquad (4.14)$$

Substituting equation 4.13 into equation 4.14 gives

$$m_{t+1,i}^{av} = \frac{m_{t+1,i}^T}{n_{0,i}^m} \qquad (4.15)$$

Where

$m_{t+1,i}^{av}$ = Average mass of rocks at time $t+1$ originally from size interval i. (kg)

A relationship between mass and diameter is quite simple for steel balls which are essentially spheres. When it comes to pebbles the shape of the rock makes this relation much more complex. In order to convert the average mass of a rock into an average diameter the *SF* was introduced. Preliminary shape factor testing revealed that the SF is a function of time and particle size. Using this data a shape factor model was generated which then allowed the average mass to be converted to an average diameter as shown below:

$$SF_{t,i} = f_{SF}(t, i) \qquad (4.16)$$

Where

$f_{SF}(t, i)$ = Shape factor function for rocks originally from size interval i evaluated at time t

$$SF_{t+1,i} = f_{SF}(t + 1, i) \qquad (4.17)$$

Where

$SF_{t+1,i}$ = Shape factor of rocks at time $t+1$ originally from size interval i.

$f_{SF}(t+1,i)$ = Shape factor function for rocks originally from size interval i evaluated at time $t+1$

Using the definition of the SF (equation 4.7) at the next time increment $t+1$ gives:

$$SF_{t+1,i} = \frac{m_{t+1,i}^{av}}{m_{t+1,i}^{s}} \qquad (4.18)$$

Where

$m_{t+1,i}^{s}$ = Mass of a sphere (kg) from size interval i given by:

$$m_{t+1,i}^{s} = \frac{\pi \times \left(d_{t+1,i}^{av}\right)^3}{6} \times \rho_{rock} \qquad (4.19)$$

Where

$d_{t+1,i}^{av}$ = Diameter of a sphere at time $t+1$ originally from size interval i. (m)

Substituting equation 4.19 into equation 4.18 gives:

$$SF_{t+1,i} = \frac{m_{t+1,i}^{av}}{\frac{\pi \times (d_{t+1,i}^{av})^3}{6} \times \rho_{rock}} \qquad (4.20)$$

Rearranging and solving for the average diameter at next time interval gives:

$$d_{t+1,i}^{av} = \sqrt[3]{\frac{6 \times m_{t+1,i}^{av}}{SF_{t+1,i} \times \rho_{rock} \times \pi}} \qquad (4.21)$$

This procedure was repeated for i size fractions present in the feed size distribution for a given period of time until average diameter became less than 3.3 mm. This is the size which separates the rocks from the fines. After all size fractions wear modelled the total mass of rocks in each size interval i was determined by summing the total mass of rock in every size interval which has an average diameter between the upper and lower limits of size interval i

$$M_i^p = \sum_t \sum_i \left[m_{t,i}^T\right]_{d_i^{bottom} < d_{t,i}^{av} < d_i^{top}} \qquad (4.22)$$

Where

M_i^p = Predicted mass of rocks in size interval i. (kg)

$$M^{tp} = \sum_i M_i^p \tag{4.23}$$

Where

M^{tp} = Total predicted mass of rocks. (kg)

$$m_i^p = \frac{M_i^p}{M^{tp}} \tag{4.24}$$

Where

m_i^p = Predicted mass fraction of rocks in size interval i.

This data is put into cumulative for form to give the predicted steady state size distribution of the charge as shown in Figure 4-15. This procedure makes it possible to predict the steady state size distribution of pebbles, given any size distribution of feed pebbles. It can be seen that the prediction is relatively accurate. For the purpose of this work the model was sufficiently accurate however improvements to the model are possible. Future work could investigate the probability of rock breakage and rock travel into smaller fractions.
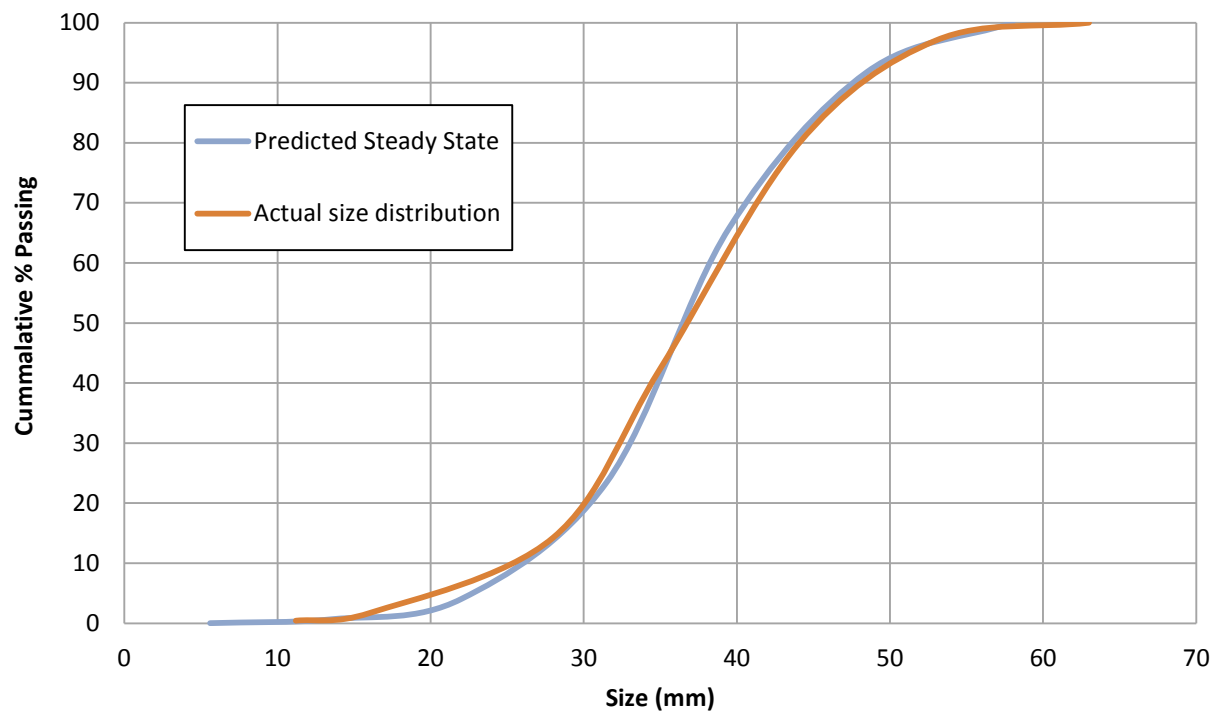
Figure 4-15: Predicted size distributions (Gold ore, 65/35mm feed size)

4.4 Tests on Gold

The main aim of this work was to optimise secondary pebble grinding by optimising the pebble feed size and the mill speed. Many difficulties arise when trying to test different operating conditions using a batch method. The difficulties arise as each condition creates a different environment for grinding. One of the main problems experienced was the change in % solids of the pulp. This was caused by the increase in the amount fines as the rocks abrade away. Since it was predicted that each operating condition would have a different wear rate and no additional water enters the mill this causes a different grinding conditions. Scoping tests revealed that without water addition the viscosity of the pulp increased to a point where it prevented grinding from occurring. The viscosity is caused by very fine particles and it should be noted that when a mill is operated in closed circuit with cyclones, the coarse particles in circulation form a large part of the slurry in the mill. Therefore, for batch tests, using ore pebbles, the pulp must be more dilute than _normal'. For this section of testing 25 litres of water was used with 20 kg of fines. This gave an initial per cent solids of about 23% on a volume basis. It was justifiable as once the wear from the rocks was accounted for, the overall per cent solids ranged from 28% to 32%. By operating in a rather dilute region the conditions within the per cent solid range are relatively constant. Unpublished tests by Professor BK Loveday showed that additional water had no effect on the product size distribution in laboratory batch tests in ball-mills and rod-mills.

In all grinding tests in this section of testing the time of grind was kept constant. The other option was to keep the energy input per ton of feed constant using a method described later on. The problem with the constant energy input method was that is required varying amounts of time. This in turn this creates inconsistent grinding conditions, which is why the constant time method was utilized.

The mines current operating condition was used to establish a base case. This was done at a set speed (83.5 % of critical speed) and using a fixed pebble feed size (65/35 mm). A review of pebble milling literature revealed no justification for the speed and pebble feed size employed at the mine. It was decided that initial tests would be conducted using the same size fraction of unrounded rock as the mine (65/35mm) and a smaller size (44/28mm). Lower mill speeds (75% and 69% of critical speed were also tested. The measured variables were power, pebble consumption, total mass of fines and the per cent of fines passing 75 μm. All these measured variables allowed for the grinding efficiency to be determined for all test. The grinding efficiency (*WI*) is defined as the energy spent to produce a ton of material finer than 75 μm and has the units of *kwh/t*.
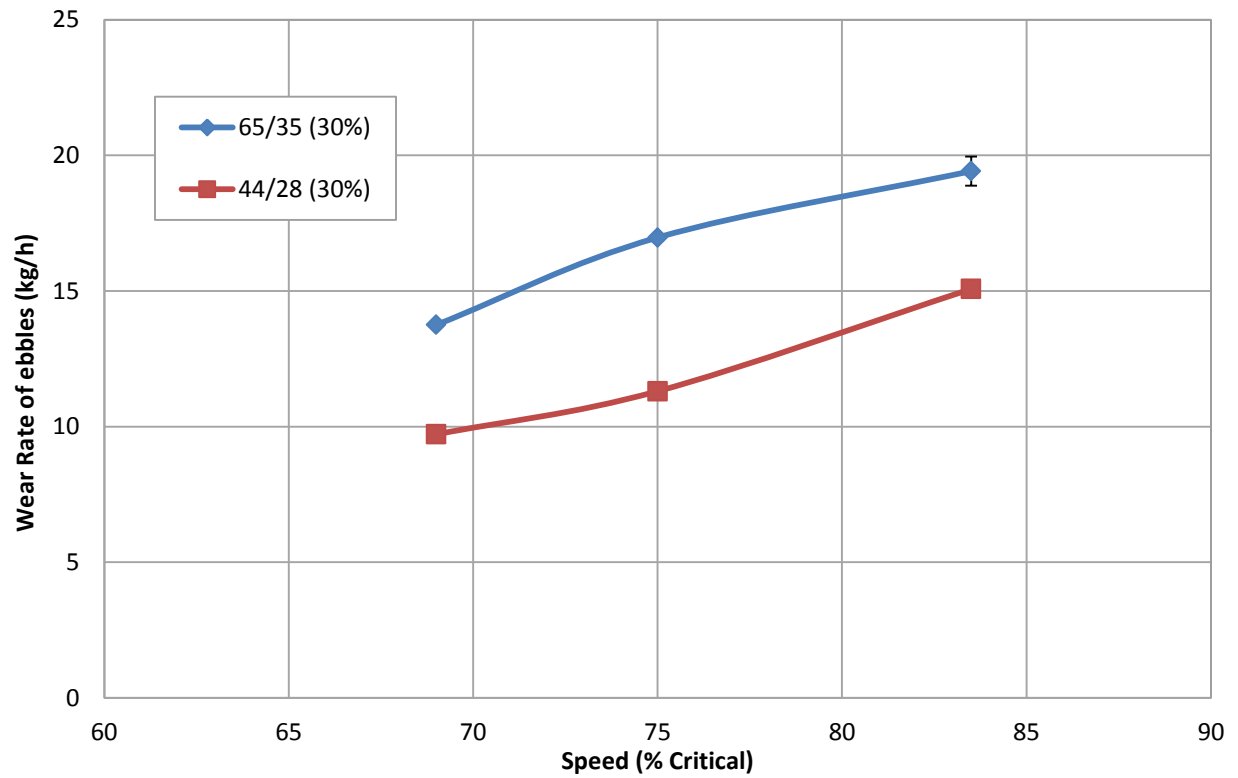
Figure 4-16: Wear Rate vs Mill Speed for different feed sizes of pebbles
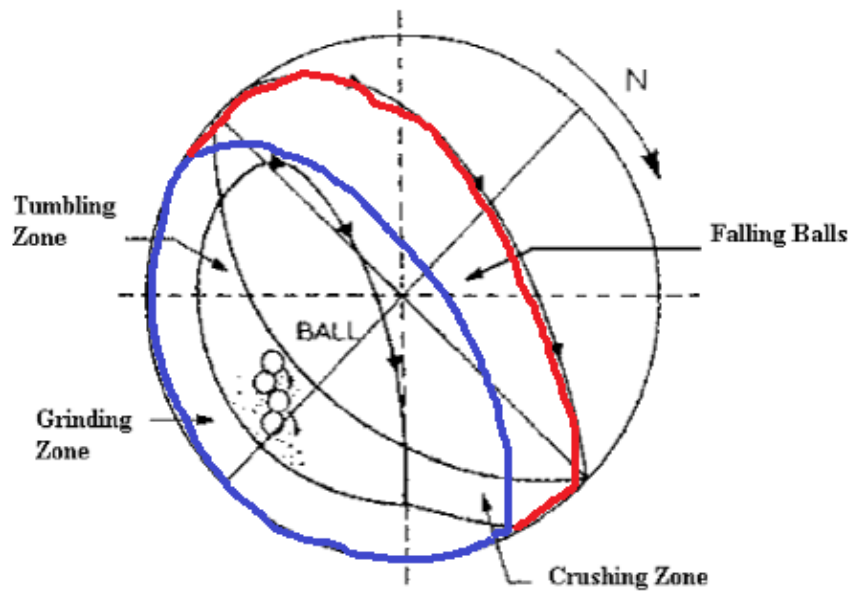
Figure 4-17: Grinding regions in a mill

The wear rate of pebbles or better defined as pebble consumption is plotted in Figure 4-16 as a function of speed for both pebble feed sizes. The effect of speed on the wear rate of pebbles is a well know principle.

Figure 4-17 shows the different grinding regions in a mill. Abrasion and attrition would take place in the grinding zone while crushing or impact grinding would take place in the crushing zone.

At lower speeds (say at about 69% critical) the media is packed closely together in the grinding zone and the trajectory shown by the blue line in Figure 4-17. A study on charge motion shows that as speeds increases the charge swells meaning there is less interaction in the grinding zone and the trajectory of the charge changes as shown in red. The maximum trajectory height increases and some rocks may be thrown clear of the charge into a region where no grinding occurs.

This means that as the mill speed increases the proportion of abrasion/attrition decreases while the proportion of crushing or impact grinding increases. Since the wear from the impact grinding process is greater than the wear from the abrasion/attrition process the total wear rate increase. The maximum trajectory height also increases with speed implying that the descending rocks have more energy to dissipate thus the impact would result in larger forces thus increasing the wear rate. In some instances the high speed may cause rocks to be thrown clear of the charge into a region where no grinding occurs and it may land directly on a lifter thus further increasing the pebble wear rate.

Figure 4-16 also demonstrates one other important principle. It shows that smaller pebbles do not wear away faster than larger pebbles. This was unexpected since the smaller rocks have a higher surface area to volume ratio on which abrasion/attrition can take place and should wear away faster. Figure 4-5 (From page 59) is repeated below to illustrate that larger pebbles would be expected to have a longer residence time and that they would wear away at a slow rate for a significant part of that life. However it is thought that the low energy descent of the smaller rocks coupled with the removal of the larger rocks results in less violent impacts in the crushing zone and thus a reduction in wear rate is observed. This also proves the hypothesis that the wear due to crushing or impact grinding is much larger than that for abrasion and attrition.

The lower wear rate in the absence of the larger rocks means that the specific wear rate (R_s) is also a function of charge size distribution. This implies that if the tagging procedure was repeated in the presence of the 44/28 mm charge size distribution, all individual specific wear rates would be lower. Instead of repeating the tagging tests it was decided to introduce a specific wear correction factor (k_s). The specific wear correction factor was used to obtain a specific wear rate plot for a different charge size distribution by assuming that the decrease in specific wear rate is proportionate across every size range. The correction factor (k_s) is obtained by taking the ratio of the total wear rate observed in the new charge size distribution to the total wear rate observed in the reference charge size distribution. The new specific wear rate plot is generated by multiplying each individual wear rate in the reference charge size distribution by the correction factor (k_s).
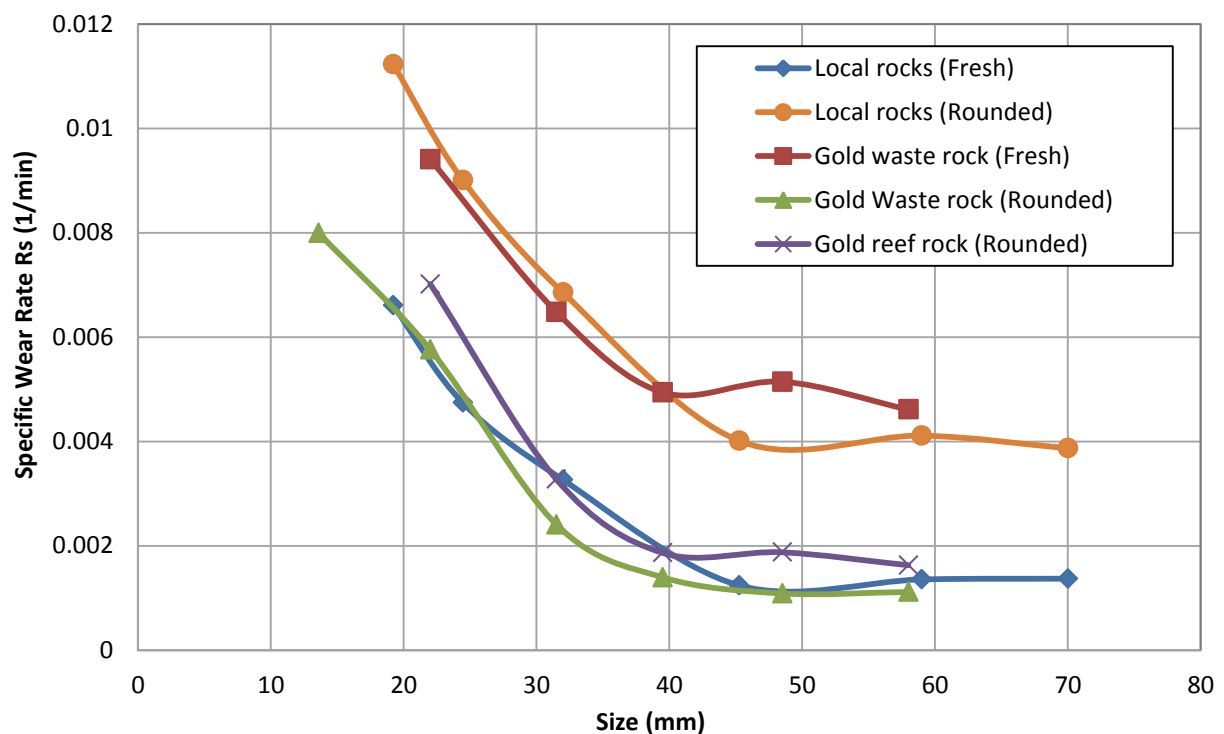
Figure 4-18: Specific wear rate for various types of rocks
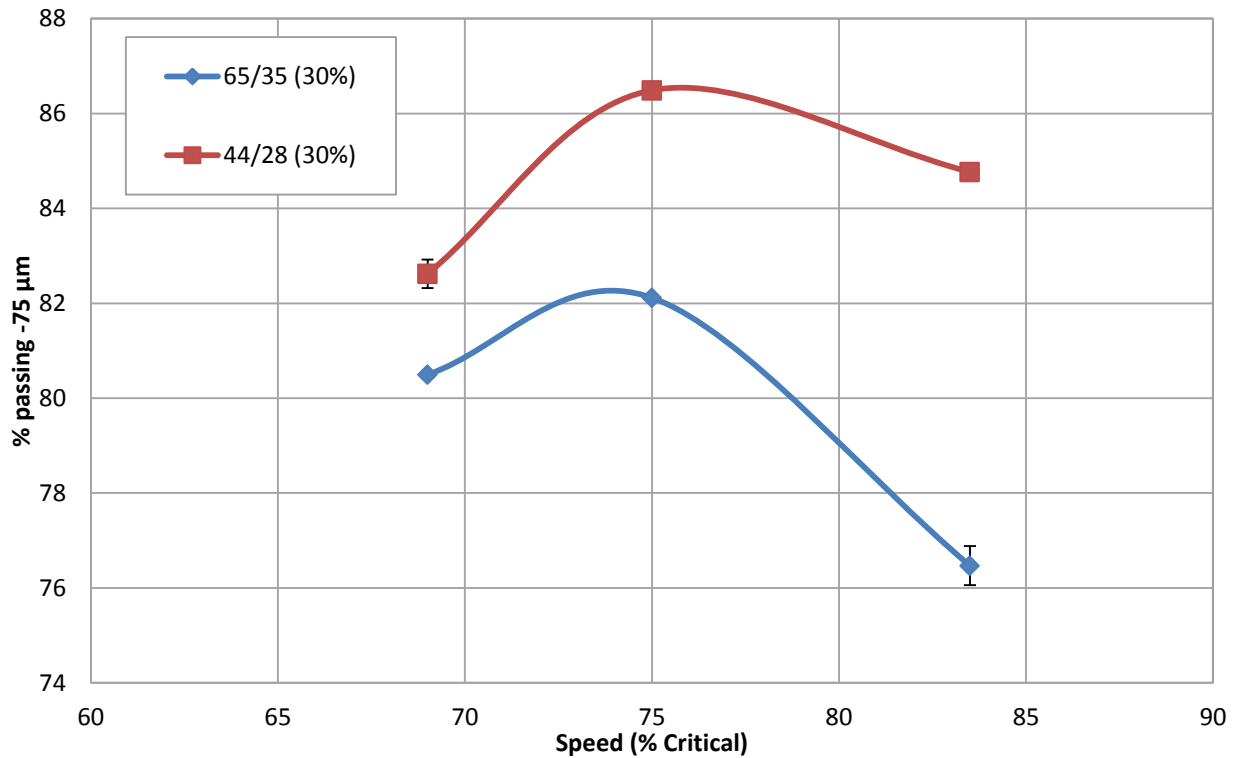
The product size (material finer than 3.3mm) is shown in Figure 4-19 as per cent passing 75 µm, plotted a function of speed for both pebble feed sizes. It can be seen from the plot that the smaller pebbles grind finer than the larger pebbles. The size of grinding media is a trade-off between two factors. A decrease in media size causes an increase in the surface area to volume ratio of rocks meaning that smaller rocks have a larger surface area on which attrition can take place. An increase in particle size creates larger forces between grinding surfaces meaning that larger particles can be broken. It is a well know principle that grinding media should be tailored to suit the size of the particles. Figure 4-19 demonstrates that the smaller pebbles are large enough to efficiently reduce the size of the pebble mill feed. The larger rocks would only be necessary if the feed was much coarser. The addition of the larger media increases that rate at which the smaller media are consumed. Nevertheless, it could be concluded that it would be beneficial to reduce the lower size limit on the range of pebble sizes. This confirms the findings of McIvor and Greenwood (1996)

As discussed before, the speed of the mill influences the proportion of each mechanism of grinding. As the mill speed increases the proportion of abrasion/attrition decreases while the

proportion of crushing or impact grinding increases. At very low speeds the charge is packed closely together promoting abrasion/attrition but is not lifted high enough for sufficient impact grinding to occur. At very high speeds the charge swells limiting the abrasion/attrition mechanism but now imparting more energy to the ore to promote impact grinding. The general shape of Figure 4-19 shows that there is an optimum speed which produces the correct proportions of each grinding mechanism to provide the highest per cent passing 75 µm. The figure shows that 75 % of critical speed is the optimum mill speed with respect to fineness of grind.

In any process there will always be a trade-off between efficiency and productivity. The ideal process should be highly productive yet highly efficient. The grinding efficiency is here defined as the energy spent to produce a ton of material finer than 75 µm, or Work Index (kwh/ton$_{-75\ µm}$). This definition implies that the lower the value the greater the efficiency. The grinding efficiency is plotted in Figure 4-20 as a function of mill speed for both pebble feed sizes. The product of this process is material with a specified proportion less than 75 µm. Hence production is proportional to rate of production of material finer than 75 µm. Thus productivity is defined, for convenience, as the rate of production of fines (minus 75 µm) and is plotted in Figure 4-21 as a function of speed for both pebble feed sizes. The total mass of fines comes from fines that enter the mill and fines that are worn from the pebbles. The ratio of fines resulting from wear (equivalent to pebble consumption) to the fines entering the mill was relatively high. For example when operating at 83.5 % critical speed using the larger pebble feed size the wear from pebble was about 11 kg while the amount of fines entering the mill was 20 kg. However, an examination of data published on the commissioning of the Nkomati Concentrator milling circuit showed similar statistics, with the pebble wear accounting for about 30 per cent of total tonnage.(Bradford et al., 1998). The rate of production of finished product is normally the primary consideration, but with the cost of electricity rising steeply, the efficiency of energy usage must be considered. Figure 2-20 and Figure 2-21 illustrate the trade-off between productivity and efficiency. An investment in larger mill shells is required to operate at lower speeds.

However, considering both graphs simultaneously on a lab scale, the basic trend observed is that as the productivity increases the efficiency decreases. At higher speeds smaller pebbles are more efficient while at lower speeds larger pebbles become more efficient. It seems that each pebble size has a corresponding mill speed which makes its use much more productive. The productivity of the larger pebbles peak at 75 % critical whilst the productivity the smaller pebbles seem to

peak at 83.5 % critical. The results of this section of tests are shown in Table 4-3. A comparison to the mines operating condition (83.5% critical speed; 65/35 mm pebble feed size) is shown in Table 4-4. The percentages shown in Table 4-4 is the change in grinding efficiency, production and pebble consumption for each operating condition.
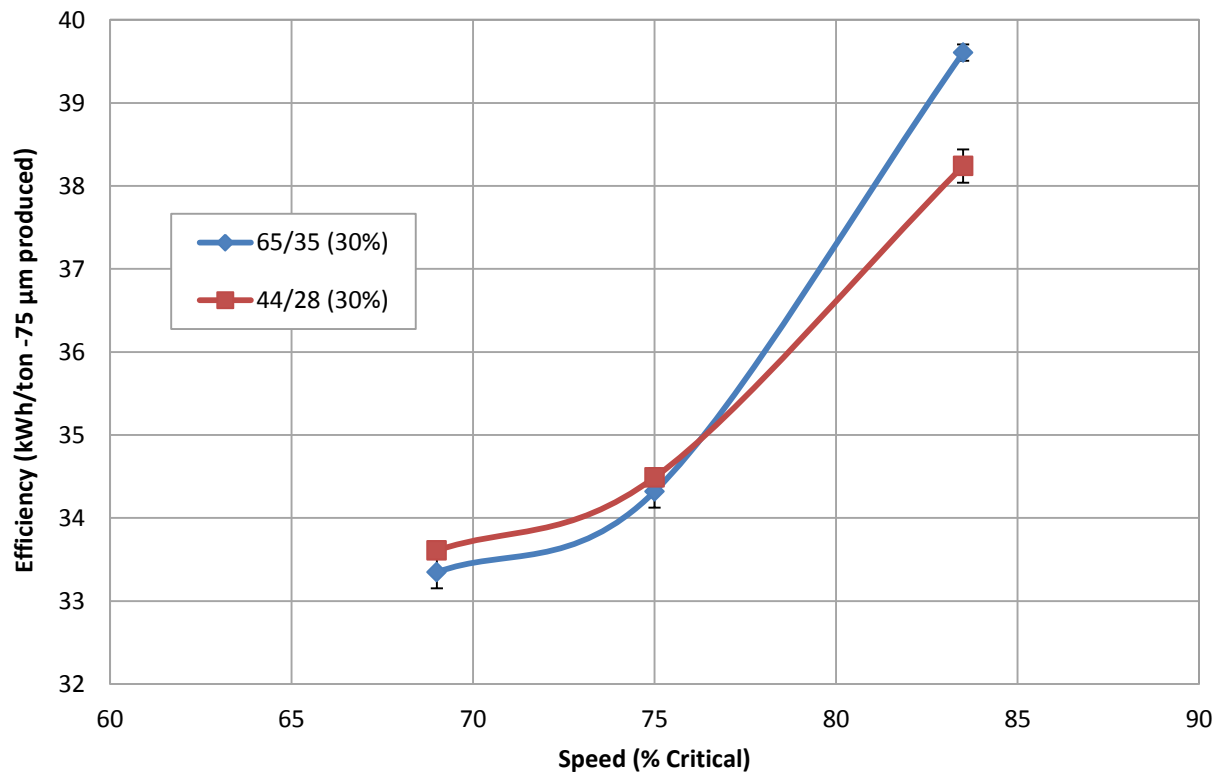
Figure 4-20: Power Consumed vs Mills Speed for different feed sizes of pebbles
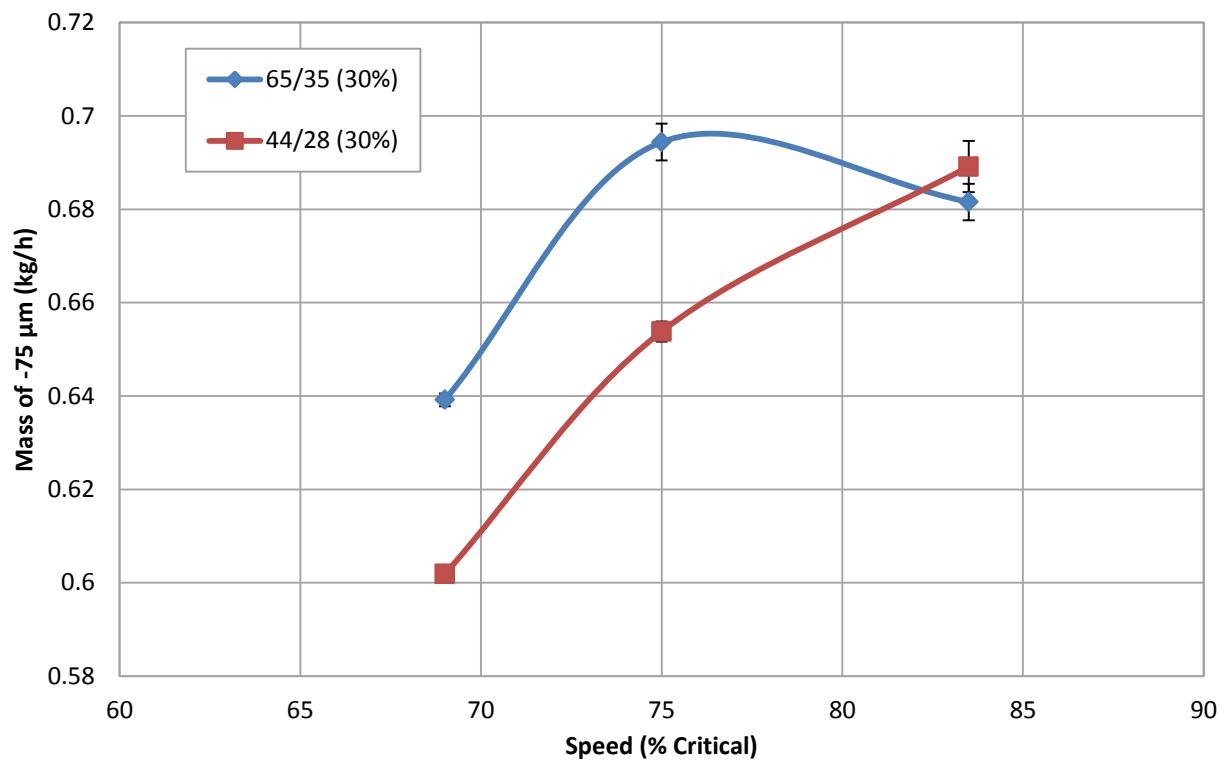
Figure 4-21: Rate of production of -75 µm vs Mills Speed for different feed sizes of pebbles

Table 4-3: Summary of results in 1.2 m diameter mill at 30% filling

Run ID (Average)	Run 1 a,b,c	Run 2 a,b	Run 3 a,b	Run 4 a,b	Run 5 a,b	Run 6 a,b
Speed (% Critical)	83.5	75	69	83.5	75	69
Pebble size (mm)	65/35	65/35	65/35	44/28	44/28	44/28
% filling	30	30	30	30	30	30
Total charge mass (g)	132200	132193	132134	131766	132205	133371
Power (kw)	1.62	1.43	1.28	1.58	1.35	1.21
Wear rate(g)	11325	9899	8020	8792	6594	5666
% passing -75 μm	76.47	82.12	80.50	84.77	86.49	82.62
Total mass of fines recovered(kg)	31.20	29.60	27.79	28.45	26.46	25.50
mass of -75(kg)	23.86	24.30	22.37	24.12	22.88	21.07
Time (min)	35	35	35	35	35	35
Efficiency (kWh/ton $_{-75\ \mu m\ produced}$)	39.61	34.32	33.35	38.24	34.49	33.61
Productivity(kg$_{-75\ \mu m\ produced}$/ h)	0.68	0.69	0.64	0.69	0.65	0.60
Energy input (kWh/ton $_{fresh\ feed}$)	47.24	41.70	37.30	46.12	39.46	35.40
Relative wear (kg$_{wear}$ /h/kw)	11.99	11.87	10.75	9.53	8.35	8.00
Wear rate(kg$_{wear}$ /h)	19.41	16.97	13.75	15.07	11.30	9.71
Per cent Wear rate (kg$_{wear}$/kg$_{charge}$)	36.15	33.11	28.62	30.54	24.79	22.07

Table 4-4: Percentage change from mines operating conditions

Speed (% Critical)	75	69	83.5	75	69
Pebble size (mm)	65/35	65/35	44/28	44/28	44/28
Plant Power Consumption (%)	-13.35%	-15.81%	-3.45%	-12.92%	-15.14%
Plant Throughput (for the same product size)	+1.88%	-6.22%	+1.11%	-4.07%	-11.70%
Pebble consumption (%)	-12.60%	-29.18%	-22.36%	-41.78%	-49.97%

4.4.1 Product size distribution analysis

There is a significant amount of mixing in a mill and residence time distribution tests have shown that perfect mixing can be assumed for simulation purposes. This results in a wide distribution of sizes in the product of mills, making the use of a classifier essential. However, all particles have the same residence time in laboratory batch tests and the coarse particles, which have relatively high breakage rates, are consumed rapidly. Hence, a relatively narrow distribution of sizes is produced and a suitably sized screen (1 – 5 mm), where ore particles are being consumed rapidly, can be used to separate the fines from the pebbles. The results of these batch tests were equivalent to the over flow of the classifier. Plant data was compared to a batch test which had a similar per cent passing 75 μm as shown in Figure 4-22.

The batch tests performed in this work therefore might be more efficient than in practice (narrow size range) and hence the plant power/ton may be a bit more. However, measurement of power in a batch test is not far off the mark, particularly with the P_{80} close to 80%.
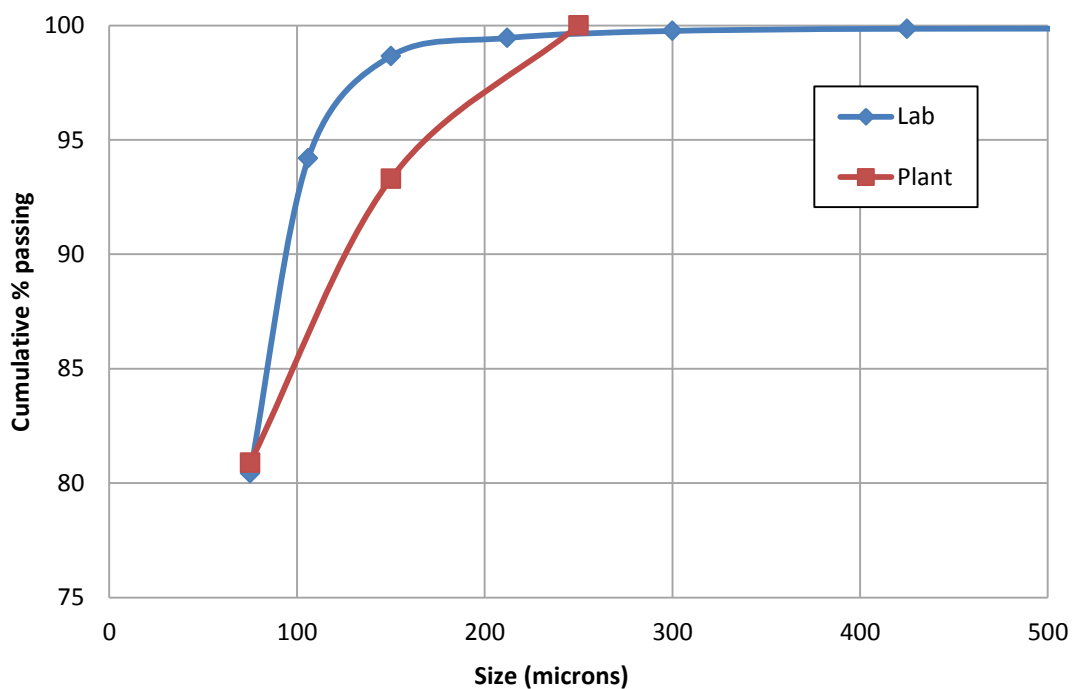
Figure 4-22: Comparison between product size distributions

The average product size distribution of each batch test for each mill condition is plotted in Figure 4-23. As discussed, in practice the size distributions of these tests are somewhat unrealistic however by comparing on a batch scale some important trends are observed. For ease of understanding Figure 4-23 was shape coded. The larger pebble feed size is plotted with a broken line while the smaller pebble feed size is plotted with a solid line. The various

speeds i.e. 69%, 75% and 83.5% critical speed are represented by ▲, ■, and ● respectively. At 83.5% critical speed the increase in the wear rate means that more fresh rock is required implying that the fast chipping mechanism produces more chips thus the coarse size distribution. It is also thought that at this speed the breakage rate of the rocks increase as direct impacts with the mill liner/lifters are more probable at this speed. This causes rock cleavage which exposes more fresh edges resulting in more chips being produced. At 75% and 69% critical speed the basic shape of the graphs are similar for both pebble feed sizes with the smaller pebble feed size giving a higher per cent passing 75 μm.
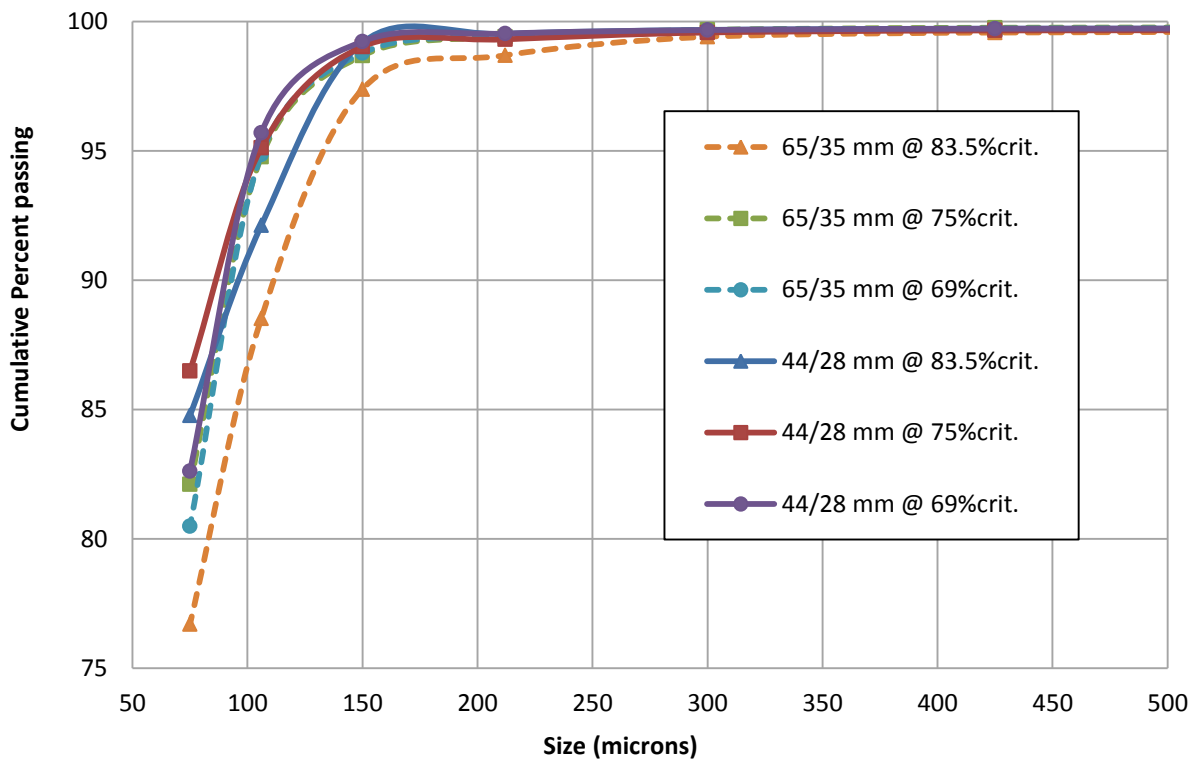
Figure 4-23: Size distributions for various conditions

4.5 Tests at higher volumetric filling

It was first thought that the smaller pebbles would wear away faster due to the larger surface area to volume ratio that the larger pebbles. However tests showed that smaller pebbles wear away slower than larger pebbles and this was thought to be due to the removal of the larger rocks. It was also thought that the low volumetric filling of the mill may cause a shortage of media in crushing zone or toe of the charge. This in turn creates larger impact forces which seem to exaggerate the wear of the larger rocks. In order to disprove the latter hypothesis and prove the former, the tests were repeated at a higher volumetric filling.

The volumetric filling was increased from 30 % to 40 % which is closer to that used in pebble milling. The mass of fines and water was determined by assuming a proportionate increase. This was done using a scaling factor of 40/30. The top-up of fresh pebbles estimated from the data at 30% filling and scaled up by 40/30. A run was only repeated if the predicted wear rate was different from the actual wear rate. However, the actual pebble consumption in all runs with the higher volumetric filling was close to the predicted value.

Milling conditions were kept similar to those at 30% of filling, by taking into account the effects of mill speed on mill power. By taking samples of the power usage early in the run the time was adjusted in order to ensure the same energy input per ton as the corresponding run at a lower volumetric filling. The energy input per ton of material entering is plotted as a function of speed in Figure 4-24. Ideally the plot should be a single line since at the lower volumetric filling for a given speed the mass of charge and the time remain constant. However the smaller pebbles seem to consume less energy as shown by the red and blue lines.

By maintaining a similar energy input a similar per cent passing was obtained even though the mass of fines was increased. The per cent passing 75 μm is shown in Figure 4-25.
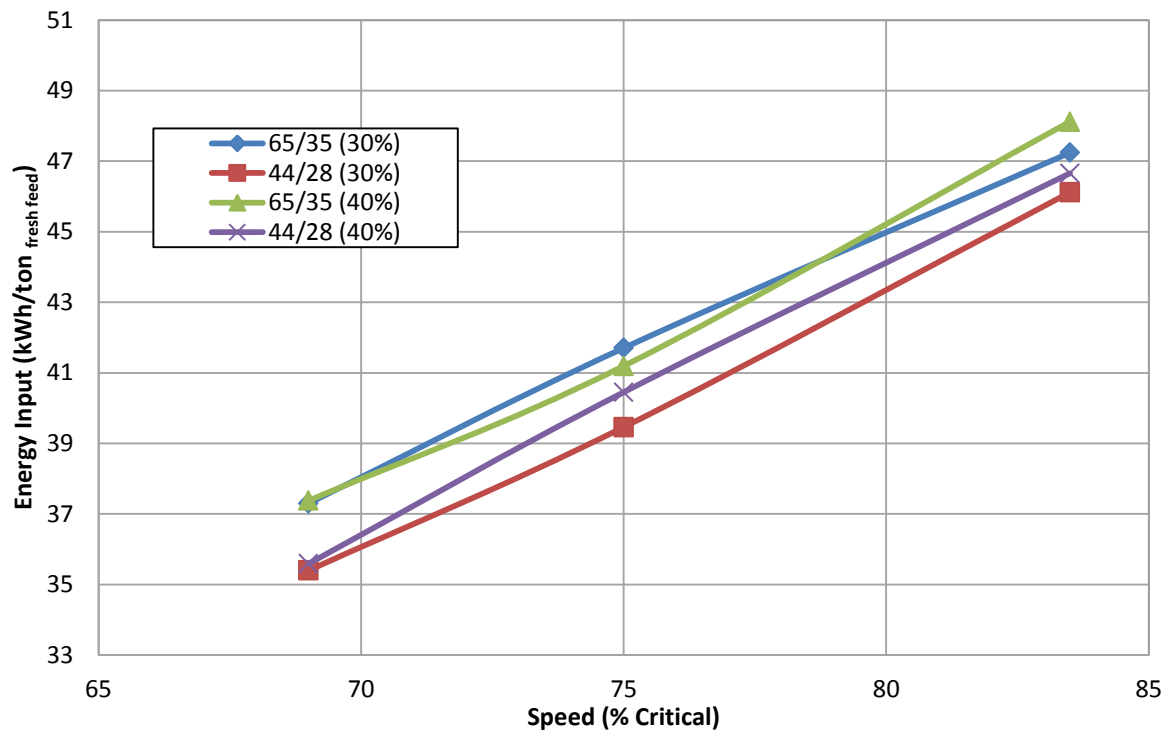
Figure 4-24: Energy input for various runs at higher mill filling
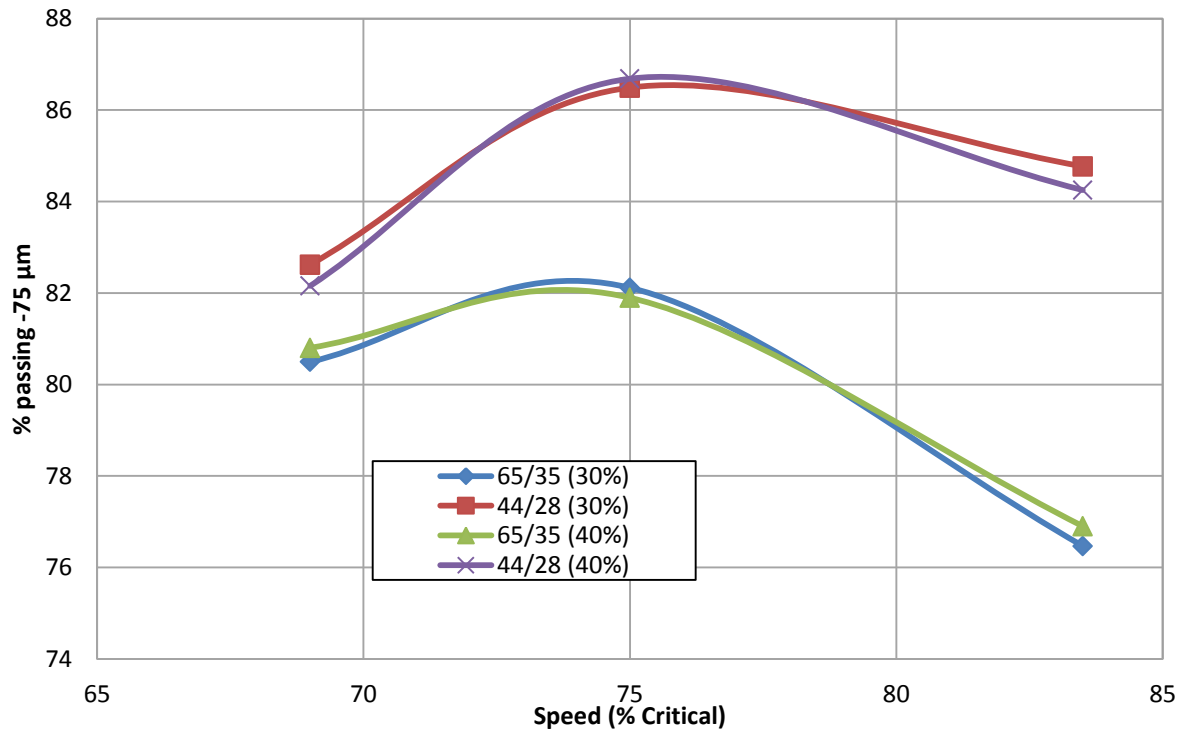
Figure 4-25: Effect of Mill Filling on Per cent passing 75 microns

The wear rate of pebbles at a higher volumetric filling is plotted as a function of mill speed in Figure 4-26. The trends observed at a higher filling were similar to the trends observed at the lower volumetric tests. This served to disprove the notion that the low volumetric filling was responsible for the exaggerated wear rate of the larger pebbles thereby confirming the original hypothesis that a reduction in the wear rate of the smaller pebbles is due to the removal of the larger rocks from the charge.
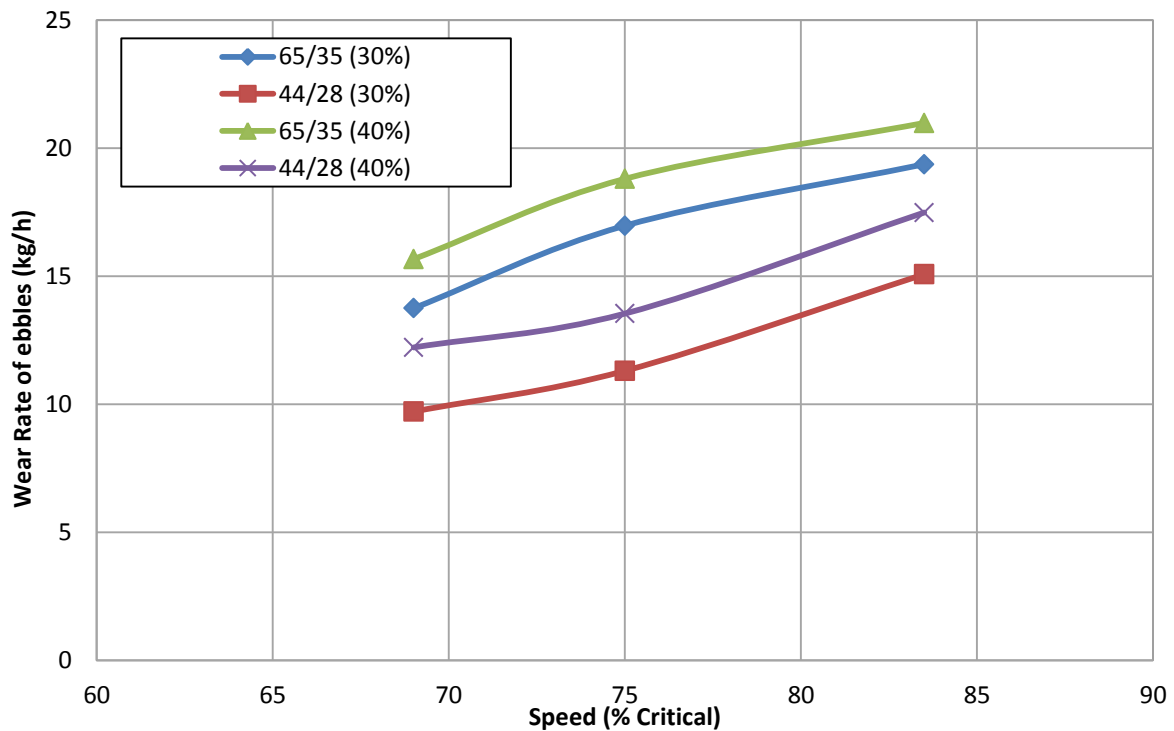
Figure 4-26: Effect of Mill Filling on Pebble Wear rate

Figure 4-26 did not allow a direct comparison between the high and low volumetric fillings, due to changes in efficiency. In order to investigate how the change in volumetric filling affected pebble wear, the wear rate per unit of energy consumed was plotted as a function of speed shown in Figure 4-27. To introduce a dimensionless way of representing pebble wear the wear rate of pebbles was expressed as a percentage of the total material entering the mill plotted as a function of speed in Figure 4-28. The total material entering the mill consisted of the mill feed and the makeup rock. By expressing the wear rate of pebbles in this way the effects of volumetric filling on wear rate could now be investigated. The wear trends observed for both high and low volumetric filling were rather similar as observed in Figure 4-26 and Figure 4-27.

91
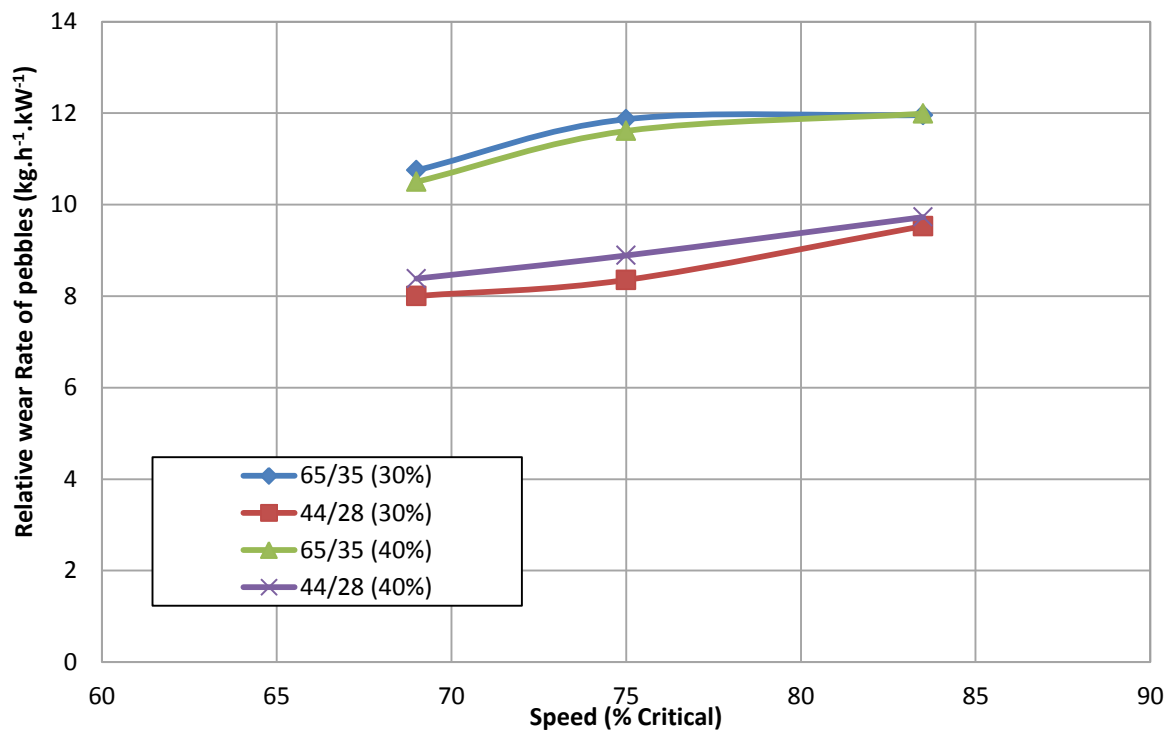
Figure 4-27: Effect of Mill Filling on Relative wear rate
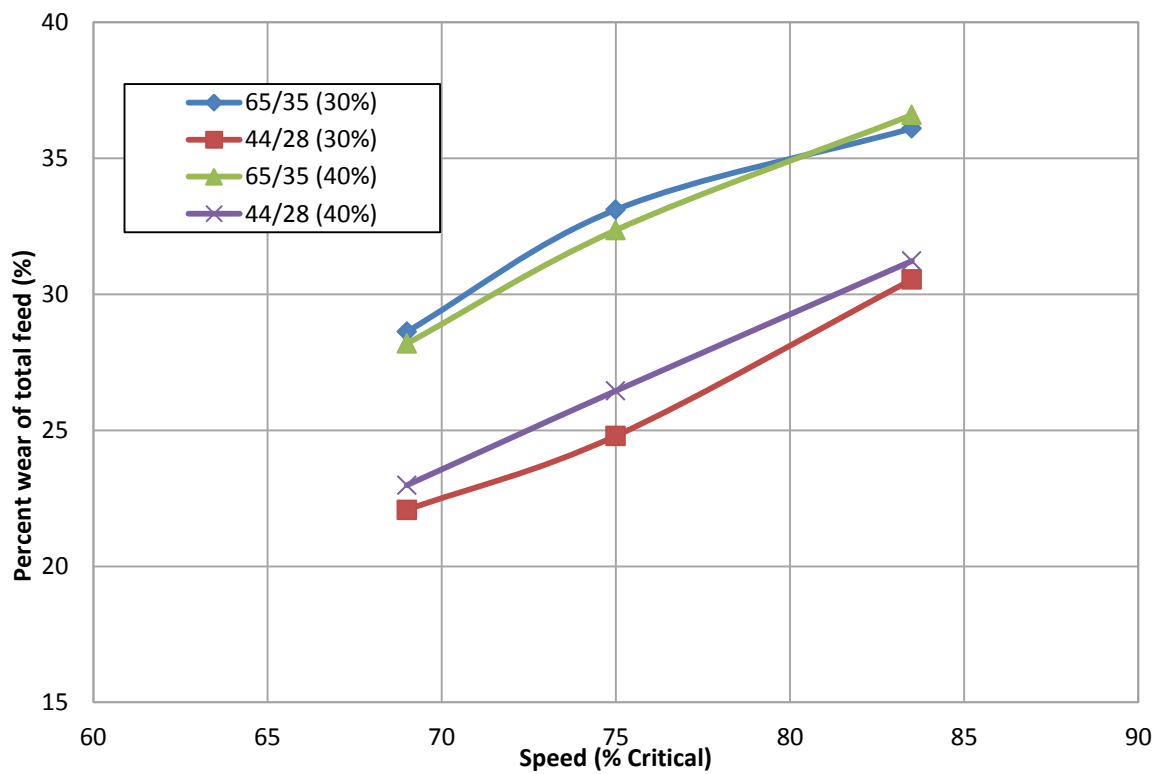
Figure 4-28: Effect of Mill Filling on Percentage wear rate

92

By using the scaling method to determine mass of fines, amount of water and predict the pebble wear rate the need for a duplicate run was prevented. By using the constant energy input method the per cent passing 75 µm was matched quite accurately. Since the wear rate was as predicted and the per cent passing 75 µm was matched, the mass of material finer than 75 µm produced in the higher volumetric filling followed the same trend as the lower volumetric filling. The trend is shown in Figure 4-29. Since the energy input was the same for each corresponding run the grinding efficiency also followed the same trend as shown in Figure 4-30. Even though the volume of charge was increased the smaller pebbles still seem to be more efficient at higher speeds while the larger pebbles still seem more efficient from an intermediate speed to a low speed. The results of this section of tests are shown in Table 4-5.
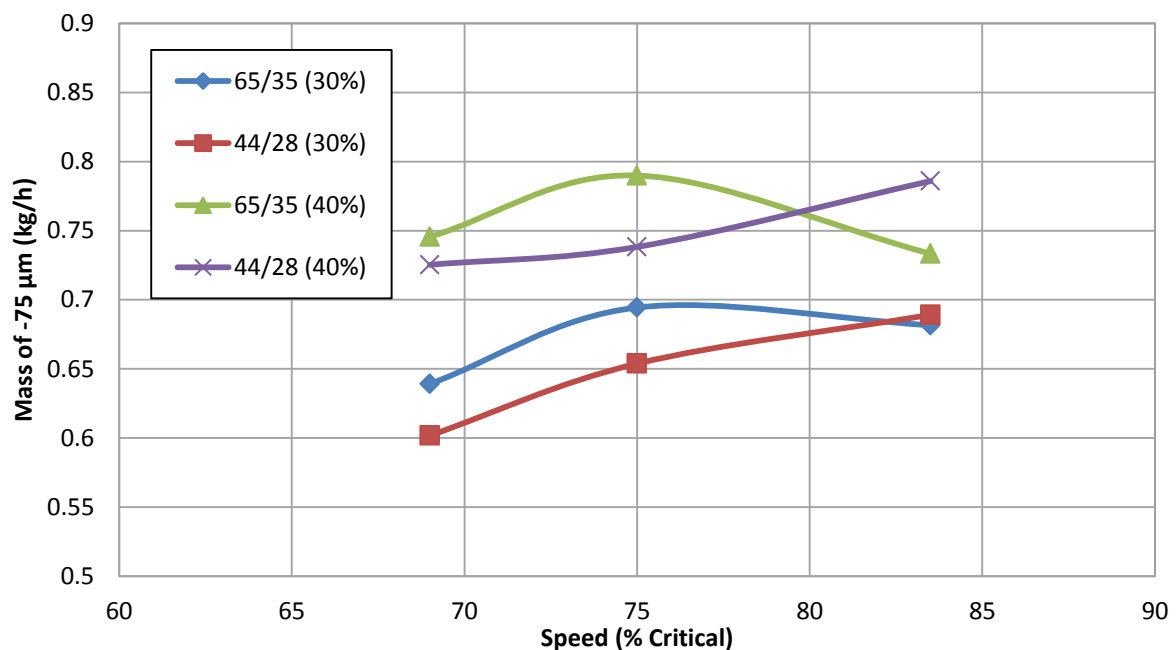
Figure 4-29: Rate of production of -75 µm vs mill Speed for different feed sizes of pebbles
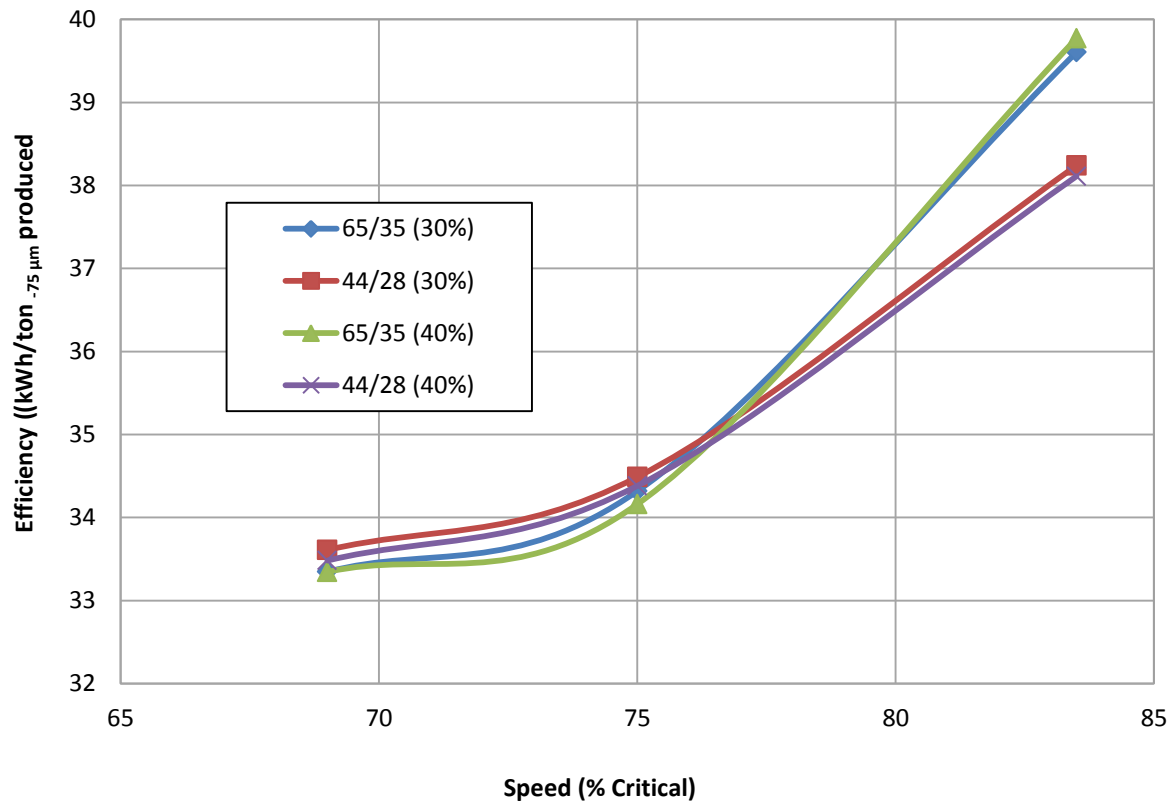
While the per cent passing 75 µm was matched, the entire size distribution of the fines was not matched exactly. The average product size distribution for all runs at a higher volumetric filling is plotted in Figure 4-31. For ease of understanding Figure 4-31was also colour and shape coded as before. The larger pebble feed size is plotted with a broken line while the smaller pebble feed size is plotted with a solid line. The various speeds i.e. 69%, 75% and 83.5% critical speed are represented by ▲, ■, and ● respectively.

Although the size distribution was not matched the trends were remarkably similar. Expect for the size distribution using the smaller pebbles at 69% critical the trends observed in all other runs were similar. The basic trends as observed before are that the greater pebble wear the greater top up of fresh rock, implying that the fast chipping mechanism produces more chips thus the coarse size distribution.
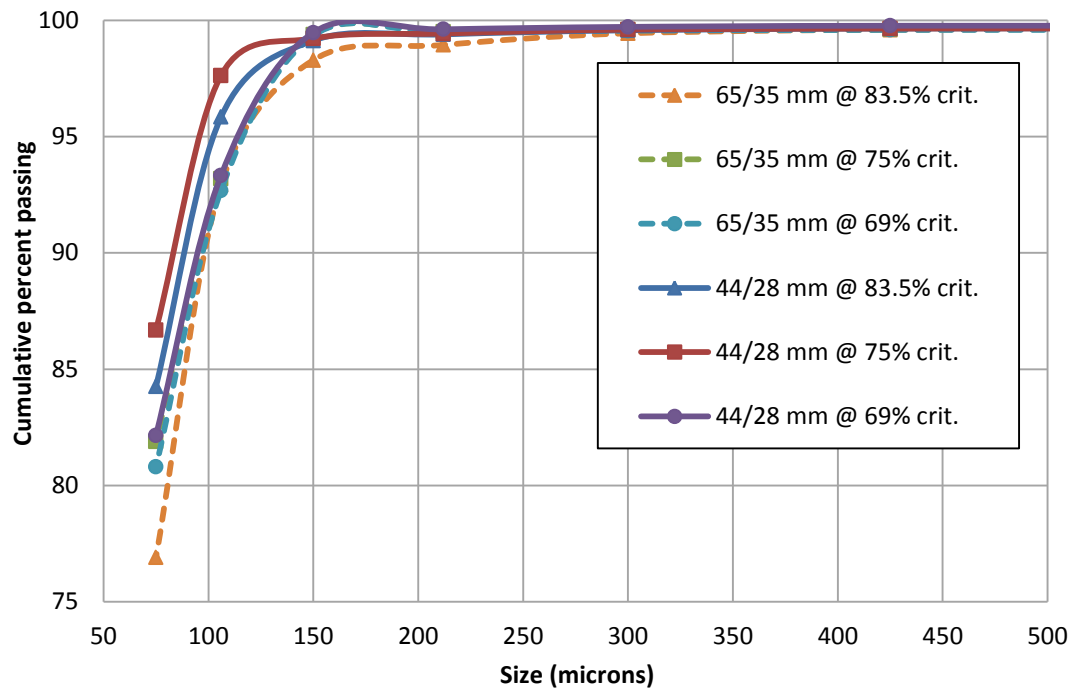
Figure 4-31: Size distributions for various conditions at higher mill filling

Table 4-5: Summary of results in 1.2 m diameter mill at 40% filling

Run ID	40 run 1	40 run 2	40 run 3	40 run 4	40 run 5	40 run 6
Speed (% Critical)	83.5	75	69	69	75	83.5
Pebble size (mm)	44/28	44/28	44/28	65/35	65/35	65/35
% filling	40	40	40	40	40	40
Total charge mass (g)	182291	184107	181437	182108	180156	184147
Power (kw)	1.80	1.52	1.46	1.49	1.62	1.75
Wear rate(g)	12528	9925	8235	10832	13202	15923
% passing -75 μm	84.25	86.68	82.16	80.80	81.90	76.90
Total mass of fines recovered(kg)	40.10	37.46	35.71	38.29	40.64	43.42
mass of -75(kg)	33.79	32.47	29.34	30.94	33.28	33.39
Time (min)	42.99	43.98	40.45	41.49	42.14	45.54
Efficiency (kWh/ton $_{-75\ \mu m\ produced}$)	38.11	34.38	33.48	33.35	34.16	39.77
Productivity(kg$_{-75\ \mu m\ produced}$/hr)	0.79	0.74	0.73	0.75	0.79	0.73
Energy input (kWh/ton $_{fresh\ feed}$)	46.66	40.45	35.59	37.38	41.19	48.12
Relative wear (kg$_{wear}$ /h/kw)	9.73	8.89	8.38	10.50	11.61	11.99
Wear rate(kg$_{wear}$ /h)	17.48	13.54	12.22	15.66	18.80	20.98
Per cent Wear rate (kg$_{wear}$/kg$_{charge}$)	31.22	26.45	22.98	28.19	32.36	36.58

4.6 The effects of mill speed and volumetric filling on power draw

In order to maximise production it is common practice to maximise the power drawn by the mill. Conventionally, this done at a fixed speed by altering the volumetric filling of the mill by changing the feed rate to the mill until maximum power draw is achieved. The net power consumed is plotted as a function of mill filling for various mill speeds in Figure 4-32. Due to the lack of resources the maximum filling that could be reached was 55%. The intercept of each graph with the y-axis is when the mill is empty (0%) and is shown by the no load power (*NLP)* for that speed. If the mill was completely full (100%) then no grinding will take and the power usage will drop down approximately the *NLP* for that speed. The only extra power consumed will be the added friction on the bearings and shafts. This implies that there exists a peak between 0% filling and 100% filling. The basic trend observed is that as the mill filling increases the power draw increase until it peaks and then begins to drop. The predicted peak power usage occurs at about 50% filling irrespective of speed. Figure 4-32 also shows how an increase in speed increases power draw until 85% critical speed, after which any increase in speed reduces the power consumption. For this reason the results of these tests were re-plotted to show the net power consumed as a function of speed for various mill fillings in Figure 4-33. It shows the peak power usage at 85% critical speed. This peak trend was expected since as the speed approaches critical (speed at which entire charge starts to centrifuge) smaller particles will start to centrifuge prematurely thus a reduction in power is observed. From these tests it is predicted that the maximum power draw for this ore will occur at 55% volumetric filling and at a mill speed of 85% critical.
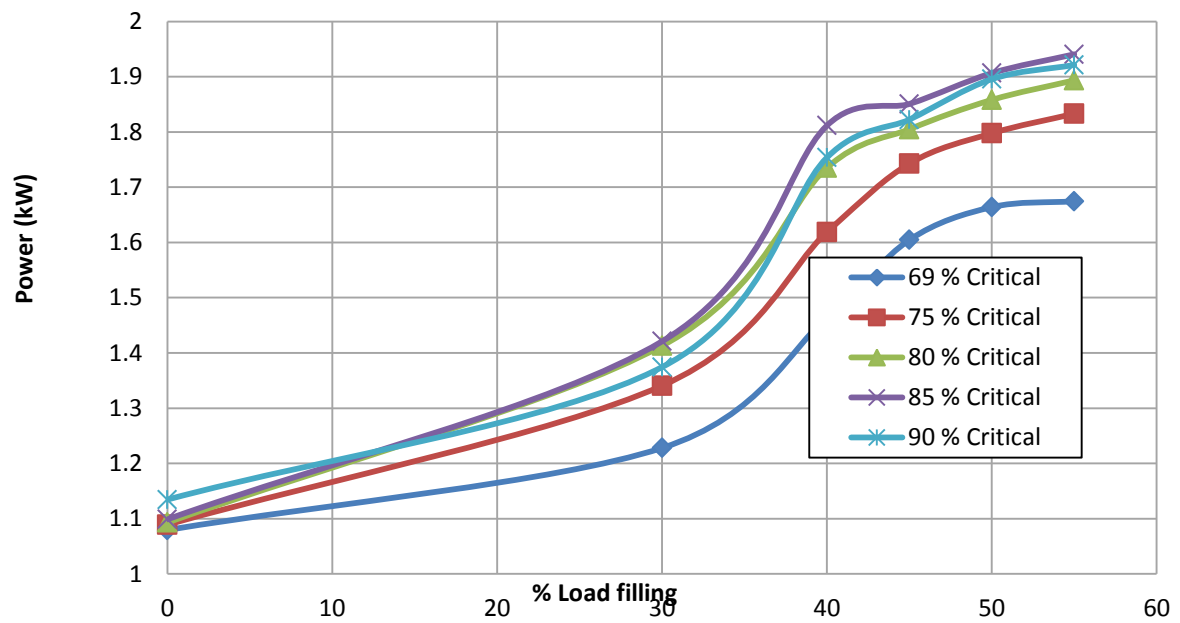
Figure 4-32: Net power vs mill filling
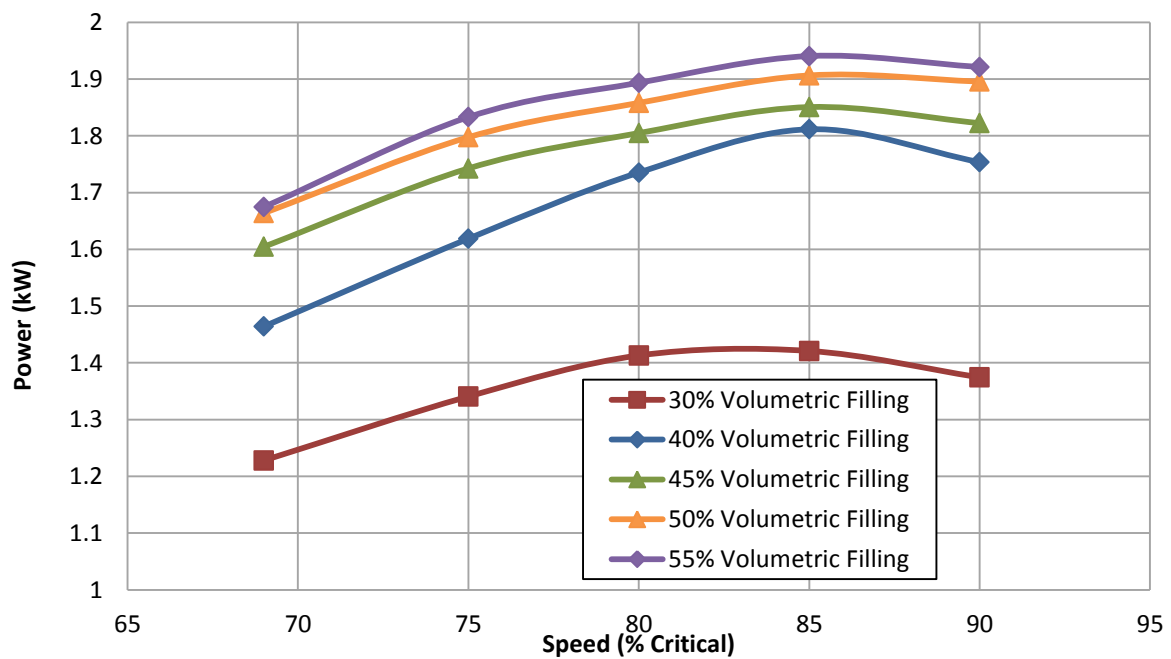
Figure 4-33: Net power vs speed

98

4.7 Comparison to steel balls

The only missing link in this work was a comparison between pebbles and steel grinding media. One constraint was the amount of metallic grinding media available. In order to fill the larger mill to 40% volumetrically about 550 kg of steel balls were required. A smaller 300 mm internal diameter by 300 mm length mill with torque measurement was readily available. The problem with smaller mill is that it was not large enough to accommodate the larger pebble feed size so only the smaller pebble feed size was tested.

The same steady state size distribution used in the larger mill was used in the smaller mill. The only difference was that the smallest size fraction (-11.2 mm) was removed. This was done because a direct comparison between balls and pebbles was done and balls smaller than 11.2 mm were not available. The pebbles and balls were within the same size fractions. The pebbles appear to be larger, because elongated and square-shaped pebbles passed through the square mesh screens (i.e. shape factors in excess of unity) as shown in Figure 4-34. Although the mass in each size fraction differed due to the difference in densities the mass fraction in each size fraction remained constant.

Figure 4-34: Various size fractions of pebbles and steel balls

The mill was filled to 40% by volume with pebbles and the mass of fines and water was determined from the 40% run in the larger mill. This was done by ensuring that the ratio between the volume of fines (and volume of water) to the total charge remained the same in

both mills. The intention was to do the test at 69% critical speed, since that is the common operating speed of a ball mill. A visual examination of the mill revealed that lifters were rather flat due to repeated impacts from steel balls during previous tests by other users. It was therefore decided that the mill speed will be increased to 75% of critical, to account for the damaged lifters and impart the correct amount of energy to the ore as if mill was running at 69% critical with proper lifters. This proved to be a justifiable adjustment. The constant energy input per ton of fine material entering method was used to determine the time of grind to ensure the per cent passing 75 μm was in a good range. A duplicate run was done to ensure the correct top up of fresh frock.

When testing the steel balls, the amount of wear from the pebbles was added to the mass of fines and the amount of water increased to ensure the same % solids as before. This was done to ensure the same grinding conditions. The constant energy input per ton of fine material entering method was used to determine the time of grind to ensure the per cent passing 75 μm was the same as the pebble run.

The energy input per ton of fine material entering the smaller mill is plotted in Figure 4-35 for pebbles and steel balls as a grinding medium. Also shown in the plot is the energy input from previous runs. The energy input should have been the same as the energy input to the smaller pebbles at 69% critical. The plot shows that the energy input was slightly higher than expected and closer to the energy input to the larger pebbles at 69% critical. This did not matter since the constant energy method was used to get the product per cent passing in the correct range.

This extra energy input is evident in Figure 4-36 which show the per cent passing -75 μm as a function of mill speed for the pebbles and steel balls in the smaller mill. By comparing the per cent passing -75 μm for previous runs the increase in the per cent passing -75 μm is attributed to the extra energy input. This was not a problem since the extra energy was added for both pebble and steel ball runs.
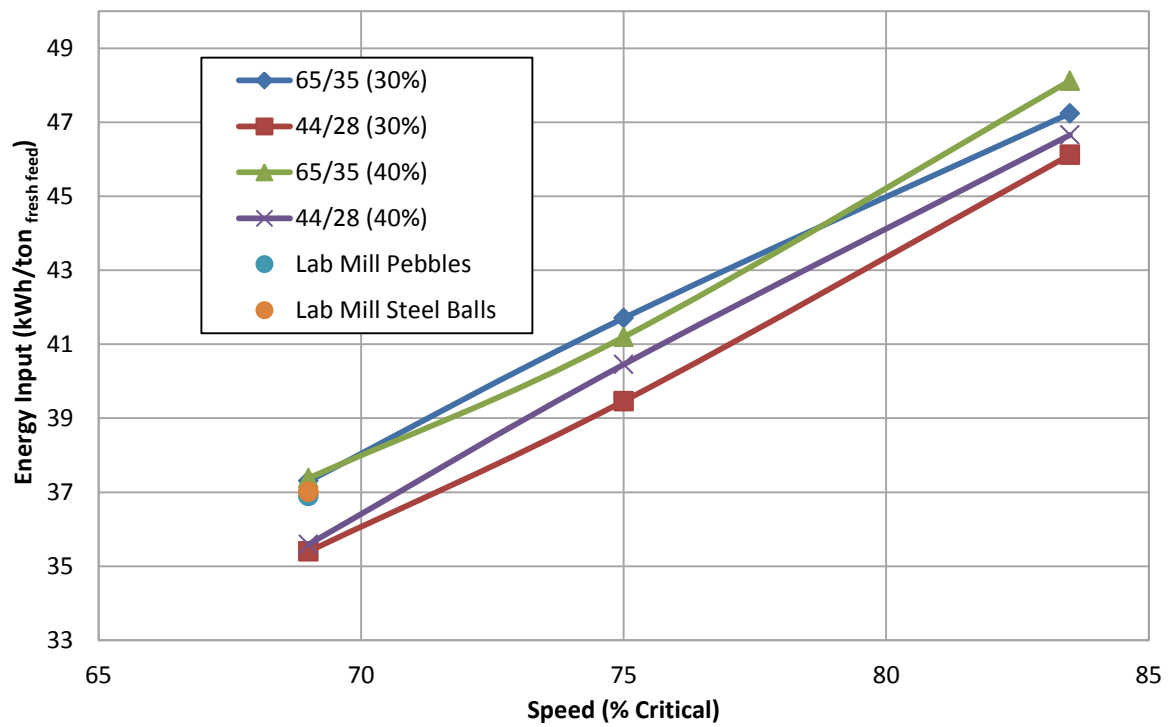
Figure 4-35: Comparison of laboratory mill data (dots) with pilot-plant data
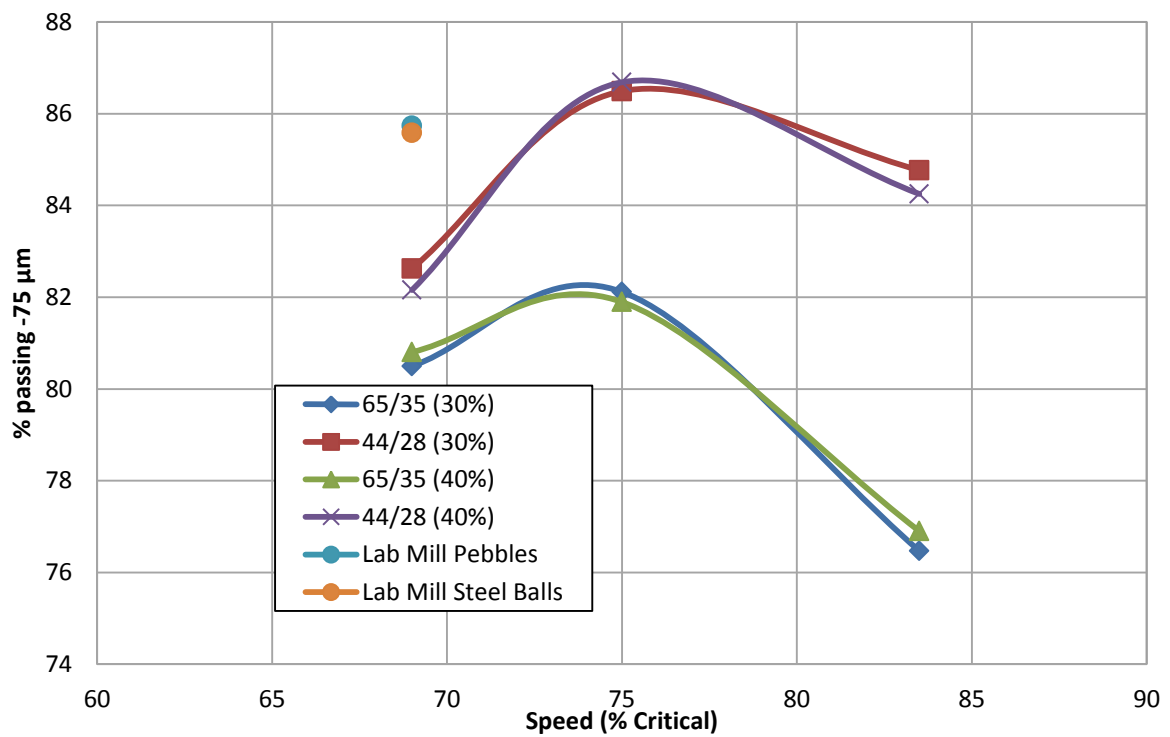
Figure 4-36: Per cent passing obtained in 0.3 m diameter mill

101

The wear rate of the rocks was an important consideration when scaling down from the larger 1.2 m diameter mill to the smaller 0.3 m diameter mill. Plotting the mass of wear per unit time would be useless since a direct comparison could not be made. By plotting the wear rate per unit energy consumed as shown in Figure 4-37 a direct comparison could be made to the larger mill. The figure shows that for the same energy input the wear rate is only slightly higher than the equivalent condition in the larger mill.

Figure 4-38 is a plot of the wear from the pebbles as a percentage of the total feed entering the mill. This total feed includes the mass of fines as well as the top up of fresh rock. The plot shows a slight drop in percentage wear from the equivalent condition in the larger mill. This method of expressing the wear rate of pebbles is a useful way of checking whether ratio of fresh rock top up to fines was affected in the scaling down process. This figure demonstrate despite the huge scale down in size the ratio of fresh rock top up to fines remained relatively constant as shown by the relatively constant percentage wear in Figure 4-38.
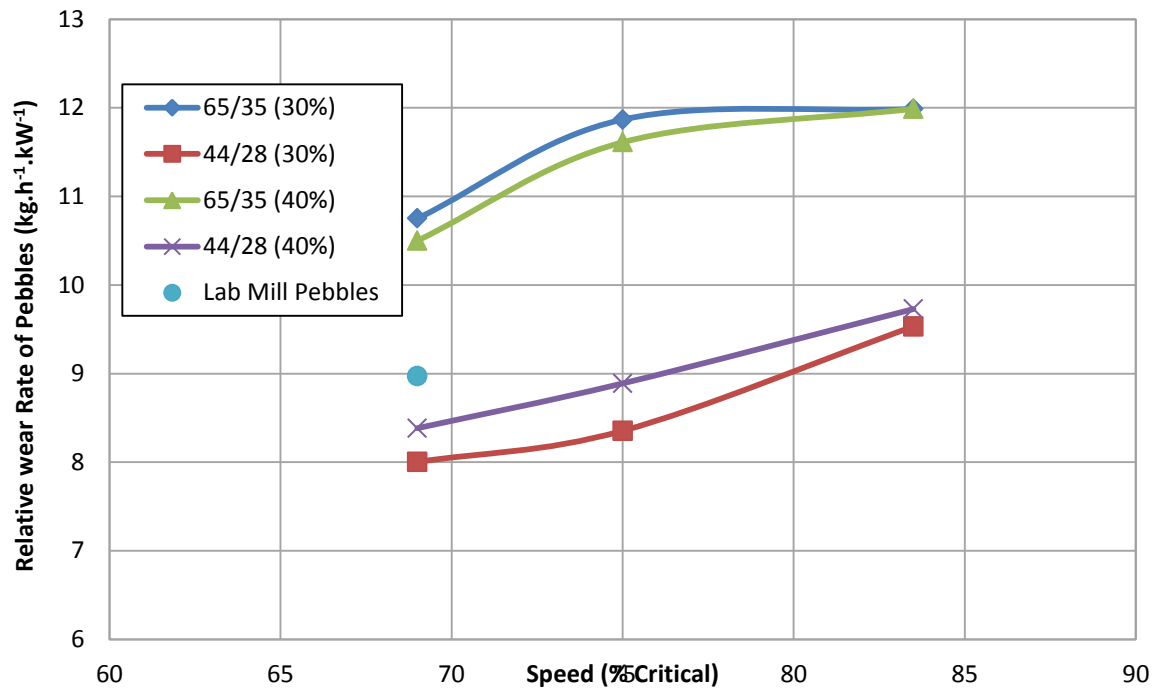
Figure 4-37: Relative wear rate obtained in 0.3 m diameter mill
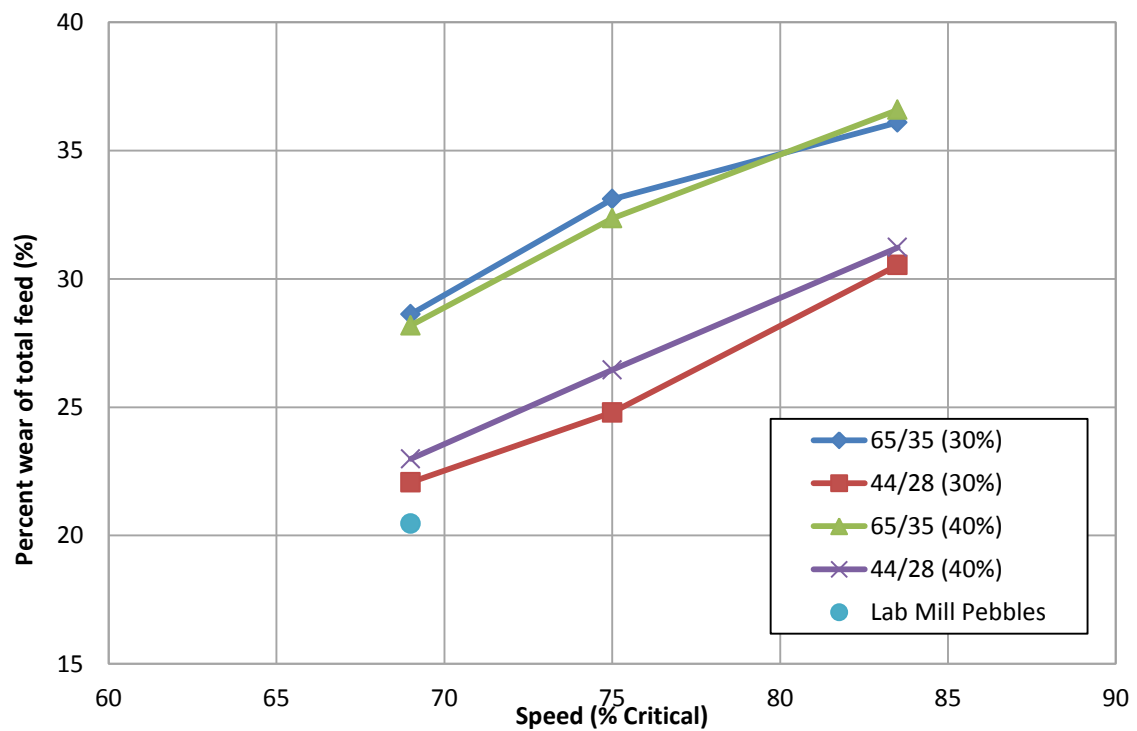
Figure 4-38: Pebble wear as percentage of total charge mass

Figure 4-39 is a plot of the grinding efficiency as a function of mill speed for the pebbles and steel balls in the smaller mill. Included in the plot is the grinding efficiency for all other runs in the larger mill. Considering the pebbles and steel balls in the smaller mill clearly the pebbles are more efficient than an equivalent size distribution of steel balls. It is well known principle that the balls size should be tailored depending on the size of the ore to grind. Evidently the entering feed is too fine for the larger balls thus the decrease in efficiency. However, the substitution of balls with pebbles, reduced the power by 42%. Hence, throughput would be adversely affected, unless the milling volume is increased. For an older mine, the milling volume could be increased by making use of the available spare mills.

When scaling down from the larger 1.2 m diameter mill to the smaller 0.3 m diameter mill it was first thought that the grinding efficiency would be higher. This principle is well known and is related to the difference in diameters of the two mills. The lower grinding efficiency may be attributed to the removal of the chips from the charge. The size distribution in the smaller mill was matched exactly to that in the larger mill but the chips were removed from the charge since equivalent sized steel balls could not be sourced. By accidently stumbling across this discovery it shows how the presence of these critical sized ore particles actually hinder the grinding process and cause a decrease in efficiency. Perhaps by screening the classifier under flow and the recycling the critical size particles to the primary mill instead of the pebble mill an increase in efficiency may be observed. The chips, which are produced during the fast chipping phase of pebble wear, probably become trapped between rocks thereby reducing abrasion/attrition thus the reason for the drop in efficiency.

Figure 4-40 is plot of the product size distribution in cumulative form for both pebbles and steel balls as a grinding medium. For similar per cent passing 75 μm the pebbles produce a finer grind with a narrow size range. The main mechanism when using steel balls as a grinding media is crushing or impact grinding with some attrition and no abrasion since there are no rocks present. When using pebbles as a grinding media size reduction occurs as a result of a combination of crushing, abrasion and attrition. The proportion of crushing to abrasion/attrition is much larger when using steel balls than when using pebbles. The fact that for similar per cent passing 75 μm the pebbles produce a finer grind proves the hypothesis that the progeny from the crushing is much coarser than the progeny from abrasion/attrition. The results of this section of tests are shown in Table 4-6. The main observation in Table 4-5 is that by using pebbles as a grinding medium the energy consumption is reduced by 26.14% however the throughput is also reduced by 42.28%.
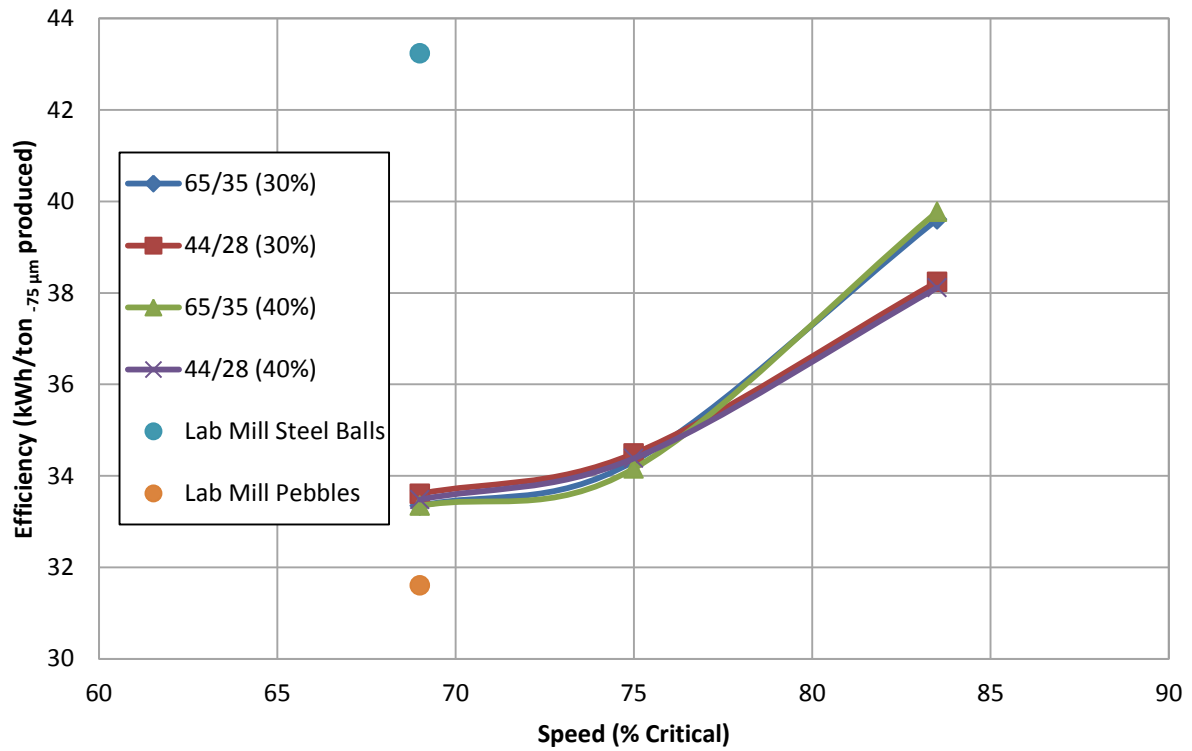
Figure 4-39: Grinding efficiency in 0.3 m diameter mill
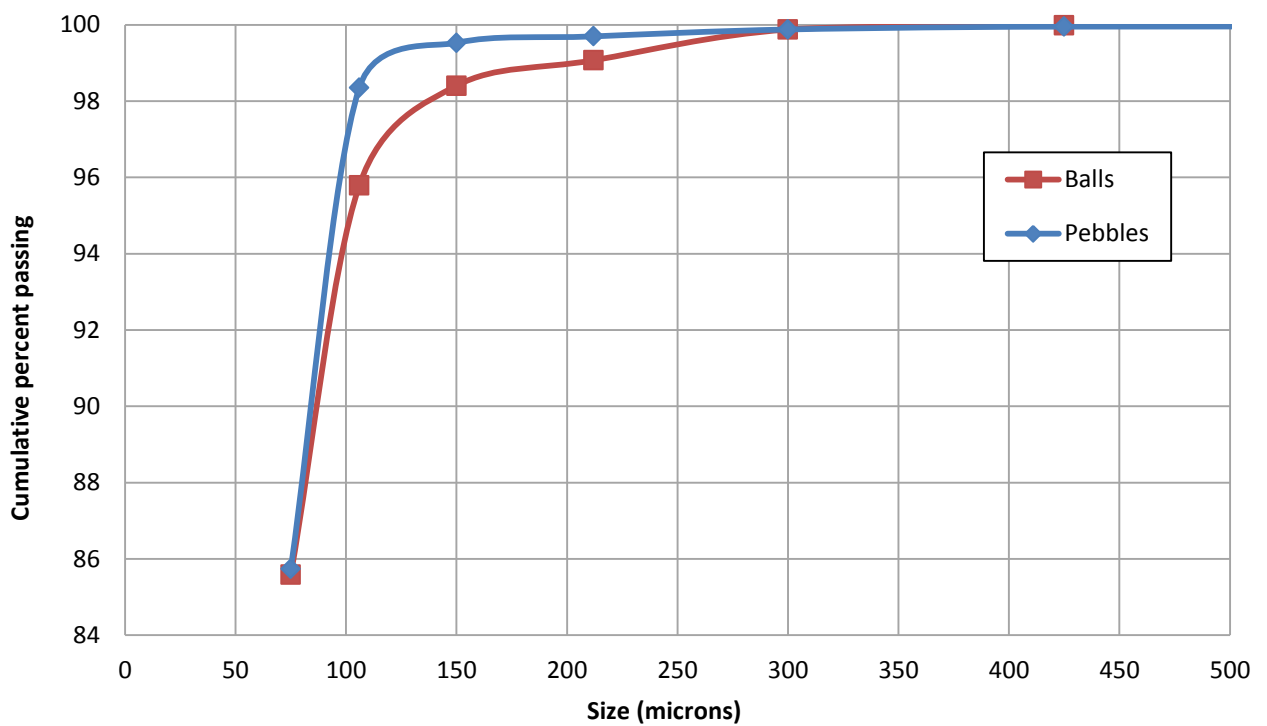
Figure 4-40: Product size distribution comparison between pebbles and balls

105

Table 4-6: Summary of results in 0.3 m diameter mill at 40% filling

Run ID (Average)	nm run 1,2	nm run 3
Speed (% Critical)	69	69
Media	Pebbles	Balls
Media Size (mm)	44/28	44/28
% filling	40%	40%
Total charge mass (g)	11264	33340
Power (W)	50	117
Wear rate(g)	571	n/a
% passing -75 μm	85.74	85.58
Total mass of fines recovered(kg)	2.29	2.29
mass of -75(kg)	1.96	1.96
Time (min)	75.16	43.30
Efficiency (kWh/ton $_{-75\ \mu m\ produced}$)	31.93	43.24
Per Cent Reduction	26.14%	0%
Productivity(kg$_{-75\ \mu m\ produced}$/min)	0.03	0.05
Per Cent Reduction	42.28%	0%
Energy input (kWh/ton $_{fresh\ feed}$)	36.89	37.01
Relative wear (kg$_{wear}$ /h/kw)	9.10	n/a
Wear rate(kg$_{wear}$ /h)	0.46	n/a
Per cent Wear rate (kg$_{wear}$/kg$_{charge}$)	20.09	n/a

4.8 Implications

The implications of the findings have different outcomes, depending on the current operating conditions of each mine. For the processing plant located on the reference gold mine with its current operating conditions and objectives the implication are somewhat different. The mine currently uses a rod mill with secondary pebble milling. The feed to this plant contains a relatively small amount of reef and most of the rock contains no gold. Waste material from above and below the reef is mined to provide sufficient space for mining activity. Waste material is also mined to provide tunnels, but a relatively small amount of reef is found mixed in this material. Hence stockpiles of ‗waste' are processed as required, when the rate of mining is reduced. The mine could choose to change the pebble feed size by simply switching the top and bottom screens from 65/35 mm to 44/28 mm which is a relatively easy and inexpensive task.

The speed of the mill could also be changed by changing the size of a gear. The implementation of each procedure would only be justified if the savings realised by the reduction in energy usage allowed for a relatively short payback period. Each change also causes a change in the throughput. A change which causes a decrease in throughput would mean that the plant would run for a longer period increasing the operating costs. An economic analysis would reveal if the potential changes are feasible.

Sometimes a mine may choose to use media in the pebble mill which is not of the ore itself. For example some mines may use waste rock as a grinding medium only. In this case the use of smaller pebbles would be more suitable. Apart from the reduction in energy usage the lower wear rate of the smaller pebbles would reduce the dilution by pebbles containing no gold. Sometimes a steady supply of pebbles is not guaranteed so the use of smaller pebbles with a lower consumption would be justified. Most gold mines in South Africa use ROM mills and are operating at reduced throughput. Spare mills are available and it may be possible to convert the ROM mills into primary mills with pebble ports. Throughput would increase, due to discharge of pebbles, which could be used for more efficient secondary milling (using spare mills).

Another application of pebble milling is in secondary milling of the feed to base metal flotation plants, or platinum flotation plants. Media consumption contributes as much as 30% to the total operating consumables. By replacing the steel balls in the secondary milling stage with pebbles, the cost associated with media consumption is eliminated. With the absence of

steel in the ground ore the flotation of sulphide ores is improved. However extra capital is needed for larger diameter secondary mills and for pebble transfer and storage.

One other important implication of this research is the development of a batch test procedure, which makes it possible to assess pebble milling, using a relatively small sample. It is envisaged that this procedure could be applied using a smaller mill (say 0.6m diameter) and possibly even on drill cores.

5. CONCLUSIONS

- A simple empirical model has been used to predict steady state size distribution and this has proved to be a resource and time saving tool. The rate of wear of size fractions of rounded pebbles should be measured using an appropriate range of pebble sizes in the mill. Even if steady-state is not reached the model would only serve to decrease the number of runs needed until steady state is reached thereby saving time and using less ore sample.

- The development of a semi-batch testing procedure has proved to be an accurate method of assessing a pebbling milling circuit using a relatively small amount of ore.

- The data obtained by testing the effects of mill speed and pebbles feed size could be used by a mine currently using a pebble milling circuit to fine tune the circuit in order to optimise it according to their needs regarding energy consumption or throughput.

- The tests have shown that the gold mine from which the sample was obtained has the following options: The various options and predicted effects are as follows:
  - Use original pebble feed size (65/35 mm) and reduce mill speed to 75% of critical speed to realise a 13.35% drop in power consumption with a 1.88% increase in production and a 12.60% decrease in pebble consumption.
  - Use original pebble feed size (65/35 mm) and reduce mill speed to 69% of critical speed to realise a 15.81% drop in power consumption with a 6.22% decrease in production and a 29.18% decrease in pebble consumption.
  - Use the original speed (83.5% of critical speed) and change the pebble feed size to 44/28 mm to realise a 3.45% drop in power consumption with a 1.11% increase in production and a 22.36% decrease in pebble consumption.
  - Reduce mill speed to 75% of critical speed and change the pebble feed size to 44/28 mm to realise a 12.92% drop in power consumption with a 4.07% decrease in production and a 41.78% decrease in pebble consumption.
  - Reduce mill speed to 69% of critical speed and change the pebble feed size to 44/28 mm to realise a 15.14% drop in power consumption with an 11.70% decrease in production and a 49.97% decrease in pebble consumption.

- Mill power was not affected by changes in the size distribution of the pebbles. This implies that the trajectory of the charge was not affected.

- The smaller pebbles grind finer than the larger pebbles. On a lab scale it seems that the larger rocks are more efficient at lower speeds while the smaller rocks are more efficient at higher speeds. There seems to be an optimum speed for each pebble size. Due to the

109

relatively high proportion of production coming from pebble wear, grinding efficiency is sensitive to pebble consumption. It was pleasing to note that pebble consumption at the Nkomati mine is of the same order (about 30 % of total production). (Bradford et al., 1998).

- Pebble consumption was reduced when the steady state mill charge and feed was changed from a simulated 65/35mm feed to a 44/28mm feed. This is thought to be due to the reduction of impact forces in the mill.

- Test repeated at a higher volumetric filling showed similar trends with respect to pebble wear, per cent passing 75 μm and power draw. i.e. the relatively low level in the mill, which was used to reduce labour, did not produce unrealistic results.

- The product size distribution revealed that the greater the top up of fresh rock the coarser the grind.

- Tests at higher speeds and volumetric fillings were used to illustrate how maximum power could be achieved. For this type of ore the optimum speed is 85% critical while the optimum volumetric filling is 55%. This may be a way of achieving maximum capacity. The trends observed at lower speeds indicated that power efficiency was likely to be far from optimum.

- The comparison to steel balls revealed that pebbles grind with a greater efficiency than steel balls but a large drop in throughput is observed. In this test a 26.14% reduction in power consumption is observed with a 42.28% drop in throughput. This is no problem for older mines where tonnage has been reduced and spare mills are available.

6. RECOMMENDATIONS

- Modelling of pebble rounding, particularly the initial phase will help quantify the potential for accumulation of chips in a pebble mill. This appears to impact on grinding efficiency
- Testing could be done on smaller scale to reduce the amount of work done by operator.
- It is recommended that the speed of the pebble mills at the reference gold mine be reduced to 75% of critical speed.
- An economic analysis should be performed on all options, particularly mines with spare capacity such as gold mines and the plant operated by Palabora Mining Company.

REFERENCES

1. AUSTIN, L. G., KLIMPEL, R. R. & LUCKIE, P. T. 1984. Ball wear and ball size selection. *Process Engineering of Size Reduction: Ball Milling,* AIME, New York**,** p426.
2. AUSTIN, L. G., MENACHO, J. M. & PEARCY, F. 1987. A general model for semi-autogenous and autogenous milling. *APCOM 87. Proceedings of the Twentieth International Symposium on the Application of Computers and Mathematics in the Mineral Industries.,* Volume 2: Metallurgy Johannesburg, SAIMM**,** pp. 107 - 126.
3. BRADFORD, L., MCINNES, C., STANGE, W., DE BEER, C., DAVID, D. & JARDIN, A. 1998. The development of the proposed milling circuit for the Nkomati main concentrator plant. *Minerals Engineering,* 11**,** 1103-1117.
4. HAHNE, R., PÅLSSON, B. I. & SAMSKOG, P. O. 2003. Ore characterisation for—and simulation of—primary autogenous grinding. *Minerals Engineering,* 16**,** 13-19.
5. HOLMBERG, K. I. & LIDSTRÖM, L. J. 1993. Fine grinding experience with vertically stirred ball mills.
6. HOWAT, D. D. & VERMEULEN, L. A. 1988. Pebbles as a grinding medium: Interrelationships of some molling parmeters. *Journal of South African Institute of Mining and Metallurgy,* 88**,** pp. 393-400.
7. JONES, S. M. & HOLMBERG, K. L. 1996. Modern Grinding Mill Designs. *Changing Scopes in Mineral Processing*.
8. KELLY, E. G. & SPOTTISWOOD, D. J. 1982. *Introduction to Mineral Processing*, John Wiley & Sons.
9. KETELHODT, L. V. 2009. Viability of optical sorting of gold waste rock dumps. *World Gold Conference 2009*.
10. KOIVISTOINEN, P. 1995. ―Significance of Comminution Circuit Design". *The XIXth International Mineral Processing Congress,* San Francisco, USA.
11. KOIVISTOINEN, P., VIRTANEN, M., EEROLA, P. & KALAPUDAS, R. 1989. A Comminution Cost Comparison of Traditional Metallic Grinding, Semiautogenous Grinding (SAG) and Two-Stage Autogenous Grinding. *International Conference on Autogenous /Semiautogenous Grinding,* Vancouver, Canada.
12. LOVEDAY, B. K. 2001. THE USE OF SMALL PEBBLES FOR SECONDARY GRINDING. *SAG 2001 Proceedings, Vancourver, BC Canada***,** Pg. 149-158.
13. LOVEDAY, B. K. 2010. The Small Pebble process for reducing ball and power comsumption in secondary grinding. *25 th International Mineral Processing Congress*.
14. LOVEDAY, B. K. & DONG, H. 2000. Optimisation of autogenous grinding. *Minerals Engineering,* 13**,** 1341-1348.
15. LOVEDAY, B. K., MORRISON, R. D., HENRY, G. & NAIDOO, U. 2006. An Investigation of Rock Abrasion and Breakage in a Pilot-scale Mill. *SAG 2006 Proceedings, Vancourver, BC Canada***,** Pg 1-8.
16. LOVEDAY, B. K. & NAIDOO, D. 1997. Rock abrasion in autogenous milling. *Minerals Engineering,* 10**,** 603-612.
17. LOVEDAY, B. K. & WHITEN, W. J. 2002. Application of a rock abrasion model top pilot-plant and plant data for fully and semi-autogenous grinding. *Trans. IMMt, Section C. 111***,** C39–C43.

18. MACLEOD, N. 2002. Geometric morphometrics and geological shape-classification systems. *Earth-Science Reviews,* 59**,** 27-47.

19. MCIVOR, R. E. & GREENWOOD, B. R. 1996. Pebble Use and Treatmentat Cleveland-Cliffs Autogenous Milling Operations. *SAG 1996 Proceedings, Vancourver, BC Canada***,** 1129-1141.

20. MELLBERG, F. & SODERMAN, A. 1996. Single autogenous grinding in Zinkgruvan. Experiences and developments of crushing critical size fractions in the grinding circuit. *In Proceedings of SAG 96,* Vancouver, September**,** pp. 1081-1103.

21. MOODLEY, R. S. 1997. A study of pulp flow and grinding efficiency in autogenous and pebble mills. *MSc thesis,* University of Natal, 1997.

22. MUSA, F. & MORRISON, R. 2009. A more sustainable approach to assessing comminution efficiency. *Minerals Engineering,* 22**,** 593-601.

23. NAIDOO, D. 2000. A laboratory-scale investigation of factors affecting autogenous milling. *MSc thesis,* University of Natal, 2000.

24. POWELL, M. S. & MCBRIDE, A. T. 2004. A three-dimensional analysis of media motion and grinding regions in mills. *Minerals Engineering,* 17**,** Pg. 1099-1109.

25. POWELL, M. S., MORRELL, S. & LATCHIREDDI, S. 2001. Developments in the understanding of South African style SAG mills. *Minerals Engineering,* 14**,** 1143-1153.

26. POWELL, M. S. & NURICK, G. N. 1996a. A study of charge motion in rotary mills Part 1—extension of the theory. *Minerals Engineering,* 9**,** 259-268.

27. POWELL, M. S. & NURICK, G. N. 1996b. A study of charge motion in rotary mills part 3—Analysis of results. *Minerals Engineering,* 9**,** 399-418.

28. POWELL, M. S., VAN DER WESTHUIZEN, A. P. & MAINZA, A. N. 2009. Applying grindcurves to mill operation and optimisation. *Minerals Engineering,* 22**,** 625-632.

29. RADZISZEWSKI, P. 2002. Exploring total media wear. *Minerals Engineering,* 15**,** 1073-1087.

30. RANTANEN S., LAHTINEN M. & W., S. 1996. Operation of ―Outogenenius" type grinding at Forestania Nickel Mines. *International Conference on Autogenous and Semiautogenous Grinding Technology 1996,* Vancouver, B.C.,Canada.

31. STANLEY, G. G. 1974. Mechanisms in the autogenous mill and their mathematical representation. *Journal of South African Institute of Mining and Metallurgy 75 (4)***,** pp. 77–98.

32. STUART, M. & JONES, S. M. 2001. Autogenous and Semiautogenous Mill. *SAG 2001 Proceedings, Vancourver, BC Canada***,** Pg. 362-372.

33. WIPF, E. 1996. To SAG or not to SAG? *In Proceedings of SAG 96,* Vancouver (September 1996)**,** pp. 1049–1062.

APPENDIX A: DERIVATION OF POWER EQUATION

$$P = \frac{W}{t} \qquad\qquad (A - 1)$$

Where P = Power (W)

　　W = Work (J)

　　t = Time (s)

Since

$$W = F \times s \qquad\qquad (A - 2)$$

Where F = Force (N)

　　s = Distance (m)

Substituting Equation A-2 into Equation A-1

$$P = \frac{F \times s}{t} \qquad\qquad (A - 3)$$

Since the effective distance travelled by the mill shell is given by:

$$s = 2\pi r \times f_r \qquad\qquad (A - 4)$$

Where r = Mill radius (m)

f_r = Rotational frequency/number of mill revolutions

Substituting Equation A-4 into Equation A-3

$$P = \frac{F \times 2\pi r \times f_r}{t} \qquad\qquad (A - 5)$$

Rearranging Equation A-5

$$P = F \times r \times 2\pi \times \frac{f_r}{t} \qquad\qquad (A - 6)$$

Grouping terms in Equation A-6 and changing units of time from seconds to minutes

$$P = (F \times r) \times \left(\frac{2\pi}{60}\right) \times \left(\frac{f_r}{t}\right) \qquad (A-6)$$

Where t = Time (min)

Since

$$RPM = \frac{f_r}{t} \qquad (A-7)$$

Where RPM = Revolutions per minute (rpm)

And Since

$$\tau = F \times r \qquad (A-8)$$

Where τ = Rotational torque (Nm)

Substituting Equation A-7 and Equation A-8 into Equation A-6 gives the power equation.

$$P = \tau \times \left(\frac{2\pi}{60}\right) \times RPM \qquad (A-9)$$

APPENDIX B1: CALIBRATION DATA (1.2 M DIAMETER MILL)

Table B1- 1: Data used for power measurement calibration

Mass(kg)	Force(N)	Torque(N.m)	Voltage(mV)
0.00	0.00	0.00	1.07
4.99	48.98	29.39	1.13
10.01	98.17	58.90	1.19
15.02	147.39	88.43	1.25
20.04	196.63	117.98	1.35
25.04	245.62	147.37	1.41
30.05	294.76	176.86	1.47
35.04	343.76	206.26	1.55
40.06	393.00	235.80	1.62
45.07	442.17	265.30	1.69
50.08	491.30	294.78	1.77
55.09	540.39	324.24	1.83
60.08	589.37	353.62	1.91
65.10	638.62	383.17	1.98
70.11	687.81	412.69	2.06
75.13	737.03	442.22	2.13
80.67	791.39	474.83	2.21
86.05	844.11	506.47	2.28
90.61	888.90	533.34	2.35
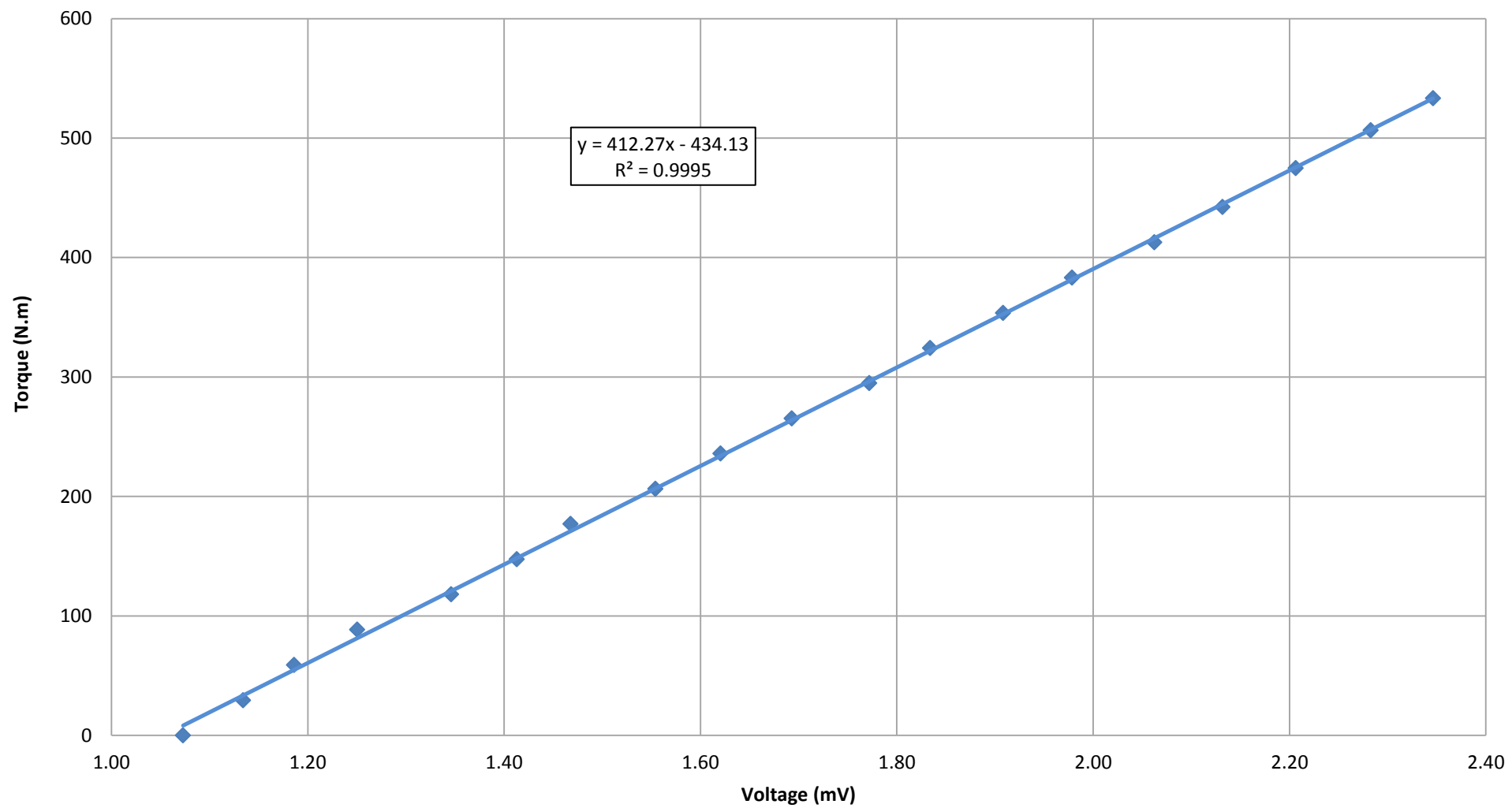
Figure B1- 1: Calibration graph showing the relation between torque and voltage

APPENDIX B2: CALIBRATION DATA (0.3 M DIAMETER MILL)

Table B2- 1: Data used for power measurement calibration

Mass(kg)	Force(N)	Torque(N.m)	Voltage(mV)
0.00	0.00	0.00	0.86
4.29	42.11	6.32	1.13
6.60	64.76	9.71	1.28
8.76	85.89	12.88	1.44
10.93	107.24	16.09	1.59
13.04	127.96	19.19	1.74
15.38	150.87	22.63	1.909
17.62	172.86	25.93	2.06
22.67	222.37	33.36	2.35
28.02	274.85	41.23	2.71

118

Table B2- 1: Data used for power measurement calibration
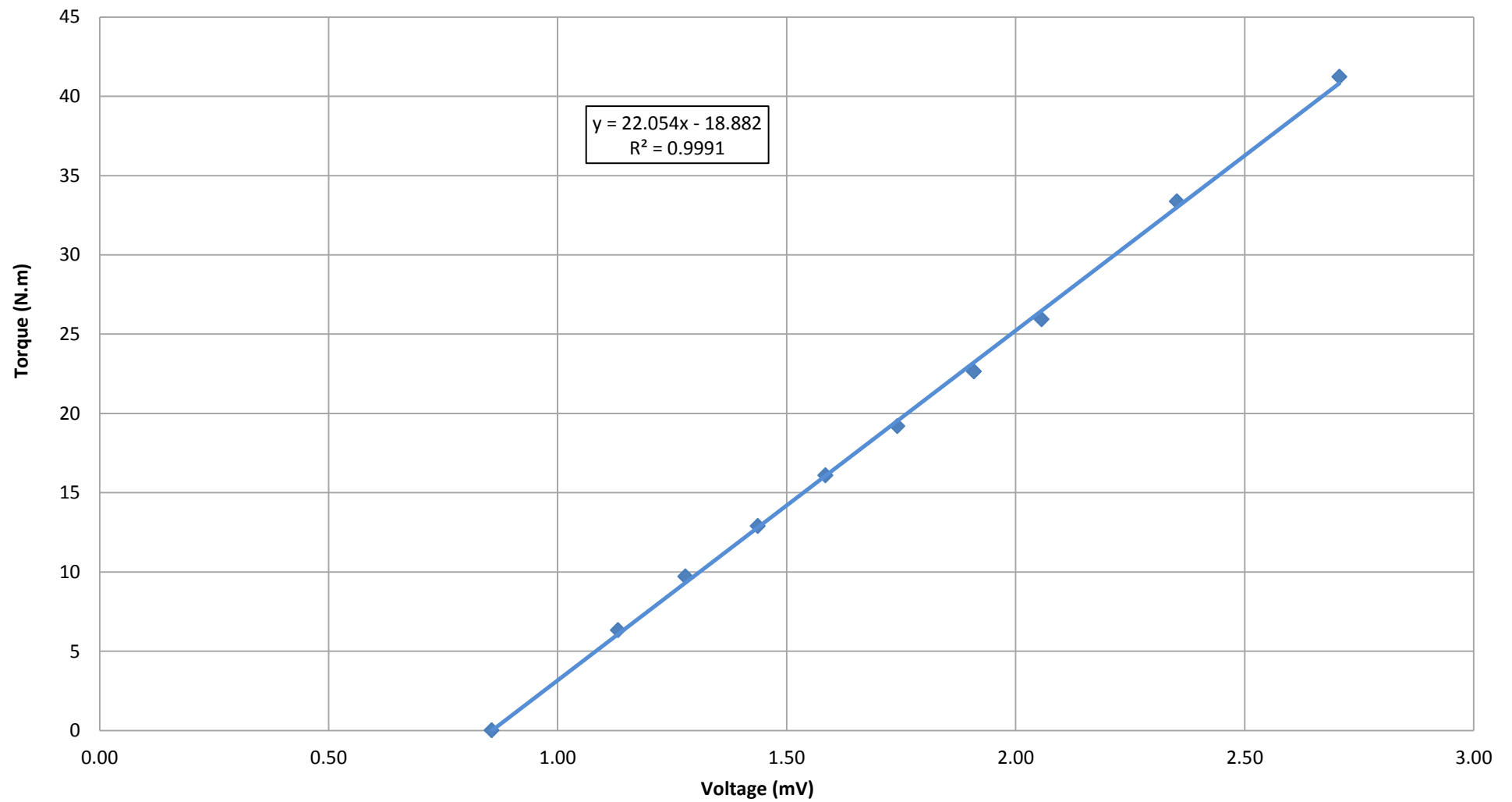
Figure B2- 1: Calibration graph showing the relation between torque and voltage

APPENDIX C: SAMPLE CALCULATION OF RECALCULATED TIME

For a given set of operating conditions i.e. mill speed (φ), volumetric filling (J), pebble feed size the energy input per ton of feed is relatively constant.

For conditions where:

Mill speed (φ) = 83.5 % Critical

Volumetric filling (J) = 30%

Pebble feed size = 44/28 mm

Required:

Mass of fines (M_1) = 20 kg

Power (P_1) = 1.578 kW

Time of grind (t_1) = 35 minutes

Then for a new set of operating conditions where:

Mill speed (φ) = 83.5 % Critical

Volumetric filling (J) = 40%

Pebble feed size = 44/28 mm

Required:

Mass of fines (M_2) = 27.58 kg

The mill was then run for a short while just to get sample of the power usage.

So that:

Power (P_2) = 1.797 kW

The new time for grinding (t_2) is determined as follows.

$$\left(\frac{total\ engery\ input}{ton\ of\ feed}\right)_{condition\ 1} = \left(\frac{total\ engery\ input}{ton\ of\ feed}\right)_{condition\ 2}$$

$$\left(\frac{P_1 t_1}{M_1}\right) = \left(\frac{P_2 t_2}{M_2}\right)$$

Rearranging:

$$t_2 = \left(\frac{M_2}{P_2}\right)\left(\frac{P_1 t_1}{M_1}\right)$$

Substituting values to calculate new time:

$$t_2 = \left(\frac{27.58 \; kg}{1.797 \; \cancel{kW}}\right)\left(\frac{1.578 \; \cancel{kW} \times 35 \; min}{20 \; \cancel{kg}}\right)$$

$$t_2 = 42.4 \; min$$

121

APPENDIX D: ADDITIONAL TABLES, FIGURES AND RAW DATA

APPENDIX D1: PRELIMINARY TESTING DATA– LOCAL ORE

Table D1- 1: Initial size distribution of 75/35 mm rocks

Size (mm)		Mass (kg)	Count	% Passing	Cum % Pass	Shape Factor
				Run 1(In)		
75	65	31.40	60	100	100	1.01
65	53	0	0	0	0	0
53	37.5	0	0	0	0	0
37.5	26.5	0	0	0	0	0
26.5	22.4	0	0	0	0	0
22.4	19	0	0	0	0	0
Total		31.40	60	100		

Table D1- 2: Change in size distribution of 75/65 mm rocks after 15 minutes

Size (mm)		Mass (kg)	Count	% Passing	Cum % Pass	Shape Factor
				Run 2 (In)		
75	65	13.93	26	51.07	100	1.03
65	53	13.35	31	48.93	48.93	1.38
53	37.5	0	0	0	0	0
37.5	26.5	0	0	0	0	0
26.5	22.4	0	0	0	0	0
22.4	19	0	0	0	0	0
Total		27.27	57	100		

Table D1- 3: Change in size distribution of 75/65 mm rocks after 30 minutes

Size (mm)		Mass (kg)	Count	% Passing	Cum % Pass	Shape Factor
				Run 3(In)		
75	65	7.89	14	31.94	100	1.08
65	53	16.81	39	68.06	68.06	1.38
53	37.5			0	0	0
37.5	26.5			0	0	0
26.5	22.4			0	0	0
22.4	19			0	0	0
Total		24.70	53	100		

Table D1- 4: Change in size distribution of 75/65 mm rocks after 60 minutes

Size (mm)		Mass (kg)	Count	% Passing	Cum % Pass	Shape Factor
Run 4(In)						
75	**65**	4.82	8	21.77	100.00	1.16
65	**53**	16.76	40	75.75	78.23	1.34
53	**37.5**	0.55	2	2.48	2.48	1.95
37.5	**26.5**	0	0	0	0	0
26.5	**22.4**	0	0	0	0	0
22.4	**19**	0	0	0	0	0
Total		22.12	50	100		

Table D1- 5: Change in size distribution of 75/65 mm rocks after 90 minutes

Size (mm)		Mass (kg)	Count	% Passing	Cum % Pass	Shape Factor
Run 5(In)						
75	**65**	4.72	8	22.91	100	1.13
65	**53**	15.37	38	74.61	77.09	1.30
53	**37.5**	0.51	2	2.48	2.48	1.82
37.5	**26.5**			0	0	0
26.5	**22.4**			0	0	0
22.4	**19**			0	0	0
Total		20.60	48	100		

123
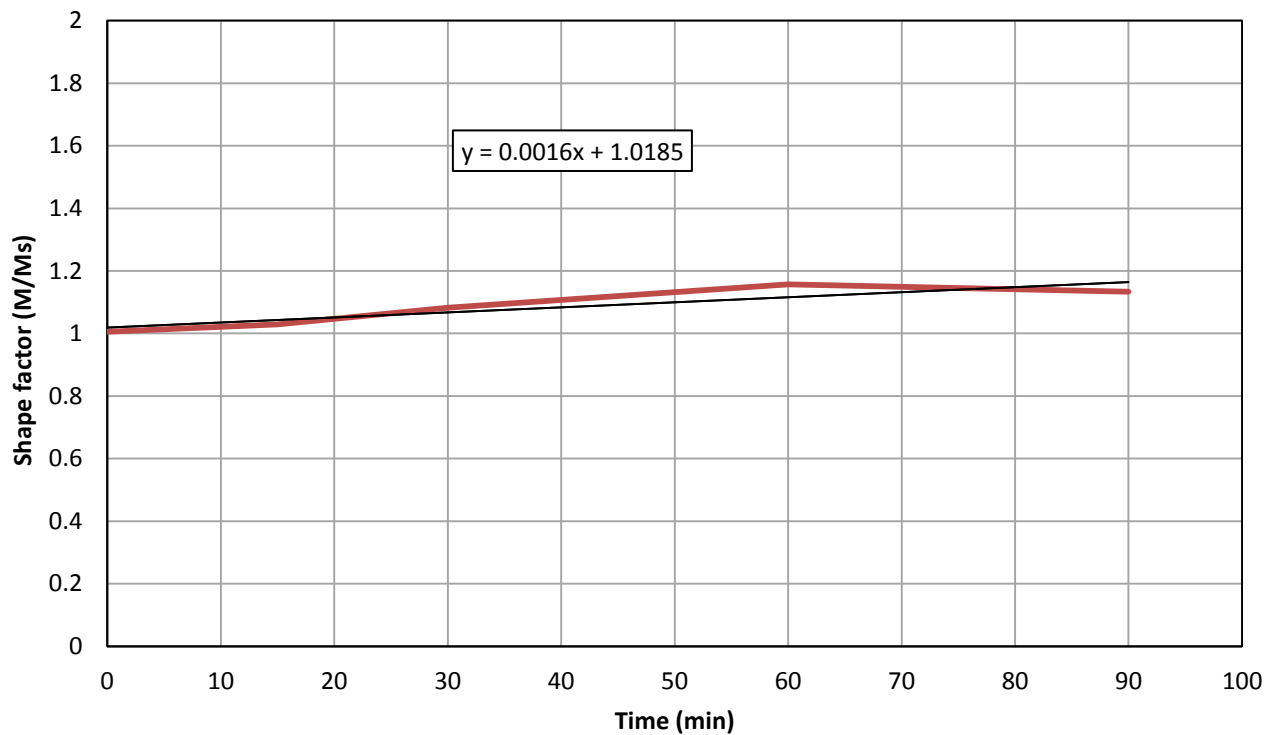
Figure D1- 1: Change in Shape factor of 75/65 rocks with time
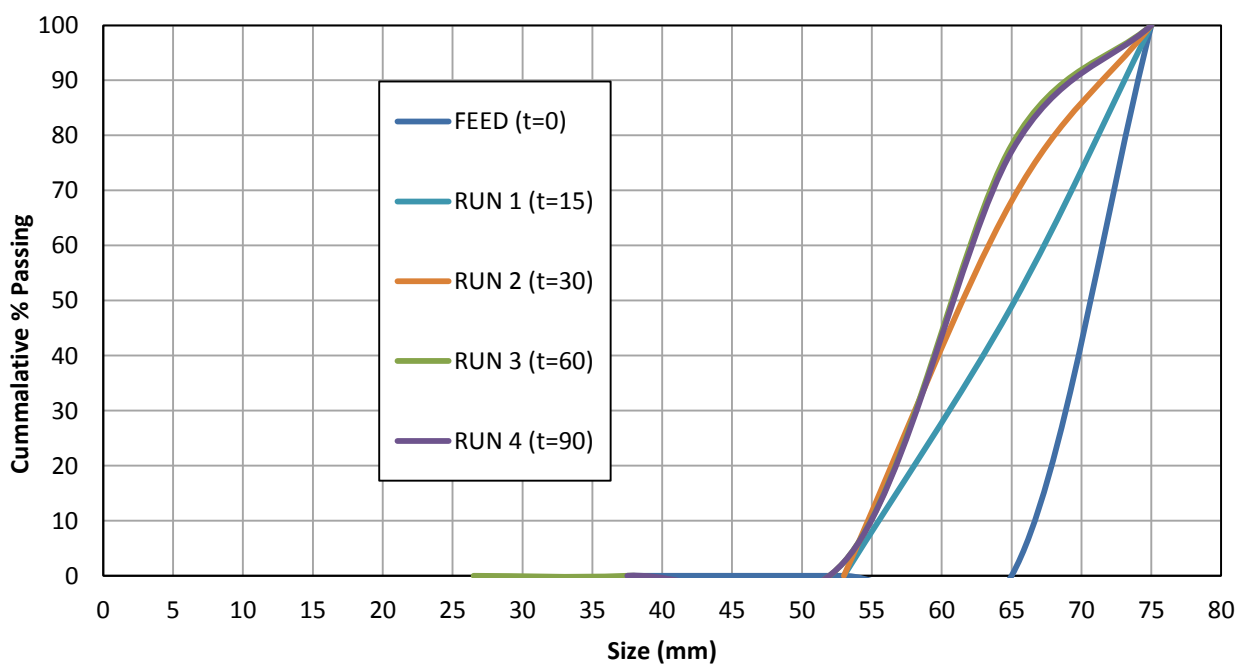
Figure D1- 2: Change in size distribution of 75/65 rocks with time

Table D1- 6: Initial size distribution of 65/53 mm rocks

Size (mm)		Mass (kg)	Count	% Passing	Cum % Pass	Shape Factor
Run 1(In)						
75	**65**	0	0	0	100	0
65	**53**	20.58	60	100	100	1.10
53	**37.5**	0	0	0	0	0
37.5	**26.5**	0	0	0	0	0
26.5	**22.4**	0	0	0	0	0
22.4	**19**	0	0	0	0	0
Total		20.58	60	100		

Table D1- 7: Change in size distribution of 65/53 mm rocks after 15 minutes

Size (mm)		Mass (kg)	Count	% Passing	Cum % Pass	Shape Factor
Run 2(In)						
75	**65**	0	0	0	100	0
65	**53**	14.05	41	78.43	100	1.10
53	**37.5**	3.87	18	21.57	21.57	1.53
37.5	**26.5**	0	0	0	0	0
26.5	**22.4**	0	0	0	0	0
22.4	**19**	0	0	0	0	0
Total		17.92	59	100		

Table D1- 8: Change in size distribution of 65/53 mm rocks after 30 minutes

Size (mm)		Mass (kg)	Count	% Passing	Cum % Pass	Shape Factor
Run 3(In)						
75	**65**	0	0	0	100	0
65	**53**	12.84	40	79.89	100	1.03
53	**37.5**	3.23	16	20.11	20.11	1.44
37.5	**26.5**			0	0	0
26.5	**22.4**			0	0	0
22.4	**19**			0	0	0
Total		16.07	56	100		

Table D1- 9: Change in size distribution of 65/53 mm rocks after 60 minutes

Run 4(In)						
Size (mm)		**Mass (kg)**	**Count**	**% Passing**	**Cum % Pass**	**Shape Factor**
75	**65**	0	0	0	100	0
65	**53**	8.22	24	60.35	100	1.10
53	**37.5**	5.21	24	38.29	39.65	1.54
37.5	**26.5**	0.19	2	1.37	1.37	1.87
26.5	**22.4**			0	0	0
22.4	**19**			0	0	0
Total		13.62	50	100		

Table D1- 10: Change in size distribution of 65/53 mm rocks after 90 minutes

Run 5(In)						
Size (mm)		**Mass (kg)**	**Count**	**% Passing**	**Cum % Pass**	**Shape Factor**
75	**65**	0	0	0	100	0
65	**53**	7.19	22	58.14	100	1.05
53	**37.5**	4.96	22	40.12	41.86	1.60
37.5	**26.5**	0.22	2	1.75	1.75	2.17
26.5	**22.4**			0	0	0
22.4	**19**			0	0	0
Total		12.37	46	100		

126
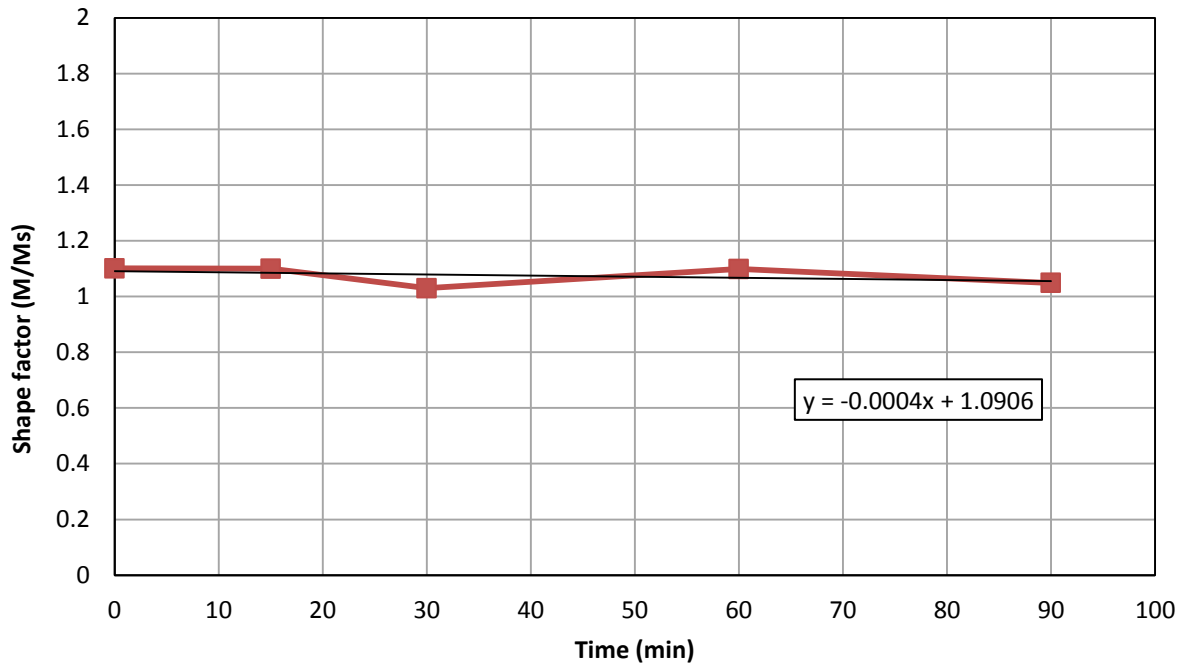
Figure D1- 3: Change in Shape factor of 65/53 rocks with time

$$y = -0.0004x + 1.0906$$
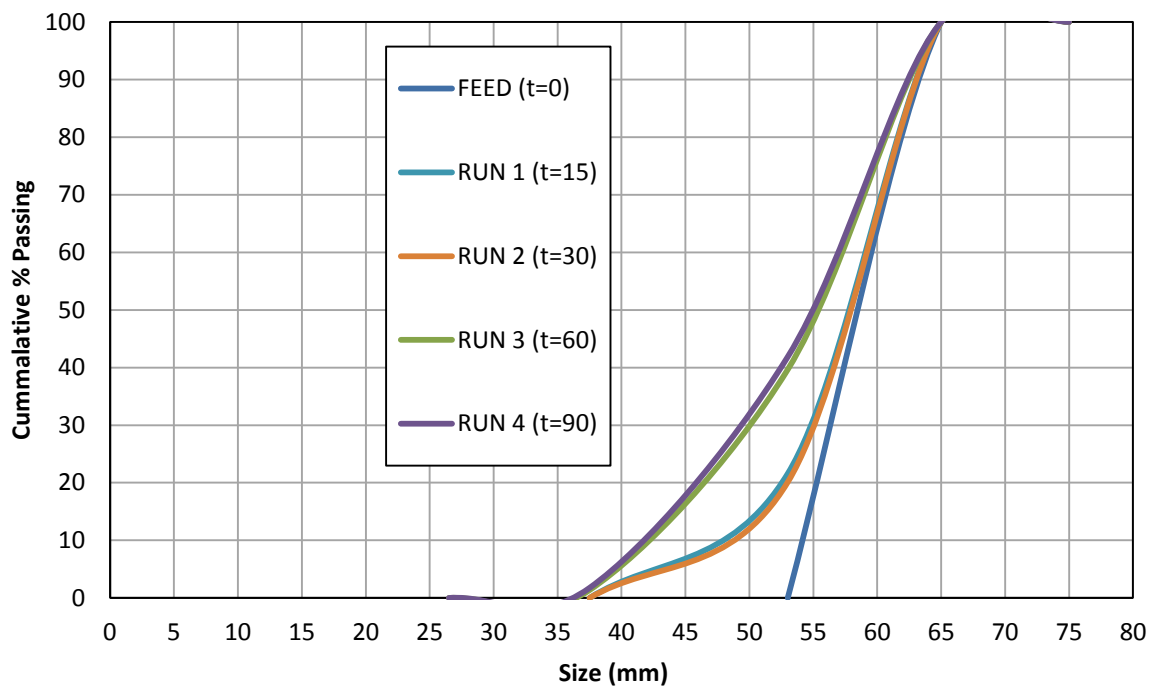
Figure D1- 4: Change in size distribution of 65/53 rocks with time

127

Table D1- 11: Initial size distribution of 53/37.5 mm rocks

Size (mm)		Mass (kg)	Count	% Passing	Cum % Pass	Shape Factor
				Run 1(In)		
75	65	0	0	0	100	0
65	53	0	0	0	100	0
53	37.5	9.66	60	100	100	1.15
37.5	26.5	0	0	0	0	0
26.5	22.4	0	0	0	0	0
22.4	19	0	0	0	0	0
Total		9.66	60	100		

Table D1- 12: Change in size distribution of 53/37.5 mm rocks after 15 minutes

Size (mm)		Mass (kg)	Count	% Passing	Cum % Pass	Shape Factor
				Run 2(In)		
75	65	0	0	0	100	0
65	53	0	0	0	100	0
53	37.5	7.90	51	92.21	100	1.10
37.5	26.5	0.67	7	7.79	7.79	1.92
26.5	22.4	0	0	0	0	0
22.4	19	0	0	0	0	0
Total		8.56	58	100		

Table D1- 13: Change in size distribution of 53/37.5 mm rocks after 30 minutes

Size (mm)		Mass (kg)	Count	% Passing	Cum % Pass	Shape Factor
				Run 3(In)		
75	65	0	0	0	100	0
65	53	0	0	0	100	0
53	37.5	6.83	43	86.96	100	1.13
37.5	26.5	1.02	12	13.04	13.04	1.72
26.5	22.4			0	0	0
22.4	19			0	0	0
Total		7.85	55	100		

Table D1- 14: Change in size distribution of 53/37.5 mm rocks after 60 minutes

Size (mm)		Mass (kg)	Count	% Passing	Cum % Pass	Shape Factor
		Run 4(In)				
75	**65**	0	0	0	100	0
65	**53**	0	0	0	100	0
53	**37.5**	5.77	36	86.90	100	1.14
37.5	**26.5**	0.87	12	13.10	13.10	1.46
26.5	**22.4**			0	0	0
22.4	**19**			0	0	0
Total		6.64	48	100		

Table D1- 15: Change in size distribution of 53/37.5 mm rocks after 90 minutes

Size (mm)		Mass (kg)	Count	% Passing	Cum % Pass	Shape Factor
		Run 5(In)				
75	**65**	0	0	0	100	0
65	**53**	0	0	0	100	0
53	**37.5**	5.37	33	82.73	100	1.16
37.5	**26.5**	1.12	16	17.27	17.27	1.41
26.5	**22.4**			0	0	0
22.4	**19**			0	0	0
Total		6.49	49	100		

129
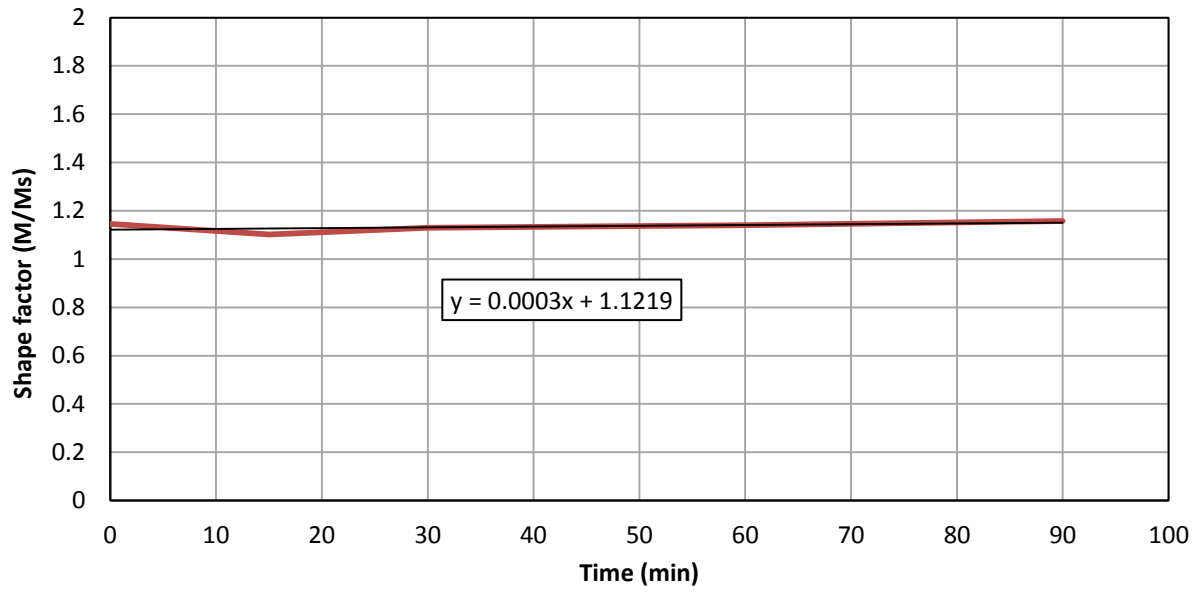
Figure D1- 5: Change in Shape factor of 53/37.5 rocks with time

$y = 0.0003x + 1.1219$
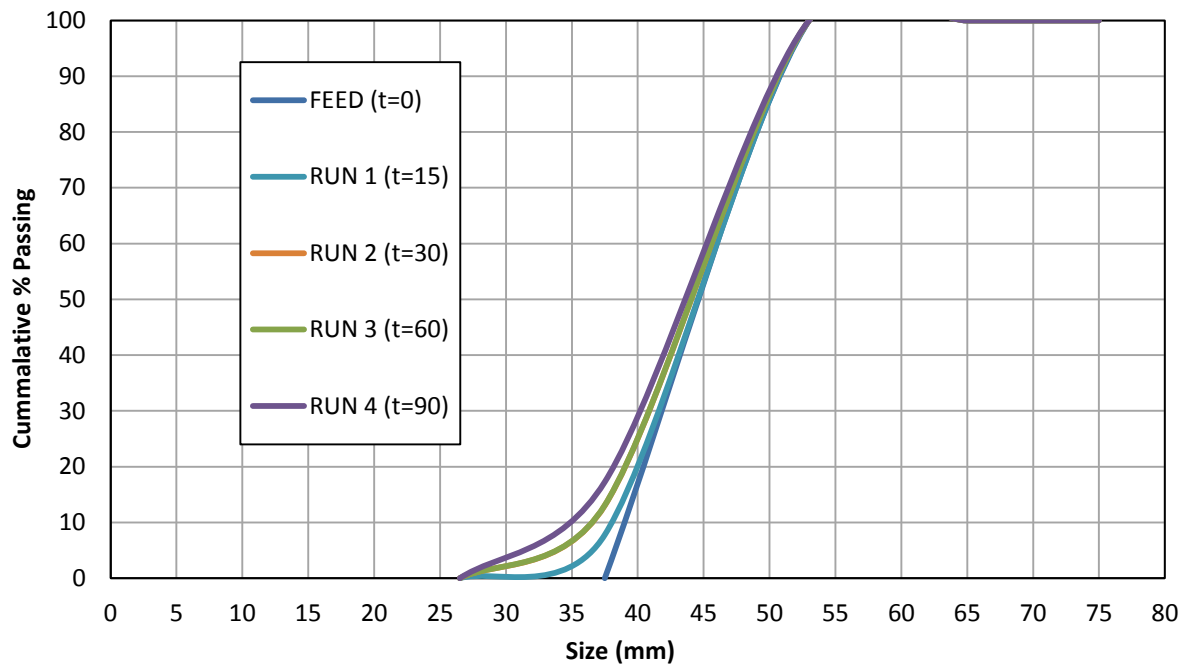
Figure D1- 6: Change in size distribution of 53/44 rocks with time

Table D1- 16: General run data for preliminary testing

	Run1 (In)	Run2 (In)	Run3 (In)	Run4 (In)	Run5 (In)
Mode	Batch	Batch	Batch	Batch	Batch
Time(min)	0	15	15	30	30
Cumulative Time (min)	0	15	30	60	90
Sand(kg)	30	30	30	30	30
Water Ratio(v/v)	0.5	0.5	0.5	0.5	0.5
Red Rock (75/65 mm)	31.40	27.27	24.70	22.12	20.60
Blue Rock (65/53 mm)	20.58	17.92	16.07	13.62	12.37
Yellow Rock (53/37.5 mm)	9.66	8.56	7.85	6.64	6.49
Used make up Rock(kg)	46.30	78.49	87.40	90.84	
Fresh make up Rock(kg)	36.21	11.28	8.69	11.92	
Total Rocks(kg)	144.15	143.52	144.70	145.13	
Count Red Rocks	60	57	53	50	48
Count Blue Rocks	60	57	53	47	44
Count Yellow Rocks	60	58	55	48	49
% Remaining (Red)(Average)	1	0.91	0.89	0.85	0.82
% Remaining (Blue) (Average)	1	0.92	0.88	0.84	0.82
% Remaining (Yellow) (Average)	1	0.92	0.89	0.86	0.82

Run ID: Run 1a

Operating conditions: Pebble Size 65/35; Speed 83.5% Critical; Volumetric filling 30%

Table D2- 1: Sample 1 product size distribution for run 1a

SIZE DISTRIBUTION SAMPLE 1					
Size (µm)		Sample mass (g)	Total mass (kg)	Mass %	% Passing
3300	1180	1.19	0.04	0.12	100.00
1180	425	0.91	0.03	0.09	99.88
425	300	1.73	0.06	0.18	99.79
300	212	8.81	0.28	0.90	99.61
212	150	19.1	0.61	1.95	98.71
150	106	147.96	4.73	15.11	96.76
106	75	52.94	1.69	5.41	81.65
75		746.47	23.89	76.24	76.24
			31.33		

Run ID: Run 1b

Operating Conditions: Pebble Size 65/35; Speed 83.5% Critical; Volumetric filling 30%

Table D2- 2: Sample 1 product size distribution for run 1b

SIZE DISTRIBUTION SAMPLE 1					
Size (µm)		Sample mass (g)	Total mass (kg)	Mass %	% Passing
3300	1180	2.08	0.07	0.21	100.00
1180	425	1.67	0.05	0.17	99.79
425	300	1.79	0.06	0.18	99.62
300	212	7.16	0.23	0.73	99.44
212	150	12.94	0.41	1.32	98.71
150	106	138.90	4.44	14.13	97.39
106	75	66.20	2.12	6.74	83.26
75		752.01	24.06	76.52	76.52
			31.45		

Table D2- 3: Sample 2 product size distribution for run 1b

SIZE DISTRIBUTION SAMPLE 2					
Size (µm)		Sample mass (g)	Total mass (kg)	Mass %	% Passing
3300	1180	1.42	0.05	0.14	100.00
1180	425	1.42	0.05	0.14	99.86
425	300	2.22	0.07	0.23	99.71
300	212	6.39	0.20	0.65	99.49
212	150	15.97	0.51	1.62	98.84
150	106	150.65	4.82	15.33	97.21
106	75	58.47	1.87	5.95	81.88
75		746.34	23.88	75.93	75.93
			31.45		

Run ID: Run 1c

Operating Conditions: Pebble Size 65/35; Speed 83.5% Critical; Volumetric filling 30%

Table D2- 4: Sample 1 product size distribution for run 1c

SIZE DISTRIBUTION SAMPLE 1					
Size (µm)		Sample mass (g)	Total mass (kg)	Mass %	% Passing
3300	1180	3.30	0.11	0.34	100.00
1180	425	1.12	0.04	0.12	99.66
425	300	1.38	0.04	0.14	99.54
300	212	6.97	0.22	0.72	99.40
212	150	10.80	0.35	1.12	98.68
150	106	57.04	1.83	5.92	97.56
106	75	141.75	4.54	14.70	91.64
75		741.65	23.73	76.93	76.93
			30.85		

Table D2- 5: Sample 2 product size distribution for run 1c

SIZE DISTRIBUTION SAMPLE 2					
Size (µm)		Sample mass (g)	Total mass (kg)	Mass %	% Passing
3300	1180	3.35	0.11	0.35	100.00
1180	425	1.70	0.05	0.18	99.65
425	300	1.40	0.04	0.15	99.47
300	212	6.50	0.21	0.68	99.33
212	150	11.20	0.36	1.16	98.65
150	106	56.00	1.79	5.82	97.49
106	75	141.45	4.53	14.71	91.66
75		739.90	23.68	76.95	76.95
			30.77		

Table D2- 6: Charge size distribution entering run 1c

SIZE DISTRIBUTION OF ROCKS (IN)						
Size (mm)		Rounded (g)	Fresh (g)	Total (g)	Mass %	% Passing
65	53	3146.40	1597.20	4743.60	3.59	100.00
53	44	15151.10	3635.60	18786.70	14.22	96.41
39.5	35	37484.50	4544.90	42029.40	31.82	82.18
35	28	41290.30	0.00	41290.30	31.26	50.36
28	16	22191.00	0.00	22191.00	16.80	19.10
16	11.2	2280.50	0.00	2280.50	1.73	2.29
11.2		747.10	0.00	747.10	0.57	0.57
		122290.90	9777.70	132068.60		

Table D2- 7: Charge size distribution exiting run 1c

SIZE DISTRIBUTION OF ROCKS (OUT)						
Size (mm)		Rounded (g)	Fresh (g)	Total (g)	Mass %	% Passing
65	53	2968.70	0.00	2968.70	2.46	100.00
53	44	15088.00	0.00	15088.00	12.48	97.54
44	35	34967.20	0.00	34967.20	28.93	85.06
35	28	40742.90	0.00	40742.90	33.70	56.14
28	16	23715.40	0.00	23715.40	19.62	22.43
16	11.2	2479.10	0.00	2479.10	2.05	2.81
11.2		919.70	0.00	919.70	0.76	0.76
		120881.00	0.00	120881.00		
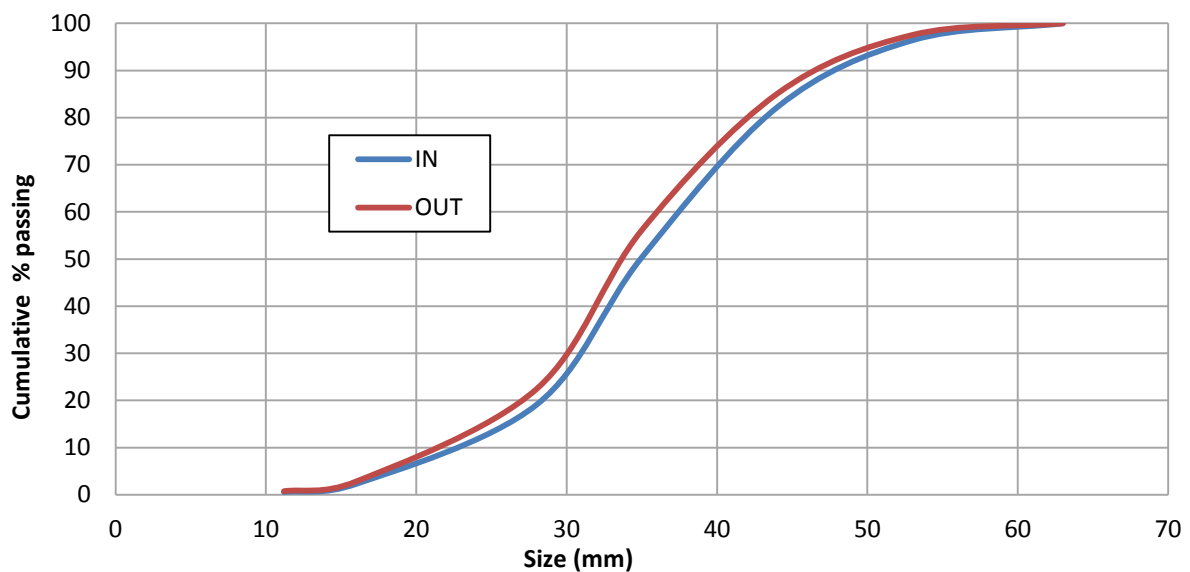
Figure D2- 1: Charge size distribution before and after run 1c

Run ID: Run 2a

Operating Conditions: Pebble Size 44/28; Speed 83.5% Critical; Volumetric filling 30%

Table D2- 8: Sample 1 product size distribution for run 2a

SIZE DISTRIBUTION SAMPLE 1					
Size (µm)		Sample mass (g)	Total mass (kg)	Mass %	% Passing
3300	1180	2.00	0.06	0.23	100.00
1180	425	0.30	0.01	0.03	99.77
425	300	0.60	0.02	0.07	99.74
300	212	1.30	0.04	0.15	99.67
212	150	4.10	0.13	0.46	99.53
150	106	49.90	1.60	5.63	99.06
106	75	73.60	2.36	8.30	93.43
75		754.60	24.15	85.13	85.13
			28.36		

Table D2- 9: Sample 2 product size distribution for run 2a

SIZE DISTRIBUTION SAMPLE 2					
Size (µm)		Sample mass (g)	Total mass (kg)	Mass %	% Passing
3300	1180	2.50	0.08	0.28	100.00
1180	425	0.30	0.01	0.03	99.72
425	300	0.30	0.01	0.03	99.68
300	212	1.50	0.05	0.17	99.65
212	150	3.00	0.10	0.34	99.48
150	106	64.70	2.07	7.35	99.14
106	75	66.90	2.14	7.60	91.78
75		740.80	23.71	84.18	84.18
			28.16		

Table D2- 10: Charge size distribution entering run 2a

SIZE DISTRIBUTION OF ROCKS (IN)						
Size (mm)		Rounded (g)	Fresh (g)	Total (g)	Mass %	% Passing
65	53	0.00	0.00	0.00	0.00	100.00
53	44	0.00	0.00	0.00	0.00	100.00
44	35	25669.70	8208.80	33878.50	25.79	100.00
35	28	44856.30	5984.10	50840.40	38.70	74.21
28	16	42517.90	0.00	42517.90	32.37	35.50
16	11.2	3050.30	0.00	3050.30	2.32	3.14
11.2		1069.10	0.00	1069.10	0.81	0.81
		117163.30	14192.90	131356.20		

Table D2- 11: Charge size distribution exiting run 2a

SIZE DISTRIBUTION OF ROCKS (OUT)						
Size (mm)		Rounded (g)	Fresh (g)	Total (g)	Mass %	% Passing
65	53	0.00	0.00	0.00	0.00	100.00
53	44	0.00	0.00	0.00	0.00	100.00
44	35	24870.70	0.00	24870.70	20.29	100.00
35	28	47791.81	0.00	47791.81	38.98	79.71
28	16	44474.13	0.00	44474.13	36.28	40.73
16	11.2	4021.22	0.00	4021.22	3.28	4.46
11.2		1444.34	0.00	1444.34	1.18	1.18
		122602.20	0.00	122602.20		
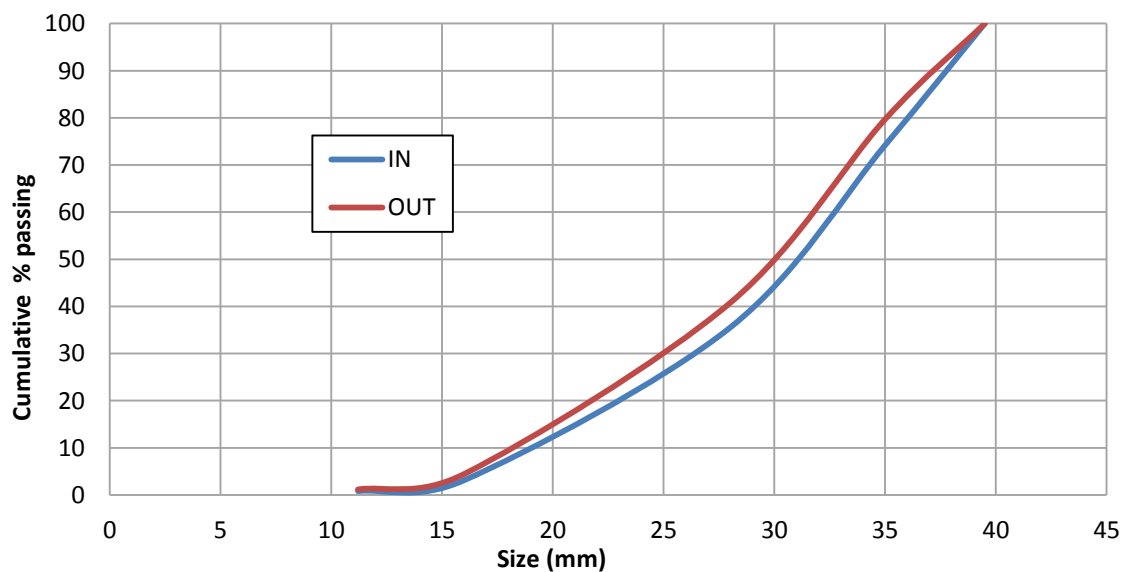
Figure D2- 2Charge size distribution before and after run 2a

Run ID: Run 2b

Operating Conditions: Pebble Size 44/28; Speed 83.5% Critical; Volumetric filling 30%

Table D2- 12: Sample 1 product size distribution for run 2b

SIZE DISTRIBUTION SAMPLE 1					
Size (µm)		Sample mass (g)	Total mass (kg)	Mass %	% Passing
3300	1180	2.10	0.07	0.23	100.00
1180	425	0.29	0.01	0.03	99.77
425	300	0.40	0.01	0.04	99.73
300	212	1.40	0.04	0.16	99.69
212	150	2.10	0.07	0.23	99.53
150	106	67.80	2.17	7.55	99.30
106	75	65.20	2.09	7.26	91.75
75		759.10	24.29	84.50	84.50
			28.75		

Table D2- 13: Sample 2 product size distribution for run 2b

SIZE DISTRIBUTION SAMPLE 2					
Size (µm)		Sample mass (g)	Total mass (kg)	Mass %	% Passing
3300	1180	1.90	0.06	0.21	100.00
1180	425	0.40	0.01	0.04	99.79
425	300	0.40	0.01	0.04	99.74
300	212	1.20	0.04	0.13	99.70
212	150	2.80	0.09	0.31	99.56
150	106	69.10	2.21	7.75	99.25
106	75	55.60	1.78	6.23	91.50
75		760.60	24.34	85.27	85.27
			28.54		

Table D2- 14: Charge size distribution entering run 2b

SIZE DISTRIBUTION OF ROCKS (IN)						
Size (mm)		Rounded (g)	Fresh (g)	Total (g)	Mass %	% Passing
65	53	0.00	0.00	0.00	0.00	100.00
53	44	0.00	0.00	0.00	0.00	100.00
39.5	35	24437.60	5541.10	29978.70	22.68	100.00
35	28	47609.30	4039.40	51648.70	39.08	77.32
28	16	45371.00	0.00	45371.00	34.33	38.24
16	11.2	3906.60	0.00	3906.60	2.96	3.92
11.2		1271.40	0.00	1271.40	0.96	0.96
		122595.90	9580.50	132176.40		

Table D2- 15: Charge size distribution entering run 2b

SIZE DISTRIBUTION OF ROCKS (OUT)						
Size (mm)		Rounded (g)	Fresh (g)	Total (g)	Mass %	% Passing
65	53	0.00	0.00	0.00	0.00	100.00
53	44	0.00	0.00	0.00	0.00	100.00
39.5	35	25021.50	0.00	25021.50	20.29	100.00
35	28	48081.60	0.00	48081.60	38.98	79.71
28	16	44743.80	0.00	44743.80	36.28	40.73
16	11.2	4045.60	0.00	4045.60	3.28	4.46
11.2		1453.10	0.00	1453.10	1.18	1.18
		123345.60	0.00	123345.60		
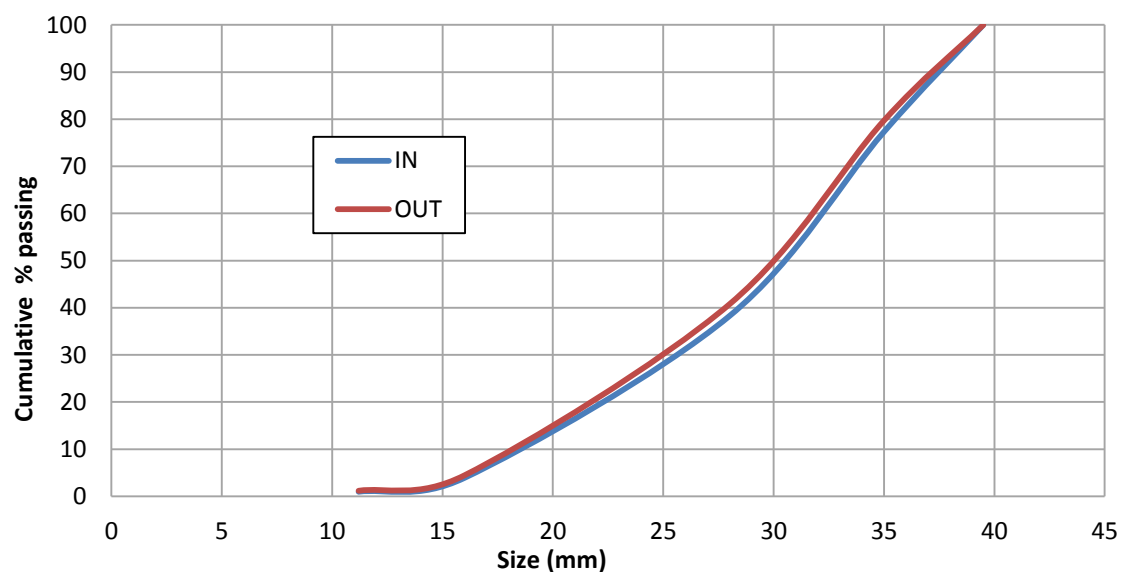
Figure D2- 3:Charge size distribution before and after run 2b

139

Run ID: Run 3a

Operating Conditions: Pebble Size 44/28; Speed 75% Critical; Volumetric filling 30%

SIZE DISTRIBUTION SAMPLE 1					
Size (µm)		Sample mass (g)	Total mass (kg)	Mass %	% Passing
3300	1180	2.90	0.09	0.35	100.00
1180	425	0.50	0.02	0.06	99.65
425	300	1.10	0.04	0.13	99.59
300	212	3.80	0.12	0.46	99.45
212	150	3.30	0.11	0.40	98.99
150	106	37.80	1.21	4.58	98.59
106	75	63.80	2.04	7.73	94.01
75		712.10	22.79	86.28	86.28
			26.41		

SIZE DISTRIBUTION SAMPLE 2					
Size (µm)		Sample mass (g)	Total mass (kg)	Mass %	% Passing
3300	1180	2.90	0.09	0.35	100.00
1180	425	0.50	0.02	0.06	99.65
425	300	1.10	0.04	0.13	99.59
300	212	3.80	0.12	0.46	99.46
212	150	3.30	0.11	0.40	99.00
150	106	36.20	1.16	4.38	98.60
106	75	64.10	2.05	7.75	94.22
75		714.80	22.87	86.46	86.46
			26.45		

Table D2- 18: Charge size distribution entering run 3a

SIZE DISTRIBUTION OF ROCKS (IN)						
Size (mm)		Rounded (g)	Fresh (g)	Total (g)	Mass %	% Passing
65	53	0.00	0.00	0.00	0.00	100.00
53	44	0.00	0.00	0.00	0.00	100.00
39.5	35	23861.50	5672.90	29534.40	22.33	100.00
35	28	48281.60	4193.50	52475.10	39.68	77.67
28	16	44743.80	0.00	44743.80	33.83	37.99
16	11.2	4045.60	0.00	4045.60	3.06	4.16
11.2		1453.10	0.00	1453.10	1.10	1.10
		122385.60	9866.40	132252.00		

Table D2- 19: Charge size distribution exiting run 3a

SIZE DISTRIBUTION OF ROCKS (OUT)						
Size (mm)		Rounded (g)	Fresh (g)	Total (g)	Mass %	% Passing
65	53	0.00	0.00	0.00	0.00	100.00
53	44	0.00	0.00	0.00	0.00	100.00
39.5	35	25154.90	0.00	25154.90	20.02	100.00
35	28	51077.00	0.00	51077.00	40.66	79.98
28	16	43634.90	0.00	43634.90	34.73	39.32
16	11.2	4340.40	0.00	4340.40	3.45	4.59
11.2		1427.00	0.00	1427.00	1.14	1.14
		125634.20	0.00	125634.20		
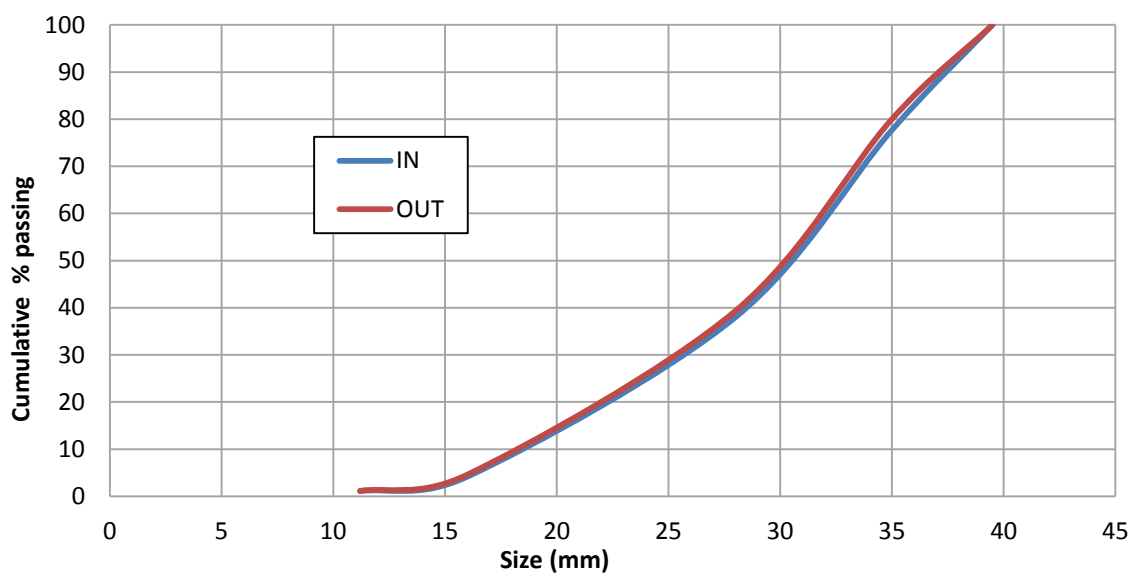
Figure D2- 4:Charge size distribution before and after run 3a

141

Run ID: Run 3b

Operating Conditions: Pebble Size 44/28; Speed 75% Critical; Volumetric filling 30%

SIZE DISTRIBUTION SAMPLE 1					
Size (μm)		Sample mass (g)	Total mass (kg)	Mass %	% Passing
3300	1180	1.93	0.06	0.23	100.00
1180	425	0.34	0.01	0.04	99.77
425	300	0.22	0.01	0.03	99.72
300	212	0.59	0.02	0.07	99.70
212	150	1.36	0.04	0.17	99.63
150	106	27.49	0.88	3.34	99.46
106	75	78.50	2.51	9.53	96.13
75		713.70	22.84	86.60	86.60
			26.37		

SIZE DISTRIBUTION SAMPLE 2					
Size (μm)		Sample mass (g)	Total mass (kg)	Mass %	% Passing
3300	1180	1.94	0.06	0.23	100.00
1180	425	0.34	0.01	0.04	99.77
425	300	0.22	0.01	0.03	99.73
300	212	0.57	0.02	0.07	99.70
212	150	1.38	0.04	0.17	99.63
150	106	27.70	0.89	3.33	99.46
106	75	79.10	2.53	9.52	96.13
75		719.90	23.04	86.61	86.61
			26.60		

SIZE DISTRIBUTION OF ROCKS (IN)						
Size (mm)		Rounded (g)	Fresh (g)	Total (g)	Mass %	% Passing
65	53	0.00	0.00	0.00	0.00	100.00
53	44	0.00	0.00	0.00	0.00	100.00
39.5	35	25154.90	3761.10	28916.00	21.88	100.00
35	28	51077.00	2763.10	53840.10	40.74	78.12
28	16	43634.90	0.00	43634.90	33.02	37.38
16	11.2	4340.40	0.00	4340.40	3.28	4.36
11.2		1427.00	0.00	1427.00	1.08	1.08
		125634.20	6524.20	132158.40		

Table D2- 23: Charge size distribution exiting run 3b

SIZE DISTRIBUTION OF ROCKS (OUT)						
Size (mm)		Rounded (g)	Fresh (g)	Total (g)	Mass %	% Passing
65	53	0.00	0.00	0.00	0.00	100.00
53	44	0.00	0.00	0.00	0.00	100.00
39.5	35	22956.00	0.00	22956.00	18.28	100.00
35	28	52584.90	0.00	52584.90	41.87	81.72
28	16	44061.90	0.00	44061.90	35.08	39.85
16	11.2	4479.70	0.00	4479.70	3.57	4.77
11.2		1506.60	0.00	1506.60	1.20	1.20
		125589.10	0.00	125589.10		
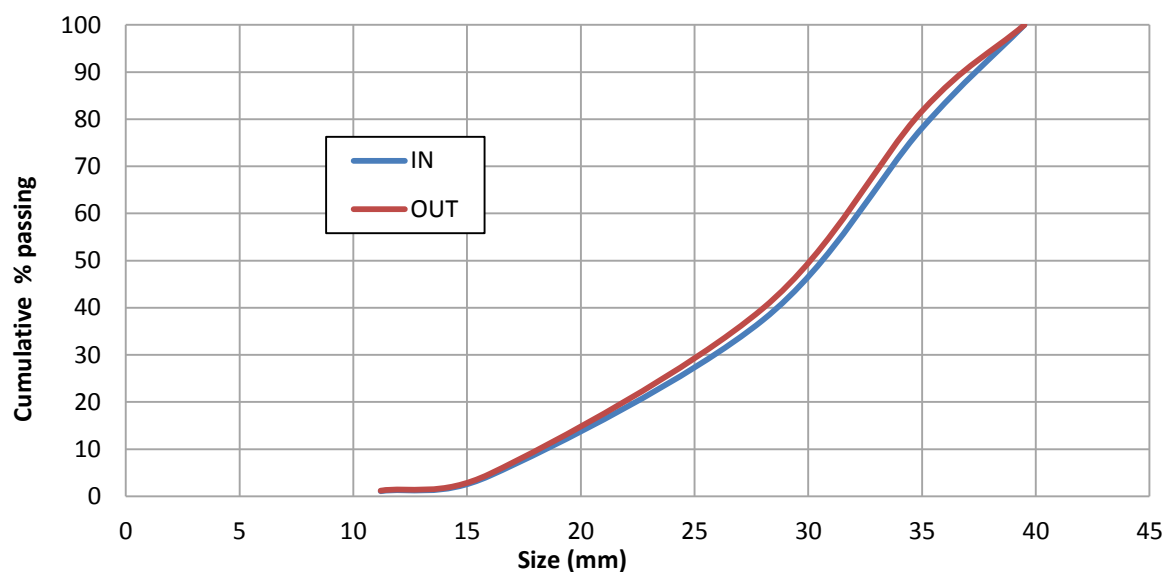
Figure D2- 5:Charge size distribution before and after run 3b

143

Run ID: Run 4a

Operating Conditions: Pebble Size 65/35; Speed 75% Critical; Volumetric filling 30%

Table D2- 24: Sample 1 product size distribution for run 4a

SIZE DISTRIBUTION SAMPLE 1					
Size (μm)		Sample mass (g)	Total mass (kg)	Mass %	% Passing
3300	1180	1.53	0.05	0.17	100.00
1180	425	0.67	0.02	0.07	99.83
425	300	0.76	0.02	0.08	99.76
300	212	2.49	0.08	0.27	99.68
212	150	6.72	0.22	0.73	99.41
150	106	36.22	1.16	3.92	98.68
106	75	117.20	3.75	12.67	94.77
75		759.10	24.29	82.09	82.09
			29.59		

Table D2- 25: Sample 2 product size distribution for run 4a

SIZE DISTRIBUTION SAMPLE 2					
Size (μm)		Sample mass (g)	Total mass (kg)	Mass %	% Passing
3300	1180	1.55	0.05	0.17	100.00
1180	425	0.68	0.02	0.07	99.83
425	300	0.77	0.02	0.08	99.76
300	212	2.51	0.08	0.27	99.68
212	150	6.78	0.22	0.73	99.41
150	106	36.50	1.17	3.91	98.68
106	75	118.12	3.78	12.66	94.77
75		765.99	24.51	82.11	82.11
			29.85		

SIZE DISTRIBUTION OF ROCKS (IN)					
Size (mm)		Rounded (g)	Fresh (g)	Total (g)	Mass %	% Passing
63	53	2861.80	1344.20	4206.00	3.18	100.00
53	44	17741.50	2905.30	20646.80	15.62	96.82
39.5	35	39937.40	3572.00	43509.40	32.92	81.20
35	28	41057.70	0.00	41057.70	31.06	48.28
28	16	20121.40	0.00	20121.40	15.22	17.22
16	11.2	1971.50	0.00	1971.50	1.49	2.00
11.2		672.60	0.00	672.60	0.51	0.51
		124363.90	7821.50	132185.40		

Table D2- 27: Charge size distribution exiting run 4a

| SIZE DISTRIBUTION OF ROCKS (OUT)					
Size (mm)		Rounded (g)	Fresh (g)	Total (g)	Mass %	% Passing
65	53	3146.40	0.00	3146.40	2.57	100.00
53	44	15151.10	0.00	15151.10	12.39	97.43
44	35	37484.50	0.00	37484.50	30.65	85.04
35	28	41290.30	0.00	41290.30	33.76	54.39
28	16	22191.00	0.00	22191.00	18.15	20.62
16	11.2	2280.50	0.00	2280.50	1.86	2.48
11.2		747.10	0.00	747.10	0.61	0.61
		122290.90	0.00	122290.90		
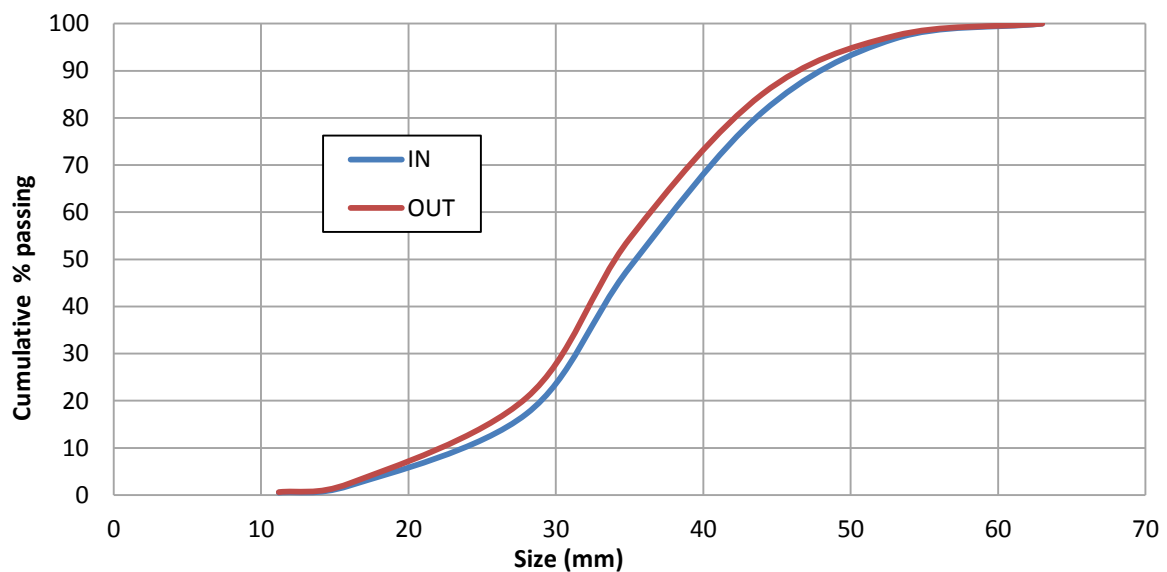
Figure D2- 6:Charge size distribution before and after run 4a

Run ID: Run 4b

Operating Conditions: Pebble Size 65/35; Speed 75% Critical; Volumetric filling 30%

Table D2- 28: Sample 1 product size distribution for run 4b

SIZE DISTRIBUTION SAMPLE 1					
Size (µm)		Sample mass (g)	Total mass (kg)	Mass %	% Passing
3300	1180	1.53	0.05	0.17	100.00
1180	425	0.66	0.02	0.07	99.83
425	300	0.76	0.02	0.08	99.76
300	212	2.48	0.08	0.27	99.68
212	150	6.69	0.21	0.73	99.41
150	106	36.06	1.15	3.92	98.68
106	75	116.69	3.73	12.68	94.76
75		755.04	24.16	82.08	82.08
			29.44		

Table D2- 29: Sample 2 product size distribution for run 4b

SIZE DISTRIBUTION SAMPLE 2					
Size (µm)		Sample mass (g)	Total mass (kg)	Mass %	% Passing
3300	1180	1.53	0.05	0.17	100.00
1180	425	0.67	0.02	0.07	99.83
425	300	0.76	0.02	0.08	99.76
300	212	2.49	0.08	0.27	99.68
212	150	6.71	0.21	0.73	99.41
150	106	36.10	1.16	3.91	98.68
106	75	116.06	3.71	12.58	94.77
75		757.91	24.25	82.18	82.18
			29.51		

Table D2- 30: Charge size distribution entering run 4b

SIZE DISTRIBUTION OF ROCKS (IN)						
Size (mm)		Rounded (g)	Fresh (g)	Total (g)	Mass %	% Passing
65	53	2861.80	1362.20	4224.00	3.20	100.00
53	44	17741.50	2905.30	20646.80	15.62	96.80
39.5	35	39937.40	3570.00	43507.40	32.91	81.19
35	28	41057.70	0.00	41057.70	31.06	48.28
28	16	20121.40	0.00	20121.40	15.22	17.22
16	11.2	1971.50	0.00	1971.50	1.49	2.00
11.2		672.60	0.00	672.60	0.51	0.51
		124363.90	7837.50	132201.40		

Table D2- 31: Charge size distribution exiting run 4b

| SIZE DISTRIBUTION OF ROCKS (OUT)						
Size (mm)		Rounded (g)	Fresh (g)	Total (g)	Mass %	% Passing
65	53	3146.40	0.00	3146.40	2.57	100.00
53	44	15171.10	0.00	15171.10	12.40	97.43
44	35	37484.50	0.00	37484.50	30.65	85.02
35	28	41285.10	0.00	41285.10	33.76	54.37
28	16	22191.00	0.00	22191.00	18.14	20.61
16	11.2	2280.50	0.00	2280.50	1.86	2.47
11.2		740.10	0.00	740.10	0.61	0.61
		122298.70	0.00	122298.70		
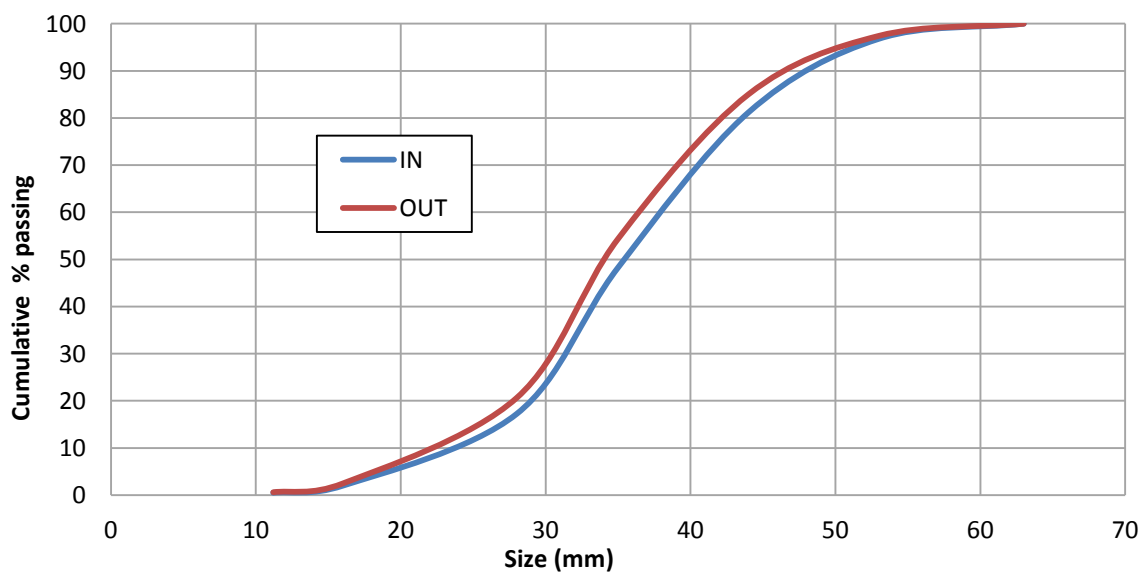
Figure D2- 7:Charge size distribution before and after run 4b

147

Run ID: Run 5a

Operating Conditions: Pebble Size 44/28; Speed 69% Critical; Volumetric filling 30%

SIZE DISTRIBUTION SAMPLE 1					
Size (μm)		Sample mass (g)	Total mass (kg)	Mass %	% Passing
3300	1180	1.73	0.06	0.22	100.00
1180	425	0.51	0.02	0.06	99.78
425	300	0.41	0.01	0.05	99.72
300	212	1.22	0.04	0.15	99.67
212	150	2.45	0.08	0.31	99.52
150	106	33.78	1.08	4.23	99.21
106	75	96.46	3.09	12.09	94.98
75		661.60	21.17	82.89	82.89
			25.54		

SIZE DISTRIBUTION SAMPLE 2					
Size (μm)		Sample mass (g)	Total mass (kg)	Mass %	% Passing
3300	1180	1.72	0.06	0.22	100.00
1180	425	0.50	0.02	0.06	99.78
425	300	0.40	0.01	0.05	99.72
300	212	1.21	0.04	0.15	99.67
212	150	2.43	0.08	0.31	99.52
150	106	33.62	1.08	4.23	99.21
106	75	96.99	3.10	12.20	94.98
75		658.00	21.06	82.78	82.78
			25.44		

Table D2- 34: Charge size distribution entering run 5a

SIZE DISTRIBUTION OF ROCKS (IN)						
Size (mm)		Rounded (g)	Fresh (g)	Total (g)	Mass %	% Passing
65	53	0.00	0.00	0.00	0.00	100.00
53	44	0.00	0.00	0.00	0.00	100.00
39.5	35	28670.10	5204.40	33874.50	25.40	100.00
35	28	47038.20	3755.70	50793.90	38.09	74.60
28	16	44567.10	0.00	44567.10	33.42	36.51
16	11.2	3050.10	0.00	3050.10	2.29	3.09
11.2		1069.40	0.00	1069.40	0.80	0.80
		124394.90	8960.10	133355.00		

Table D2- 35: Charge size distribution exiting run 5a

| SIZE DISTRIBUTION OF ROCKS (OUT)						
Size (mm)		Rounded (g)	Fresh (g)	Total (g)	Mass %	% Passing
65	53	0.00	0.00	0.00	0.00	100.00
53	44	0.00	0.00	0.00	0.00	100.00
39.5	35	26908.50	0.00	26908.50	21.08	100.00
35	28	51219.10	0.00	51219.10	40.13	78.92
28	16	45023.20	0.00	45023.20	35.27	38.79
16	11.2	3310.40	0.00	3310.40	2.59	3.52
11.2		1180.30	0.00	1180.30	0.92	0.92
		127641.50	0.00	127641.50		
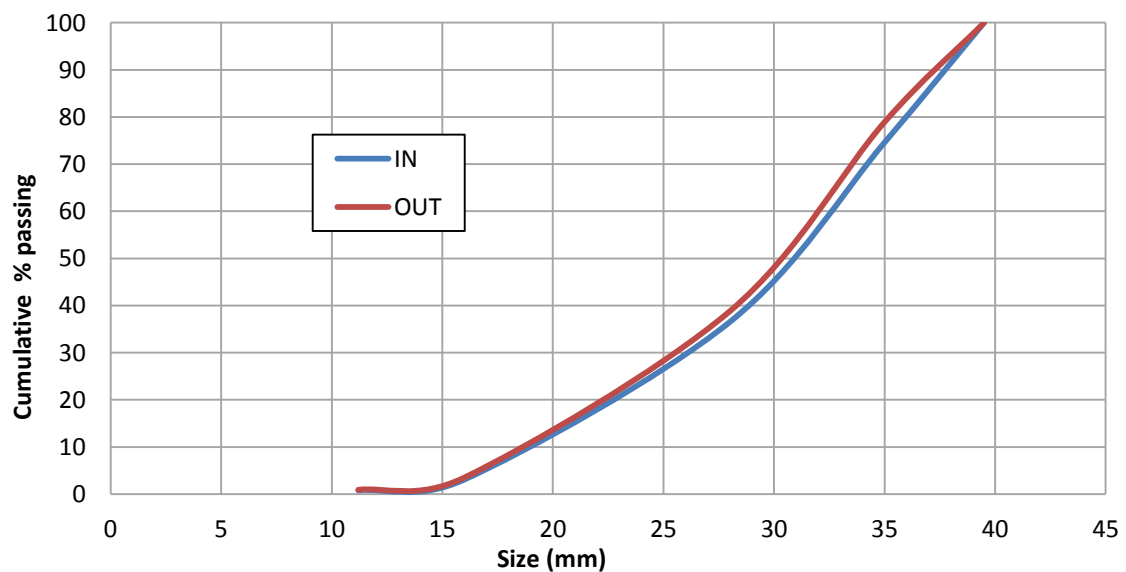
Figure D2- 8:Charge size distribution before and after run 5a

149

Run ID: Run 5b

Operating Conditions: Pebble Size 44/28; Speed 69% Critical; Volumetric filling 30%

SIZE DISTRIBUTION SAMPLE 1					
Size (µm)		Sample mass (g)	Total mass (kg)	Mass %	% Passing
3300	1180	1.88	0.06	0.24	100.00
1180	425	0.31	0.01	0.04	99.76
425	300	0.41	0.01	0.05	99.72
300	212	0.94	0.03	0.12	99.67
212	150	2.41	0.08	0.30	99.56
150	106	22.55	0.72	2.83	99.25
106	75	111.40	3.56	13.99	96.42
75		656.34	21.00	82.43	82.43
			25.48		

SIZE DISTRIBUTION SAMPLE 2					
Size (µm)		Sample mass (g)	Total mass (kg)	Mass %	% Passing
3300	1180	1.89	0.06	0.24	100.00
1180	425	0.31	0.01	0.04	99.76
425	300	0.42	0.01	0.05	99.72
300	212	0.94	0.03	0.12	99.67
212	150	2.42	0.08	0.30	99.55
150	106	22.65	0.72	2.84	99.25
106	75	111.89	3.58	14.03	96.41
75		657.22	21.03	82.39	82.39
			25.53		

Table D2- 38: Charge size distribution entering run 5b

SIZE DISTRIBUTION OF ROCKS (IN)						
Size (mm)		Rounded (g)	Fresh (g)	Total (g)	Mass %	% Passing
65	53	0.00	0.00	0.00	0.00	100.00
53	44	0.00	0.00	0.00	0.00	100.00
39.5	35	26908.50	3310.00	30218.50	22.65	100.00
35	28	51219.10	2436.30	53655.40	40.23	77.35
28	16	45023.20	0.00	45023.20	33.75	37.12
16	11.2	3310.40	0.00	3310.40	2.48	3.37
11.2		1180.30	0.00	1180.30	0.88	0.88
		127641.50	5746.30	133387.80		

Table D2- 39: Charge size distribution exiting run 5b

| SIZE DISTRIBUTION OF ROCKS (OUT)						
Size (mm)		Rounded (g)	Fresh (g)	Total (g)	Mass %	% Passing
65	53	0.00	0.00	0.00	0.00	100.00
53	44	0.00	0.00	0.00	0.00	100.00
39.5	35	26293.20	0.00	26293.20	20.58	100.00
35	28	50950.10	0.00	50950.10	39.88	79.42
28	16	45495.60	0.00	45495.60	35.61	39.55
16	11.2	3841.50	0.00	3841.50	3.01	3.94
11.2		1189.70	0.00	1189.70	0.93	0.93
		127770.10	0.00	127770.10		
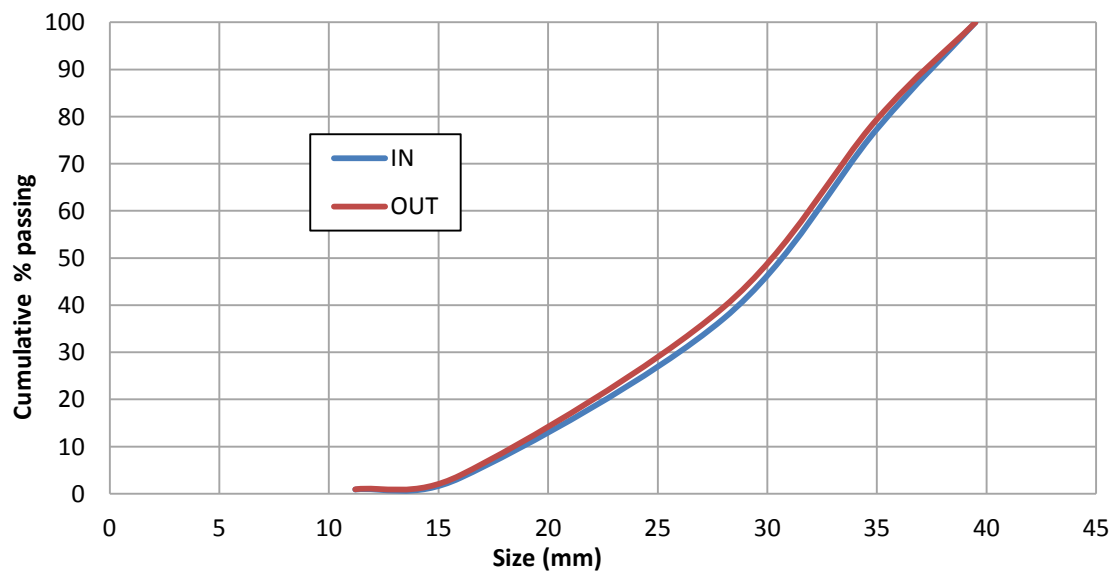
Figure D2- 9:Charge size distribution before and after run 5b

151

Run ID: Run 6a

Operating Conditions: Pebble Size 65/35; Speed 69% Critical; Volumetric filling 30%

Table D2- 40: Sample 1 product size distribution for run 6a

SIZE DISTRIBUTION SAMPLE 1					
Size (μm)		Sample mass (g)	Total mass (kg)	Mass %	% Passing
3300	1180	0.90	0.03	0.10	100.00
1180	425	0.35	0.01	0.04	99.90
425	300	0.81	0.03	0.09	99.86
300	212	2.69	0.09	0.31	99.76
212	150	6.95	0.22	0.80	99.45
150	106	38.69	1.24	4.47	98.65
106	75	118.22	3.78	13.65	94.18
75		697.69	22.33	80.54	80.54
			27.72		

Table D2- 41: Sample 2 product size distribution for run 6a

SIZE DISTRIBUTION SAMPLE 2					
Size (μm)		Sample mass (g)	Total mass (kg)	Mass %	% Passing
3300	1180	0.90	0.03	0.10	100.00
1180	425	0.35	0.01	0.04	99.90
425	300	0.81	0.03	0.09	99.86
300	212	2.69	0.09	0.31	99.76
212	150	6.90	0.22	0.79	99.45
150	106	38.79	1.24	4.47	98.66
106	75	119.52	3.82	13.76	94.19
75		698.40	22.35	80.43	80.43
			27.79		

Table D2- 42: Charge size distribution entering run 6a

SIZE DISTRIBUTION OF ROCKS (IN)						
Size (mm)		Rounded (g)	Fresh (g)	Total (g)	Mass %	% Passing
65	53	2258.60	1689.60	3948.20	2.99	100.00
53	44	19122.90	3761.60	22884.50	17.32	97.01
39.5	35	44792.30	4494.60	49286.90	37.29	79.70
35	28	37241.40	0.00	37241.40	28.18	42.40
28	16	16550.10	0.00	16550.10	12.52	14.22
16	11.2	1676.70	0.00	1676.70	1.27	1.70
11.2		571.40	0.00	571.40	0.43	0.43
		122213.40	9945.80	132159.20		

Table D2- 43: Charge size distribution exiting run 6a

| SIZE DISTRIBUTION OF ROCKS (OUT)						
Size (mm)		Rounded (g)	Fresh (g)	Total (g)	Mass %	% Passing
65	53	2244.50	0.00	2244.50	1.81	100.00
53	44	17653.40	0.00	17653.40	14.22	98.19
44	35	42748.50	0.00	42748.50	34.43	83.97
35	28	39567.10	0.00	39567.10	31.87	49.55
28	16	19339.80	0.00	19339.80	15.58	17.68
16	11.2	1892.70	0.00	1892.70	1.52	2.10
11.2		718.30	0.00	718.30	0.58	0.58
		124164.30	0.00	124164.30		
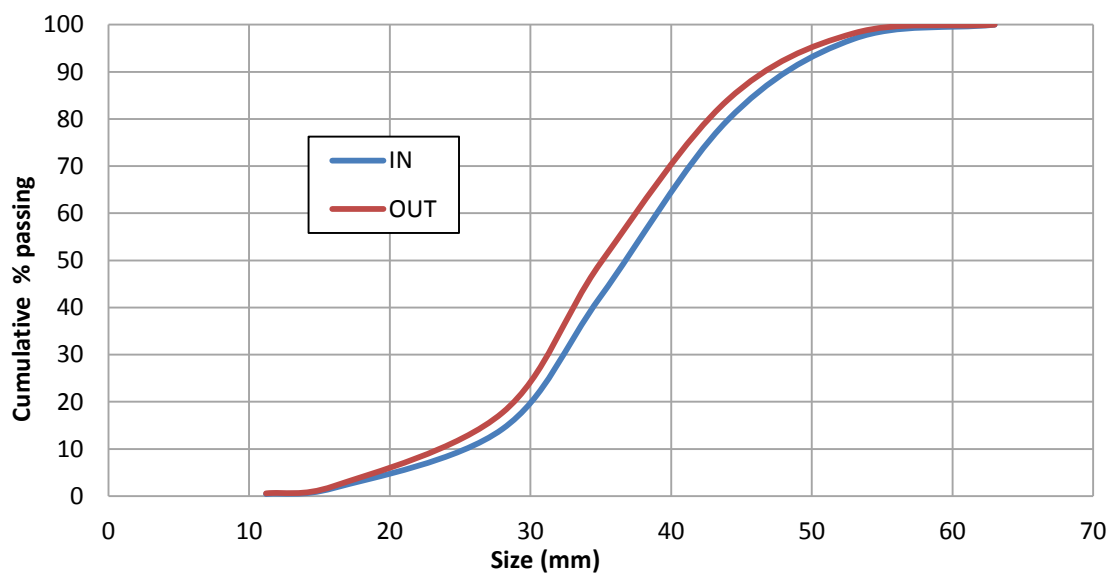
Figure D2- 10:Charge size distribution before and after run 6a

153

Run ID: Run 6b

Operating Conditions: Pebble Size 65/35; Speed 69% Critical; Volumetric filling 30%

Table D2- 44: Sample 1 product size distribution for run 6b

SIZE DISTRIBUTION SAMPLE 1					
Size (μm)		*Sample mass (g)*	*Total mass (kg)*	*Mass %*	*% Passing*
3300	*1180*	2.30	0.07	0.26	100.00
1180	*425*	0.50	0.02	0.06	99.74
425	*300*	0.50	0.02	0.06	99.68
300	*212*	1.60	0.05	0.18	99.62
212	*150*	5.30	0.17	0.61	99.44
150	*106*	32.40	1.04	3.73	98.83
106	*75*	126.50	4.05	14.57	95.09
75		699.30	22.38	80.53	80.53
			27.79		

Table D2- 45: Sample 2 product size distribution for run 6b

SIZE DISTRIBUTION SAMPLE 2					
Size (μm)		*Sample mass (g)*	*Total mass (kg)*	*Mass %*	*% Passing*
3300	*1180*	2.20	0.07	0.25	100.00
1180	*425*	0.50	0.02	0.06	99.75
425	*300*	0.60	0.02	0.07	99.69
300	*212*	1.70	0.05	0.20	99.62
212	*150*	5.40	0.17	0.62	99.43
150	*106*	32.50	1.04	3.73	98.81
106	*75*	127.00	4.06	14.58	95.07
75		701.00	22.43	80.49	80.49
			27.87		

Table D2- 46: Charge size distribution entering run 6b

SIZE DISTRIBUTION OF ROCKS (IN)						
Size (mm)		Rounded (g)	Fresh (g)	Total (g)	Mass %	% Passing
65	53	2244.50	1335.80	3580.30	2.71	100.00
53	44	17653.40	2920.70	20574.10	15.57	97.29
39.5	35	42748.50	3688.30	46436.80	35.15	81.72
35	28	39567.10	0.00	39567.10	29.95	46.57
28	16	19339.80	0.00	19339.80	14.64	16.62
16	11.2	1892.70	0.00	1892.70	1.43	1.98
11.2		718.30	0.00	718.30	0.54	0.54
		124164.30	7944.80	132109.10		

Table D2- 47: Charge size distribution exiting run 6b

SIZE DISTRIBUTION OF ROCKS (OUT)						
Size (mm)		Rounded (g)	Fresh (g)	Total (g)	Mass %	% Passing
65	53	2561.80	0.00	2561.80	2.06	100.00
53	44	17741.50	0.00	17741.50	14.30	97.94
44	35	39937.40	0.00	39937.40	32.19	83.63
35	28	41057.70	0.00	41057.70	33.09	51.44
28	16	20121.40	0.00	20121.40	16.22	18.35
16	11.2	1971.50	0.00	1971.50	1.59	2.13
11.2		672.60	0.00	672.60	0.54	0.54
		124063.90	0.00	124063.90		
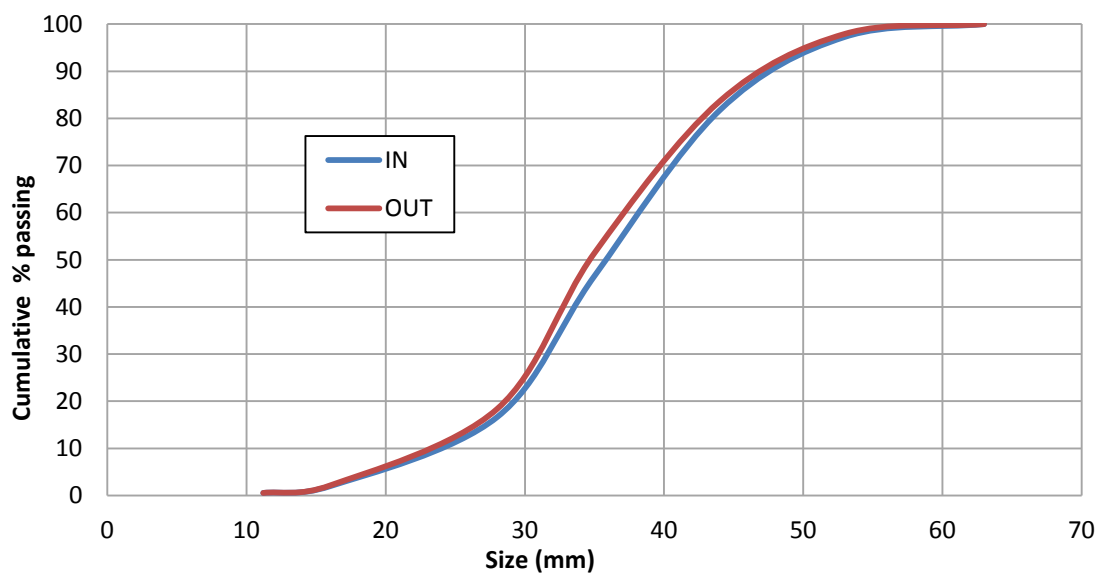
Figure D2- 11:Charge size distribution before and after run 6b

83.5 % Critical Speed (33 rpm)				
	Voltage(mV)	Torque(N.m)	Power (kW)	Net Power (kW)
NLP	1.093	16.467	0.057	n/a
run 1 a	2.231	485.505	1.678	1.621
run 1 b	2.233	486.459	1.681	1.624
run 1 c	2.226	483.486	1.671	1.614
run 2 a	2.201	473.133	1.635	1.578
run 2 b	2.205	474.893	1.641	1.584

75 % Critical Speed (30 rpm)				
	Voltage(mV)	Torque(N.m)	Power (kW)	Net Power (kW)
NLP	1.089	14.932	0.047	n/a
run 3 a	2.134	445.571	1.400	1.353
run 3 b	2.134	445.619	1.400	1.353
run 4 a	2.193	470.073	1.477	1.430
run 4 b	2.193	469.945	1.476	1.429

69 % Critical Speed (27.5 rpm)				
	Voltage(mV)	Torque(N.m)	Power (kW)	Net Power (kW)
NLP	1.079	10.897	0.031	n/a
run 5 a	2.103	433.011	1.247	1.216
run 5 b	2.100	431.681	1.243	1.212
run 6 a	2.159	456.114	1.314	1.282
run 6 b	2.154	453.820	1.307	1.276

Run ID: 40 Run 1

Operating Conditions: Pebble Size 44/28; Speed 83.5% Critical; Volumetric filling 40%

Table D2- 51: Sample 1 product size distribution for 40 run 1

SIZE DISTRIBUTION SAMPLE 1					
Size (µm)		Sample mass (g)	Total mass (kg)	Mass %	% Passing
3300	1180	2.00	0.13	0.32	100.00
1180	425	0.48	0.03	0.08	99.68
425	300	0.57	0.04	0.09	99.60
300	212	0.95	0.06	0.15	99.51
212	150	1.62	0.10	0.26	99.36
150	106	26.14	1.67	4.18	99.10
106	75	66.49	4.26	10.64	94.92
75		526.80	33.72	84.28	84.28
			40.00		

Table D2- 52: Sample 2 product size distribution for 40 run 1

SIZE DISTRIBUTION SAMPLE 2					
Size (µm)		Sample mass (g)	Total mass (kg)	Mass %	% Passing
3300	1180	1.44	0.09	0.23	100.00
1180	425	0.48	0.03	0.08	99.77
425	300	0.39	0.02	0.06	99.69
300	212	1.25	0.08	0.20	99.63
212	150	1.73	0.11	0.28	99.43
150	106	15.03	0.96	2.39	99.16
106	75	78.79	5.04	12.54	96.76
75		529.07	33.86	84.22	84.22
			40.20		

SIZE DISTRIBUTION OF ROCKS (IN)						
Size (mm)		Rounded (g)	Fresh (g)	Total (g)	Mass %	% Passing
65	53	0.00	0.00	0.00	0.00	100.00
53	44	0.00	0.00	0.00	0.00	100.00
44	35	39110.50	7648.40	46758.90	25.65	100.00
35	28	64623.00	5506.80	70129.80	38.47	74.35
28	16	59700.90	0.00	59700.90	32.75	35.88
16	11.2	4225.00	0.00	4225.00	2.32	3.13
11.2		1475.90	0.00	1475.90	0.81	0.81
		169135.30	13155.20	182290.50		

Table D2- 54: Charge size distribution exiting40 run 1

SIZE DISTRIBUTION OF ROCKS (OUT)						
Size (mm)		Rounded (g)	Fresh (g)	Total (g)	Mass %	% Passing
65	53	0.00	0.00	0.00	0.00	100.00
53	44	0.00	0.00	0.00	0.00	100.00
44	35	39191.80	0.00	39191.80	23.09	100.00
35	28	64280.40	0.00	64280.40	37.86	76.91
28	16	59685.90	0.00	59685.90	35.16	39.05
16	11.2	5184.00	0.00	5184.00	3.05	3.89
11.2		1420.50	0.00	1420.50	0.84	0.84
		169762.60	0.00	169762.60		
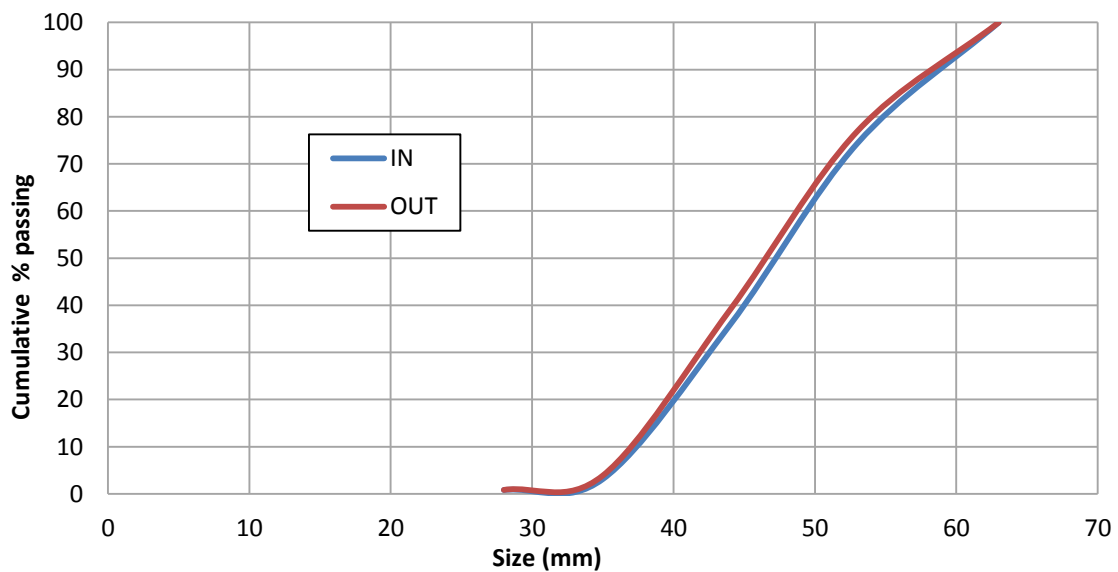
Figure D2- 12:Charge size distribution before and after 40 run 1

158

Run ID: 40 run 2

Operating Conditions: Pebble Size 44/28; Speed 75% Critical; Volumetric filling 40%

Table D2- 55: Sample 1 product size distribution for 40 run 2

SIZE DISTRIBUTION SAMPLE 1					
Size (μm)		Sample mass (g)	Total mass (kg)	Mass %	% Passing
3300	1180	1.80	0.11	0.31	100.00
1180	425	0.27	0.02	0.05	99.69
425	300	0.27	0.02	0.05	99.65
300	212	0.99	0.06	0.17	99.60
212	150	1.17	0.07	0.20	99.43
150	106	9.43	0.60	1.61	99.23
106	75	63.06	4.04	10.76	97.62
75		508.97	32.57	86.86	86.86
			37.50		

Table D2- 56: Sample 2 product size distribution for 40 run 2

SIZE DISTRIBUTION SAMPLE 2					
Size (μm)		Sample mass (g)	Total mass (kg)	Mass %	% Passing
3300	1180	1.80	0.11	0.31	100.00
1180	425	0.27	0.02	0.05	99.69
425	300	0.27	0.02	0.05	99.65
300	212	0.99	0.06	0.17	99.60
212	150	1.30	0.08	0.22	99.43
150	106	9.20	0.59	1.57	99.21
106	75	65.06	4.16	11.13	97.64
75		505.78	32.37	86.51	86.51
			37.42		

SIZE DISTRIBUTION OF ROCKS (IN)						
Size (mm)		Rounded (g)	Fresh (g)	Total (g)	Mass %	% Passing
65	53	0.00	0.00	0.00	0.00	100.00
53	44	0.00	0.00	0.00	0.00	100.00
44	35	42104.60	5239.30	47343.90	25.72	100.00
35	28	66626.90	3785.60	70412.50	38.25	74.28
28	16	59690.90		59690.90	32.42	36.04
16	11.2	5184.00		5184.00	2.82	3.62
11.2		1475.70		1475.70	0.80	0.80
		175082.10	9024.90	184107.00		

SIZE DISTRIBUTION OF ROCKS (OUT)						
Size (mm)		Rounded (g)	Fresh (g)	Total (g)	Mass %	% Passing
65	53	0.00	0.00	0.00	0.00	100.00
53	44	0.00	0.00	0.00	0.00	100.00
44	35	39133.20	0.00	39133.20	22.47	100.00
35	28	70456.40	0.00	70456.40	40.45	77.53
28	16	57187.40	0.00	57187.40	32.83	37.08
16	11.2	5819.10	0.00	5819.10	3.34	4.25
11.2		1586.20	0.00	1586.20	0.91	0.91
		174182.30	0.00	174182.30		
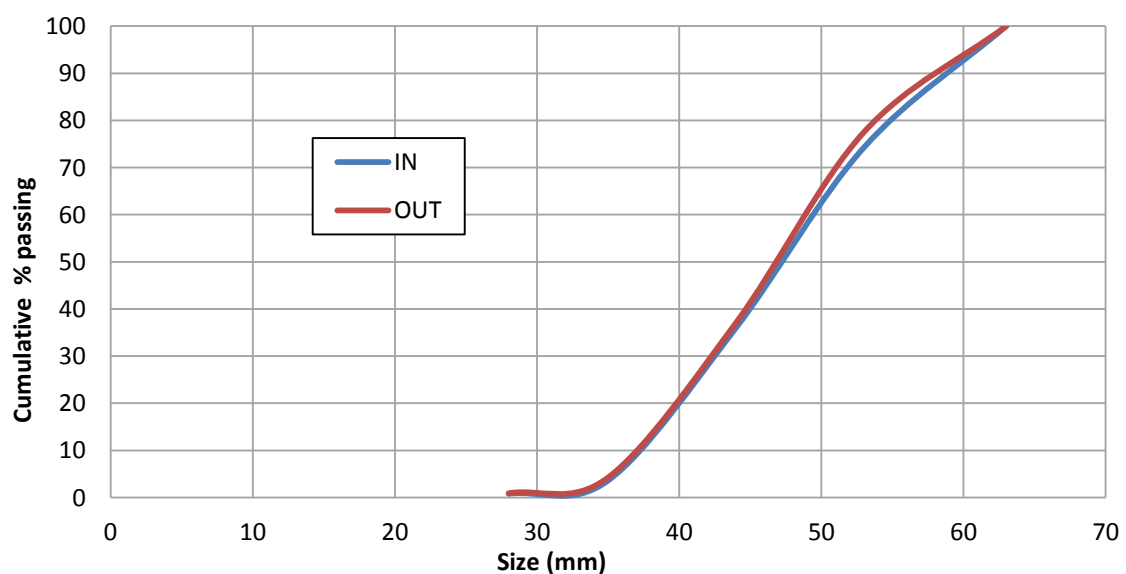
Figure D2- 13:Charge size distribution before and after 40 run 2

160

Run ID: 40 run 3

Operating Conditions: Pebble Size 44/28; Speed 69% Critical; Volumetric filling 40%

SIZE DISTRIBUTION SAMPLE 1					
Size (µm)		Sample mass (g)	Total mass (kg)	Mass %	% Passing
3300	1180	1.96	0.13	0.35	100.00
1180	425	0.16	0.01	0.03	99.65
425	300	0.16	0.01	0.03	99.62
300	212	0.39	0.03	0.07	99.59
212	150	0.70	0.05	0.13	99.52
150	106	33.90	2.17	6.09	99.40
106	75	61.86	3.96	11.11	93.30
75		457.50	29.28	82.19	82.19
			35.62		

Table D2- 60: Sample 2 product size distribution for 40 run 3

SIZE DISTRIBUTION SAMPLE 2					
Size (µm)		Sample mass (g)	Total mass (kg)	Mass %	% Passing
3300	1180	0.31	0.02	0.06	100.00
1180	425	0.16	0.01	0.03	99.94
425	300	0.39	0.03	0.07	99.92
300	212	0.78	0.05	0.14	99.85
212	150	0.86	0.06	0.15	99.71
150	106	34.71	2.22	6.21	99.55
106	75	62.78	4.02	11.22	93.35
75		459.29	29.39	82.12	82.12
			35.79		

SIZE DISTRIBUTION OF ROCKS (IN)					
Size (mm)		Rounded (g)	Fresh (g)	Total (g)	Mass %	% Passing
65	53			0.00	0.00	100.00
53	44			0.00	0.00	100.00
44	35	39561.10	5465.10	45026.20	24.82	100.00
35	28	66929.90	4099.10	71029.00	39.15	75.18
28	16	59694.70		59694.70	32.90	36.04
16	11.2	4215.00		4215.00	2.32	3.13
11.2		1472.20		1472.20	0.81	0.81
		171872.90	9564.20	181437.10		

Table D2- 62: Charge size distribution exiting40 run 3

| SIZE DISTRIBUTION OF ROCKS (OUT)					
Size (mm)		Rounded (g)	Fresh (g)	Total (g)	Mass %	% Passing
65	53			0.00	0.00	100.00
53	44			0.00	0.00	100.00
44	35	39526.70		39526.70	22.82	100.00
35	28	65013.40		65013.40	37.54	77.18
28	16	62460.80		62460.80	36.06	39.64
16	11.2	4752.50		4752.50	2.74	3.58
11.2		1448.50		1448.50	0.84	0.84
		173201.90	0.00	173201.90		
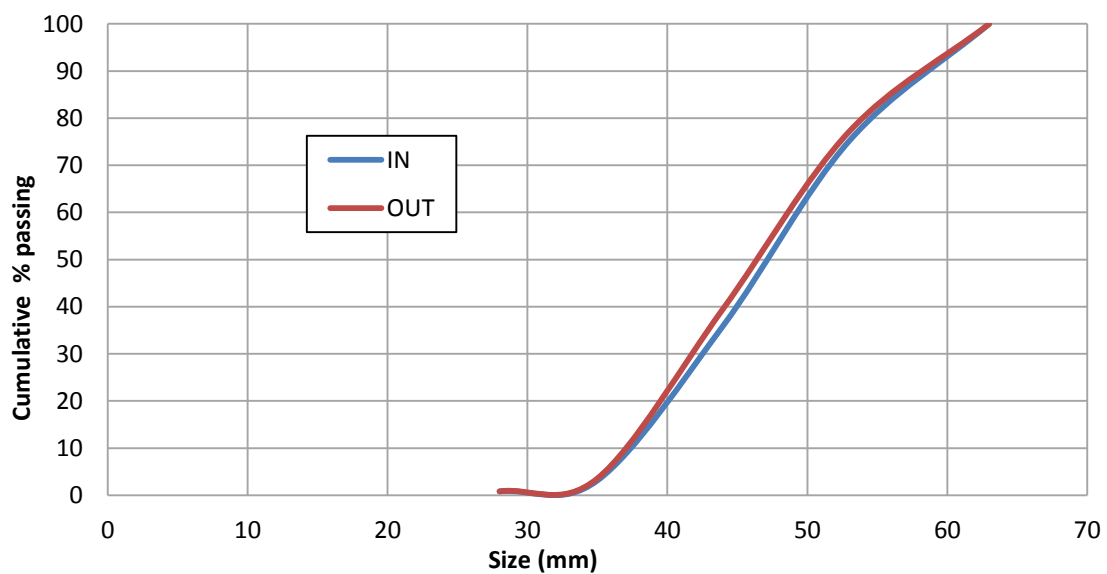
Figure D2- 14:Charge size distribution before and after 40 run 3

162

Run ID: 40 run 4

Operating Conditions: Pebble Size 65/35; Speed 69% Critical; Volumetric filling 40%

SIZE DISTRIBUTION SAMPLE 1					
Size (µm)		Sample mass (g)	Total mass (kg)	Mass %	% Passing
3300	1180	2.23	0.14	0.37	100.00
1180	425	0.18	0.01	0.03	99.63
425	300	0.18	0.01	0.03	99.60
300	212	0.45	0.03	0.07	99.57
212	150	0.80	0.05	0.13	99.49
150	106	38.56	2.47	6.44	99.36
106	75	70.36	4.50	11.75	92.92
75		486.08	31.11	81.17	81.17
			38.33		

SIZE DISTRIBUTION SAMPLE 2					
Size (µm)		Sample mass (g)	Total mass (kg)	Mass %	% Passing
3300	1180	2.30	0.15	0.38	100.00
1180	425	0.22	0.01	0.04	99.62
425	300	0.22	0.01	0.04	99.58
300	212	0.44	0.03	0.07	99.54
212	150	0.88	0.06	0.15	99.47
150	106	41.06	2.63	6.87	99.32
106	75	71.83	4.60	12.02	92.45
75		480.71	30.77	80.43	80.43
			38.25		

SIZE DISTRIBUTION OF ROCKS (IN)					
Size (mm)		Rounded (g)	Fresh (g)	Total (g)	Mass %	% Passing
65	53	3015.00	1826.90	4841.90	2.66	100.00
53	44	24341.30	4112.20	28453.50	15.62	97.34
44	35	58912.50	5051.80	63964.30	35.12	81.72
35	28	54548.00		54548.00	29.95	46.59
28	16	26696.00		26696.00	14.66	16.64
16	11.2	2613.90		2613.90	1.44	1.98
11.2		990.40		990.40	0.54	0.54
		171117.10	10990.90	182108.00		

Table D2- 66: Charge size distribution exiting40 run 4

| SIZE DISTRIBUTION OF ROCKS (OUT)					
Size (mm)		Rounded (g)	Fresh (g)	Total (g)	Mass %	% Passing
65	53	4329.50		4329.50	2.53	100.00
53	44	22847.70		22847.70	13.34	97.47
44	35	52088.50		52088.50	30.41	84.13
35	28	57423.50		57423.50	33.53	53.72
28	16	30634.00		30634.00	17.89	20.19
16	11.2	2970.00		2970.00	1.73	2.31
11.2		982.50		982.50	0.57	0.57
		171275.70	0.00	171275.70		
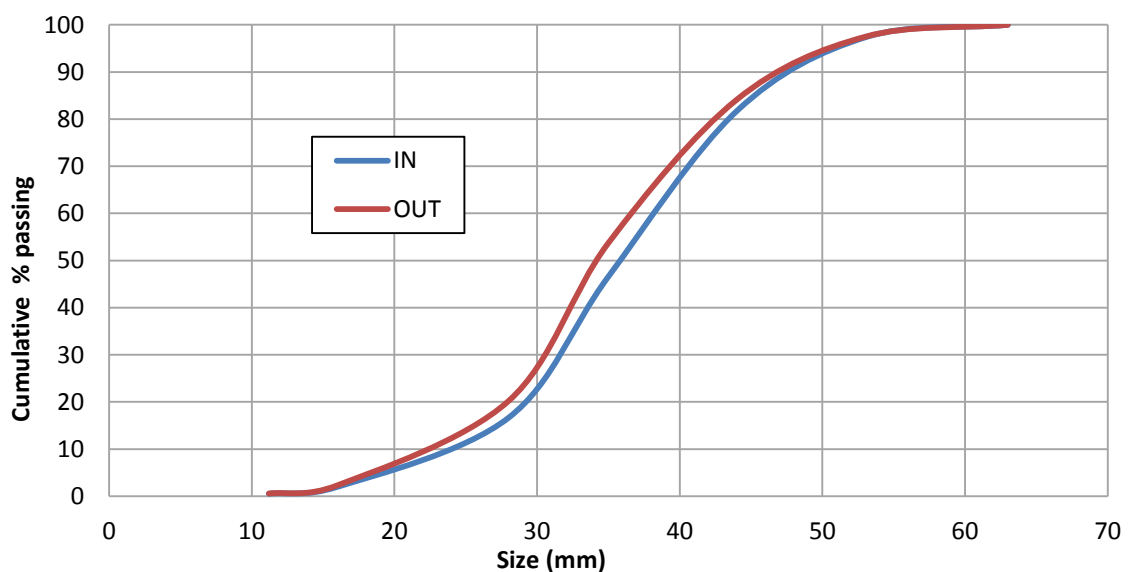
Figure D2- 15:Charge size distribution before and after 40 run 4

164

Run ID: 40 run 5

Operating Conditions: Pebble Size 65/35; Speed 75% Critical; Volumetric filling 40%

Table D2- 67: Sample 1 product size distribution for 40 run 5

SIZE DISTRIBUTION SAMPLE 1					
Size (μm)		Sample mass (g)	Total mass (kg)	Mass %	% Passing
3300	1180	2.26	0.14	0.35	100.00
1180	425	0.18	0.01	0.03	99.65
425	300	0.18	0.01	0.03	99.62
300	212	0.45	0.03	0.07	99.59
212	150	0.81	0.05	0.13	99.52
150	106	39.06	2.50	6.14	99.39
106	75	71.27	4.56	11.21	93.25
75		521.75	33.39	82.04	82.04
			40.70		

Table D2- 68: Sample 2 product size distribution for 40 run 5

SIZE DISTRIBUTION SAMPLE 2					
Size (μm)		Sample mass (g)	Total mass (kg)	Mass %	% Passing
3300	1180	2.28	0.15	0.36	100.00
1180	425	0.18	0.01	0.03	99.64
425	300	0.18	0.01	0.03	99.61
300	212	0.46	0.03	0.07	99.58
212	150	0.82	0.05	0.13	99.51
150	106	39.57	2.53	6.24	99.38
106	75	72.20	4.62	11.39	93.14
75		518.33	33.17	81.75	81.75
			40.58		

SIZE DISTRIBUTION OF ROCKS (IN)

Size (mm)		Rounded (g)	Fresh (g)	Total (g)	Mass %	% Passing
65	53	2651.40	2286.80	4938.20	2.74	100.00
53	44	23434.00	5036.40	28470.40	15.80	97.26
44	35	55714.40	6252.30	61966.70	34.40	81.46
35	28	54528.20		54528.20	30.27	47.06
28	16	26654.90		26654.90	14.80	16.79
16	11.2	2614.60		2614.60	1.45	2.00
11.2		982.50		982.50	0.55	0.55
		166580.00	13575.50	180155.50		

Table D2- 70: Charge size distribution exiting40 run 5

SIZE DISTRIBUTION OF ROCKS (OUT)

| Size (mm)		Rounded (g)	Fresh (g)	Total (g)	Mass %	% Passing
65	53	3619.40		3619.40	2.17	100.00
53	44	23734.60		23734.60	14.22	97.83
44	35	51090.80		51090.80	30.60	83.62
35	28	54973.50		54973.50	32.93	53.01
28	16	29209.60		29209.60	17.50	20.09
16	11.2	3274.70		3274.70	1.96	2.59
11.2		1051.30		1051.30	0.63	0.63
		166953.90	0.00	166953.90		
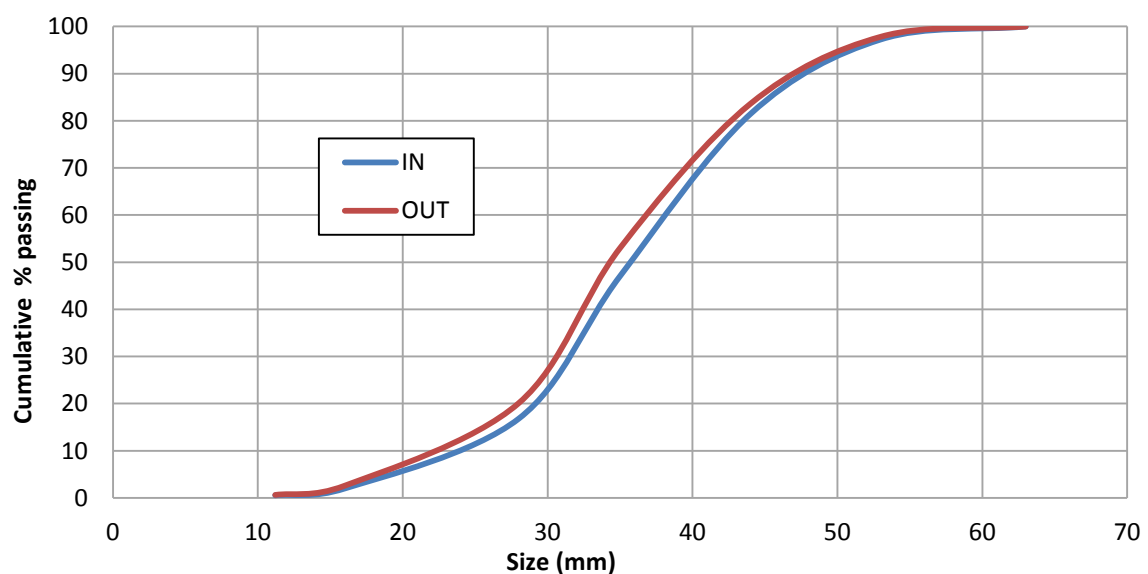
Figure D2- 16:Charge size distribution before and after 40 run 5

166

Run ID: 40 run 6

Operating Conditions: Pebble Size 65/35; Speed 83.5% Critical; Volumetric filling 40%

SIZE DISTRIBUTION SAMPLE 1					
Size (μm)		Sample mass (g)	Total mass (kg)	Mass %	% Passing
3300	1180	1.66	0.11	0.25	100.00
1180	425	1.02	0.07	0.15	99.75
425	300	1.02	0.07	0.15	99.60
300	212	3.33	0.21	0.49	99.45
212	150	4.35	0.28	0.64	98.96
150	106	35.71	2.29	5.26	98.32
106	75	106.82	6.84	15.73	93.06
75		525.18	33.61	77.33	77.33
			43.46		

SIZE DISTRIBUTION SAMPLE 2					
Size (μm)		Sample mass (g)	Total mass (kg)	Mass %	% Passing
3300	1180	1.73	0.11	0.25	100.00
1180	425	1.06	0.07	0.16	99.75
425	300	1.06	0.07	0.16	99.59
300	212	3.45	0.22	0.51	99.43
212	150	4.52	0.29	0.67	98.92
150	106	37.05	2.37	5.47	98.26
106	75	110.62	7.08	16.32	92.79
75		518.32	33.17	76.47	76.47
			43.38		

Table D2- 73: Charge size distribution entering 40 run 6

SIZE DISTRIBUTION OF ROCKS (IN)						
Size (mm)		Rounded (g)	Fresh (g)	Total (g)	Mass %	% Passing
65	53	2418.10	2563.80	4981.90	2.71	100.00
53	44	22798.60	5655.70	28454.30	15.45	97.29
44	35	58896.50	6985.50	65882.00	35.78	81.84
35	28	54559.20		54559.20	29.63	46.07
28	16	26663.70		26663.70	14.48	16.44
16	11.2	2615.10		2615.10	1.42	1.96
11.2		990.70		990.70	0.54	0.54
		168941.90	15205.00	184146.90		

Table D2- 74: Charge size distribution exiting40 run 6

SIZE DISTRIBUTION OF ROCKS (OUT)						
Size (mm)		Rounded (g)	Fresh (g)	Total (g)	Mass %	% Passing
65	53	3191.60		3191.60	1.90	100.00
53	44	21045.80		21045.80	12.51	98.10
44	35	53508.00		53508.00	31.81	85.59
35	28	57691.80		57691.80	34.29	53.78
28	16	28617.80		28617.80	17.01	19.49
16	11.2	3221.30		3221.30	1.91	2.48
11.2		947.90		947.90	0.56	0.56
		168224.20	0.00	168224.20		
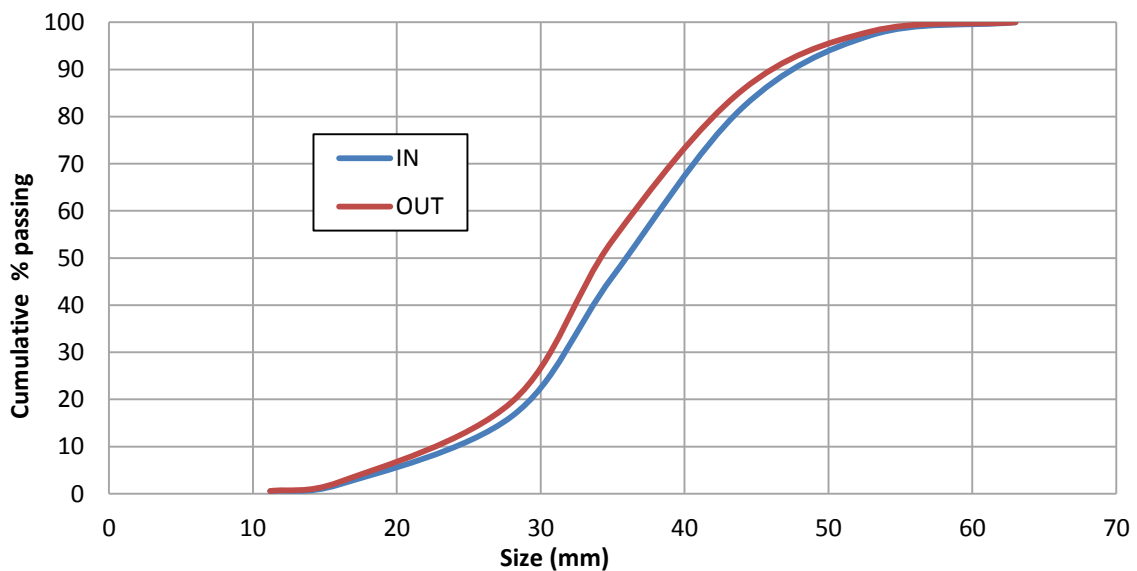
Figure D2- 17:Charge size distribution before and after 40 run 6

168

Table D2- 75: Power draw data for runs at various speeds at 40% filling

Speed	Run ID	Voltage(mV)	Torque(N.m)	Power (kW)	Net Power (kW)
83.50%	NLP	1.093	16.467	0.057	
	40 run 1*	2.337	529.233	1.829	1.772
	40 run 1	2.354	536.491	1.854	1.797
	40 run 6*	2.267	500.588	1.730	1.673
	40 run 6	2.321	522.827	1.807	1.750
75%	NLP	1.089	14.932	0.047	
	40 run 2*	2.236	487.588	1.532	1.485
	40 run 2	2.265	499.711	1.570	1.523
	40 run 5*	2.354	536.393	1.685	1.638
	40 run 5	2.339	530.277	1.666	1.619
69%	NLP	1.079	10.897	0.031	
	40 run 3*	2.298	513.124	1.478	1.446
	40 run 3	2.307	516.877	1.488	1.457
	40 run 4*	2.336	528.919	1.523	1.492
	40 run 4	2.336	528.920	1.523	1.492

Power used to find recalculated time

Table D2- 76: Data used to recalculate milling time in 40% filling tests

Run ID	t_2 (min)	t_1 (min)	M_2 (kg)	M_1 (kg)	P_1 (kw)	P_2 (kw)
40 run 1	42.99	35.00	27.59	20.00	1.578	1.772
40 run 2	43.98	35.00	27.59	20.00	1.353	1.485
40 run 3	40.45	35.00	27.59	20.00	1.212	1.446
40 run 4	41.49	35.00	27.59	20.00	1.282	1.492
40 run 5	42.14	35.00	27.59	20.00	1.430	1.638
40 run 6	45.54	35.00	27.59	20.00	1.578	1.673

APPENDIX D3: VOLUMETRIC AND SPEED TESTING DATA

Table D3- 1: Power data at 30% filling for various speeds

	Speed (% Critical)	Voltage(mV)	Torque(N.m)	Net Torque(N.m)	Net POWER(kW)
No load power	69	1.079	10.897	-	-
	75	1.089	14.932	-	-
	80	1.093	16.467	-	-
	85	1.099	18.863	-	-
	90	1.135	33.623	-	-
	69	2.114	437.312	426.415	1.228
	75	2.124	441.690	426.758	1.341
	80	2.116	438.121	421.653	1.413
	85	2.067	417.955	399.092	1.421
	90	2.019	398.192	364.569	1.374

Table D3- 2: Power data at 40% filling for various speeds

	Speed (% Critical)	Voltage(mV)	Torque(N.m)	Net Torque(N.m)	Net POWER(kW)
No load power	69	1.079	10.897	-	-
	75	1.089	14.932	-	-
	80	1.093	16.467	-	-
	85	1.099	18.863	-	-
	90	1.135	33.623	-	-
	69	2.313	519.299	508.402	1.464
	75	2.339	530.200	515.268	1.619
	80	2.349	534.297	517.829	1.735
	85	2.333	527.662	508.799	1.812
	90	2.263	498.793	465.170	1.754

Table D3- 3: Power data at 45% filling for various speeds

	Speed (% Critical)	Voltage(mV)	Torque(N.m)	Net Torque(N.m)	Net POWER(kW)
			45% Volumetric Filling		
No load power	69	1.079	10.897	-	-
	75	1.089	14.932	-	-
	80	1.093	16.467	-	-
	85	1.099	18.863	-	-
	90	1.135	33.623	-	-
	69	2.431	568.078	557.182	1.605
	75	2.435	569.620	554.688	1.743
	80	2.399	555.060	538.592	1.805
	85	2.360	538.653	519.790	1.851
	90	2.307	517.031	483.408	1.822

Table D3- 4: Power data at 50% filling for various speeds

	Speed (% Critical)	Voltage(mV)	Torque(N.m)	Net Torque(N.m)	Net POWER(kW)
			50% Volumetric Filling		
No load power	69	1.079	10.897	-	-
	75	1.089	14.932	-	-
	80	1.093	16.467	-	-
	85	1.099	18.863	-	-
	90	1.135	33.623	-	-
	69	2.481	588.677	577.781	1.664
	75	2.477	587.122	572.190	1.798
	80	2.438	570.941	554.474	1.858
	85	2.398	554.316	535.452	1.906
	90	2.354	536.445	502.823	1.896

Table D3- 5: Power data at 55% filling for various speeds

	Speed (% Critical)	Voltage(mV)	Torque(N.m)	Net Torque(N.m)	Net POWER(kW)
	55% Volumetric Filling				
No load power	*69*	1.079	10.897	-	-
	75	1.089	14.932	-	-
	80	1.093	16.467	-	-
	85	1.099	18.863	-	-
	90	1.135	33.623	-	-
	69	2.490	592.400	581.504	1.675
	75	2.505	598.403	583.471	1.833
	80	2.464	581.527	565.059	1.894
	85	2.421	563.897	545.034	1.941
	90	2.371	543.271	509.648	1.921

Run ID: nm run 1

Operating Conditions: Pebbles; Speed 69% Critical; Volumetric filling 40%

Table D4- 1: Sample 1 product size distribution for nm run 1

SIZE DISTRIBUTION SAMPLE 1					
Size (µm)		Sample mass (g)	Total mass (kg)	Mass %	% Passing
3300	1180	0.20	0.00	0.01	100.00
1180	425	0.20	0.00	0.01	99.99
425	300	2.70	0.00	0.12	99.98
300	212	6.50	0.01	0.28	99.86
212	150	3.70	0.00	0.16	99.58
150	106	21.10	0.02	0.92	99.42
106	75	293.90	0.29	12.84	98.50
75		1960.10	1.96	85.65	85.65
			2.29		

Table D4- 2: Charge size distribution entering nm run 1

SIZE DISTRIBUTION OF ROCKS (IN)						
Size (mm)		Rounded (g)	Fresh (g)	Total (g)	Mass %	% Passing
65	53	0.00	0.00	0.00	0.00	100.00
53	44	0.00	0.00	0.00	0.00	100.00
44	35	2331.40	591.20	2922.60	25.95	100.00
35	28	3933.50	441.60	4375.10	38.85	74.05
28	16	3698.30	0.00	3698.30	32.84	35.19
16	11.2	264.60	0.00	264.60	2.35	2.35
11.2		0.00	0.00	0.00	0.00	0.00
		10227.80	1032.80	11260.60		

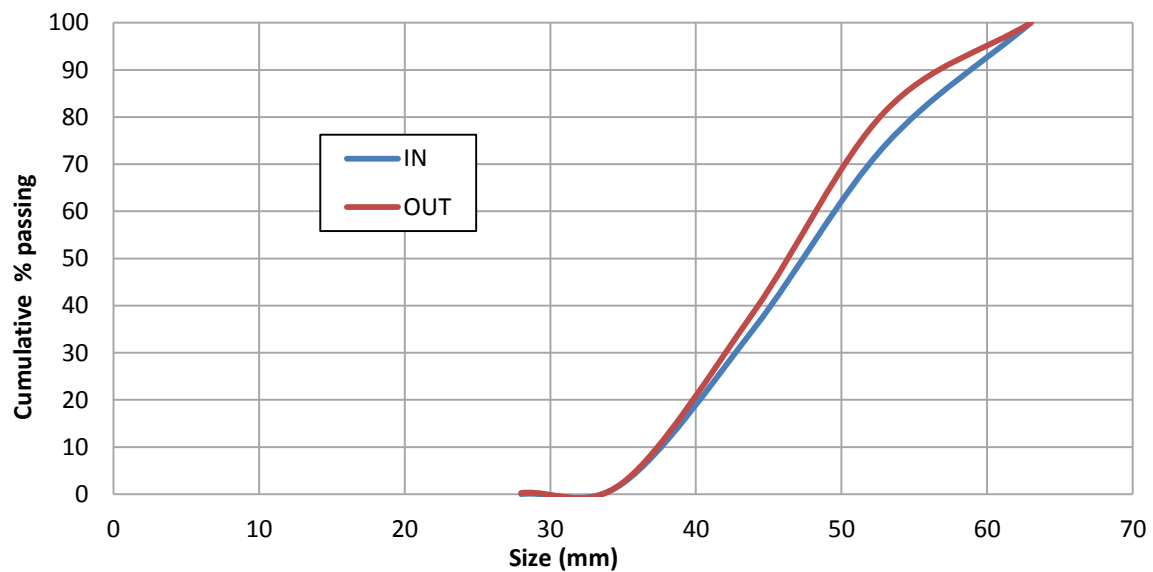| SIZE DISTRIBUTION OF ROCKS (OUT)						
Size (mm)		Rounded (g)	Fresh (g)	Total (g)	Mass %	% Passing
65	53	0.00	0.00	0.00	0.00	100.00
53	44	0.00	0.00	0.00	0.00	100.00
44	35	2003.90	0.00	2003.90	18.77	100.00
35	28	4530.90	0.00	4530.90	42.44	81.23
28	16	3875.50	0.00	3875.50	36.30	38.79
16	11.2	237.60	0.00	237.60	2.23	2.50
11.2		29.00	0.00	29.00	0.27	0.27
		10676.90	0.00	10676.90		

Figure D4- 1:Charge size distribution before and after nm run 1

Run ID: nm run 2

Operating Conditions: Pebbles; Speed 69% Critical; Volumetric filling 40%

Table D4- 4: Sample 1 product size distribution for nm run 2

SIZE DISTRIBUTION SAMPLE 1					
Size (µm)		Sample mass (g)	Total mass (kg)	Mass %	% Passing
3300	1180	1.20	0.00	0.05	100.00
1180	425	0.60	0.00	0.03	99.95
425	300	0.70	0.00	0.03	99.92
300	212	1.80	0.00	0.08	99.89
212	150	4.10	0.00	0.18	99.81
150	106	32.80	0.03	1.43	99.63
106	75	283.90	0.28	12.38	98.20
75		1968.10	1.97	85.82	85.82
			2.29		

Table D4- 5: Charge size distribution entering nm run 2

SIZE DISTRIBUTION OF ROCKS (IN)						
Size (mm)		Rounded (g)	Fresh (g)	Total (g)	Mass %	% Passing
65	53	0.00	0.00	0.00	0.00	100.00
53	44	0.00	0.00	0.00	0.00	100.00
44	35	2003.90	360.40	2364.30	20.98	100.00
35	28	4530.90	258.70	4789.60	42.51	79.02
28	16	3875.50	0.00	3875.50	34.40	36.51
16	11.2	237.60	0.00	237.60	2.11	2.11
11.2		0.00	0.00	0.00	0.00	0.00
		10647.90	619.10	11267.00		

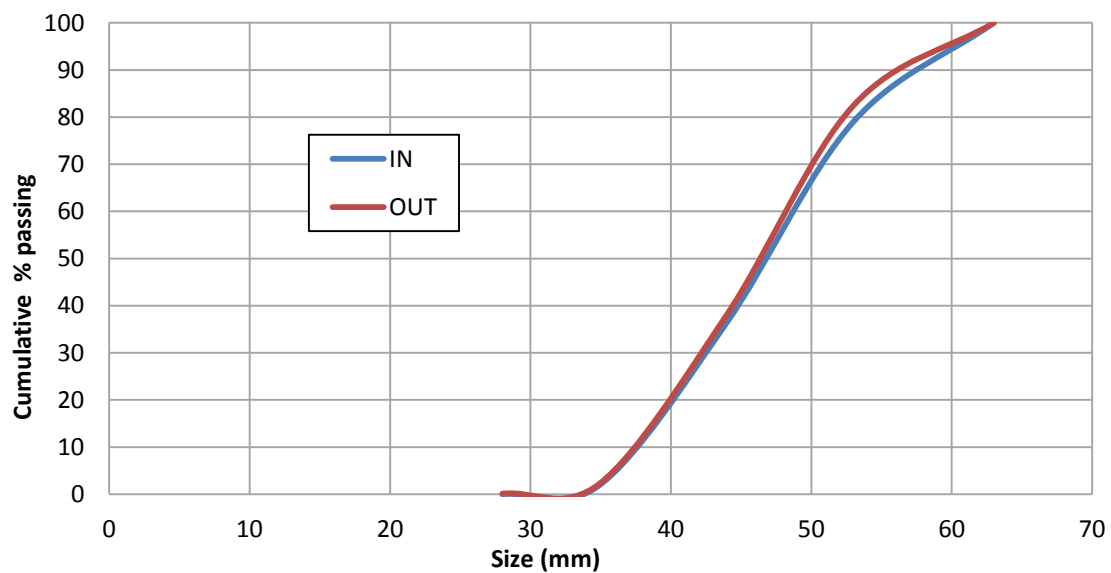| SIZE DISTRIBUTION OF ROCKS (OUT)					
Size (mm)		Rounded (g)	Fresh (g)	Total (g)	Mass %	% Passing
65	53	0.00	0.00	0.00	0.00	100.00
53	44	0.00	0.00	0.00	0.00	100.00
44	35	1880.60	0.00	1880.60	17.56	100.00
35	28	4742.90	0.00	4742.90	44.29	82.44
28	16	3825.20	0.00	3825.20	35.72	38.15
16	11.2	247.60	0.00	247.60	2.31	2.43
11.2		12.80	0.00	12.80	0.12	0.12
		10709.10	0.00	10709.10		

Figure D4- 2:Charge size distribution before and after nm run 2

Run ID: nm run 3

Operating Conditions: Steel balls; Speed 69% Critical; Volumetric filling 40%

SIZE DISTRIBUTION SAMPLE 1					
Size (µm)		Sample mass (g)	Total mass (kg)	Mass %	% Passing
3300	1180	0.00	0.00	0.00	100.00
1180	425	0.30	0.00	0.01	100.00
425	300	2.50	0.00	0.11	99.99
300	212	18.50	0.02	0.81	99.88
212	150	15.30	0.02	0.67	99.07
150	106	59.90	0.06	2.62	98.40
106	75	233.70	0.23	10.20	95.79
75		1960.10	1.96	85.58	85.58
			2.29		

SIZE DISTRIBUTION OF ROCKS (IN)					
Size (mm)		Rounded (g)	Fresh (g)	Total (g)	Mass %	% Passing
65	53	0.00	0.00	0.00	0.00	100.00
53	44	0.00	0.00	0.00	0.00	100.00
44	35	8662.10	0.00	8662.10	25.98	100.00
35	28	12924.90	0.00	12924.90	38.77	74.02
28	16	10977.90	0.00	10977.90	32.93	35.25
16	11.2	774.70	0.00	774.70	2.32	2.32
11.2		0.00	0.00	0.00	0.00	0.00
		33339.60	0.00	33339.60		

SIZE DISTRIBUTION OF ROCKS (OUT)					
Size (mm)		Rounded (g)	Fresh (g)	Total (g)	Mass %	% Passing
65	53	0.00	0.00	0.00	0.00	100.00
53	44	0.00	0.00	0.00	0.00	100.00
44	35	8497.10	0.00	8497.10	25.50	100.00
35	28	13251.50	0.00	13251.50	39.77	74.50
28	16	10797.20	0.00	10797.20	32.40	34.73
16	11.2	774.60	0.00	774.60	2.32	2.32
11.2		0.00	0.00	0.00	0.00	0.00
		33320.40	0.00	33320.40		

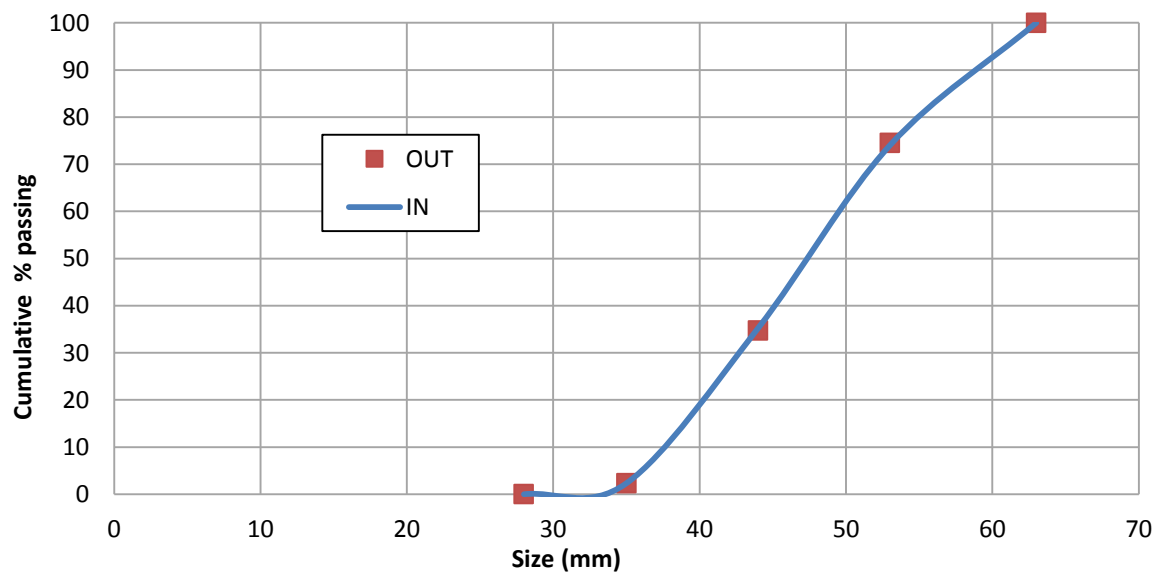Figure D4- 3:Charge size distribution before and after nm run 3

178

Table D4- 10:Power draw data for runs in small mill

Run ID	Voltage (mV)	Torque (N.m)	Power (kW)	Net Power (kW)
NLP	1.007	3.323	0.022	n/a
nmrun1*	1.359	11.094	0.072	0.050
nmrun1	1.359	11.094	0.072	0.050
nmrun2*	1.360	11.104	0.072	0.051
nmrun2	1.354	10.975	0.071	0.050
nmrun3*	1.827	21.412	0.139	0.117
nmrun3	1.827	21.412	0.139	0.117

Power used to find recalculated time

Table D4- 11:Data used to recalculate milling time in small mill tests

Run ID	t_2 (min)	t_1 (min)	M_2 (kg)	M_1 (kg)	P_1(kw)	P_2(kw)
nmrun1	75.21	35.00	1.70	20.00	1.276	0.050
nmrun2	75.11	35.00	1.70	20.00	1.276	0.051
nmrun3	43.30	75.11	2.28	1.70	0.051	0.117